Seismic interpretation and evaluation of the Cenozoic uplift in the southwestern Barents Sea

Mauricio Reyes Canales

ABSTRACT

Several studies have suggested considerable uplift and erosion in the western Barents Sea and Svalbard margin during Cenozoic times. After continental breakup of the Norwegian-Greenland Sea, a primary tectonic uplift was induced as consequence of the heat transfer during the margin transform stage. This Cenozoic uplift caused a sub-aerial terrain that was massively eroded, creating prograding wedges along western Barents Sea margin. This massive erosion, related to intense glacial activity during Pliocene-Pleistocene times generated a secondary isostatic uplift that maintained an elevated glaciated terrain.

Seven 2D seismic lines and two wells have been studied to understand the Cenozoic geological history of the southwestern Barents Sea. To describe the main features based on seismic images, and to study the magnitude and consequences of the major Cenozoic uplift and erosion in the southwestern Barents Sea were the main objectives of this thesis.

The methodology to interpret these profiles consisted primarily in observing the main seismic features of these images. After this, the main reflections were marked and then a geological model was proposed. Finally, these geological models were tied with previous regional investigations, making possible the understanding of the geological history for each line. The first interpreted image was a seismic line intersected by one of the wells, from which a seismic-well tie was done. This well and previous studies provided key information in order to date the main reflections and have a better understanding of the geological evolution and lithological composition of the study area.

Almost all the seismic lines show similar features and have a close-related geologic history. The Vestbakken Volcanic Province (VVP) was marked during the seismic interpretation and is linked with the continental breakup of Norwegian-Greenland Sea. These volcanic flows were easy to distinguish in the seismic lines and their presence was confirmed by one of the wells. The pre-glacial sediments (Paleocene-Lower Miocene) were deposited and affected during the shear margin setting that dominated the southwestern Barents Sea during those times. Transpression and transtension during this stage could explain the configuration of these strata.

The glacial sediments (Pliocene-Pleistocene) were deposited after the Cenozoic uplift and massive glacial erosion, an evidence of this is the main truncation that separates the pre-glacial and glacial sediments. These glacial sediments formed the massive prograding wedges (ex. Bjørnøya fan) visible along the margin.

By studying the available well data it was possible to infer the magnitude of the uplift. To estimate the magnitude of the total uplift during Cenozoic times, a method based in the use of empirical depth-porosity shale/sand trends was applied and then compared with depth-porosity trends calculated from the well logs. When comparing the obtained results (900±100 m of uplift) with previous estimations (from 700 m up to 1500 m of uplift), there is a good correlation between the depth-porosity trend method and the variable estimated range for the total uplift in this area of the southwestern Barents Sea margin.

ACKNOWLEDGMENTS

Thanks to God for giving me life, wisdom, and the perseverance to make this achievement possible.

Thanks to my Mom, for her affection, comprehension and giving me invaluable principles. Thanks to my aunts, uncles, cousins, and to all my wonderful family for your love and support throughout all the moments of my life. Your knowledge and values have enriched me as a person and made me into a man who works for the humanity and for a better world.

I would like to express my gratitude to my supervisor Prof. Ståle Emil Johansen for giving me the opportunity to work on this thesis. His continuous support, patience, motivation, and knowledge were fundamental to making this project possible.

Thanks to the members and professors of the USB (Universidad Simón Bolívar) and NTNU who provided me the knowledge all these years necessary to reach this achievement. Thanks to the people in the laboratory K-73, your support for this project has been unmatched and has helped in improving this thesis.

Last but not the least; I would like to thank my dear friends that I met in Trondheim. You are amazing people and my stay in Norway could not be better without your friendship and solidarity.

TABLE OF CONTENTS

LIST OF FIGURES

ABBREVIATIONS

Abbreviation	Complete name
BQ	Base Quaternary/ Base Pleistocene
BP	Base Pliocene
BO	Base Oligocene
EE-LP	Early Eocene – Late Paleocene
HAR	High amplitude reflections
ILM	Intra Lower Miocene
ILO	Intra Lower Oligocene
IME (1,2,3)	Intra Middle Eocene (I,II,III)
IO	Intra Oligocene
IP (1,2,3,4,5,6)	Intra Pliocene (I,II,III,IV,V,VI)
IQ (1,2)	Intra Quaternary (I and II)
VVP	Vestbakken Volcanic Province

1. INTRODUCTION

The southwestern Barents Sea margin was formed in response to the Paleocene-Eocene continental breakup and opening of the Norwegian-Greenland Sea. This passive margin was not formed by normal or near normal extension; the tectonic development included a transform margin stage, giving it particular geological features. The tectonic history of this margin could be simplified in three main stages: (1) Rifting and continental breakup, including shear setting between continental crusts; (2) Sea floor spreading and generation of an active transform margin; (3) Passive margin stage and late Cenozoic uplift and erosion.

The Vestbakken Volcanic Province is located at a rifted margin segment southwest of Bjørnøya (see figure 1). These volcanic rocks were originated during Paleocene-Eocene times as consequence of rifting and continental breakup. Evidence from this volcanic activity is present in seismic images and in the well data. Transtensional and transpressional tectonism during the transform margin stage was also present along the area.

Several studies have suggested that the southwestern Barents Sea and Svalbard margin have experienced considerable uplift and erosion during Cenozoic times. This uplift took place after the continental breakup of the Norwegian–Greenland Sea as consequence of the heat transfer during the transform margin stage. This Cenozoic uplift caused a high sub-aerial elevated terrain that was massively eroded, creating prograding wedges (also known as fans) along the western Barents Sea margin. This massive erosion, helped by the intense glacial activity, generated a secondary isostatic uplift that maintains an elevated glaciated terrain.

A wide variety of methods have been proposed to estimate the Cenozoic uplift and erosion: mass balance, vitrinite reflectance, shale compaction, interval velocities, clay mineral diagenesis, computational modelling of heat transfer, etc. The exact origin of this uplift is still in debate, but heat transfer is one of the most accepted explanations.

The understanding of this major event is fundamental to comprehend the recent geological history of the area and their impact in oil exploration. The maturity of sources rocks, timing and trap generation have been affected by this regional event, changing dramatically the potential petroleum systems in the area.

The present study consisted in the interpretation of 2D seismic lines and the use of two wells. The main focus consisted in finding and estimating the magnitude of the Cenozoic uplift along the southwestern Barents Sea margin. For this reason, a detailed understanding of the geological events based in the seismic images, well data and previous studies was necessary. Finding and describing main erosive truncations and other uplift generated structures was one of the main purposes of this work. Finally, a method to estimate the Cenozoic uplift in the area was applied based on the use of depth-porosity empirical shale/sand trends and well data.
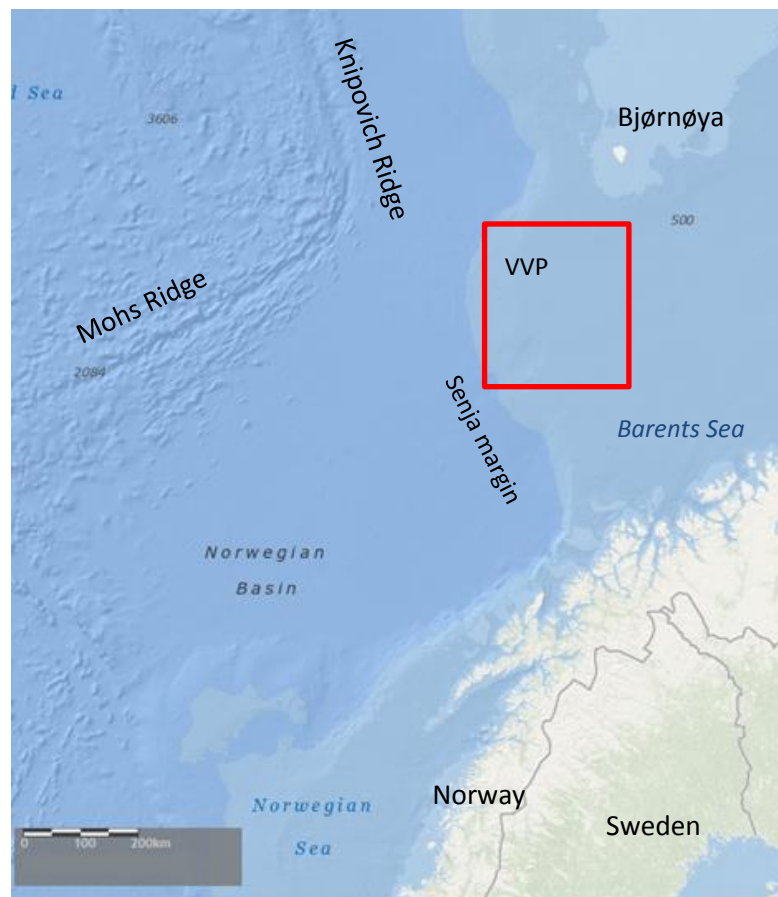
Figure 1. Bathymetry of the southwestern Barents Sea and Norwegian Sea. The red rectangle shows the area of study, entirely over the continental side of the margin. VVP= Vestbakken Volcanic Province. (Modified from NOAA).

2. GEOLOGICAL BACKGROUND

2.1. DEVELOPMENT OF A PASSIVE MARGIN

The passive margin concept involves several types of geological margins, widely studied particularly for their relevance in oil exploration. Passive margins usually results from the succession of three main events: initial rifting phase, Sea floor spreading and formation of oceanic crust (Bradley, 2008). The location and ages of modern passive margins are possible to determinate using bathymetry maps, seismicity and magnetic anomalies (Bradley, 2008).

Nowadays, the western Barents Sea margin is considered a passive margin. However, during some period between the continental breakup and the modern passive margin, the western Barents Sea showed a transform margin setting.

To understand the western Barents Sea geological evolution is necessary study previous geological models that explain the formation of a passive margin including a shear margin stage. In this section it will be show some concepts and models that describe the main features and formation of a passive margin.

2.1.1.   RIFTING AND CONTINENTAL BREAKUP

The process of continental breakup has been studied by different authors for long time. There are several models to explain the continental breakup. Passive rifting models explain extension and thinning of the lithosphere as a result of force distribution (McKenzie, 1978). Active rifting models explain breakup as result of ascending mantle plume (Morgan, 1983).

McKenzie's model (see figure 2) is described like a pure-shear extension model. It Consist in the stretching of continental lithosphere than led thinning of continental crust and upwelling of asthenospheric material (McKenzie, 1978). This stage also led block faulting and subsidence. Thickening of lithosphere occurs after cooling of upwelled asthenosphere, this upwelling asthenosphere becomes a new part of lithosphere (McKenzie, 1978). McKenzie's pure shear model is considered a symmetrical model (Lister et al., 1986).

Wernicke's model (see figure 2) suggests simple shear for explain continental rifting. This model proposes a detachment-related zone cutting the whole thickness of the lithosphere (Lister et al., 1986). Extension is obtained as a result of one part being pulled out from the other beneath, creating a low angle detachment fault. Upwelling of the asthenosphere material occurs beneath the detachment zone. Wernicke's simple shear model is considered an asymmetrical model (Lister et al., 1986). Other models propose and active rifting during the continental breakup. Morgan's model suggests that breakup is caused by continental drift over hot spots. As continents move over hot spots, through the lithosphere will be a creation of weakness paths. Millions of years later, continents are split along these lines (Morgan, 1983)

Thinning of lithosphere induce asthenospheric ascension. This asthenosphere will partially melt through the ascension, and the volume of melted material depends on the amount of lithospheric thinning and the temperature of the asthenosphere (White and McKenzie, 1989). The magmatism caused by this asthenospheric ascension will follow through the lithosphere until the surface. This melt rock will reach the surface, producing voluminous flood basalts. The eruptive basalts will flow laterally onto the contiguous areas.
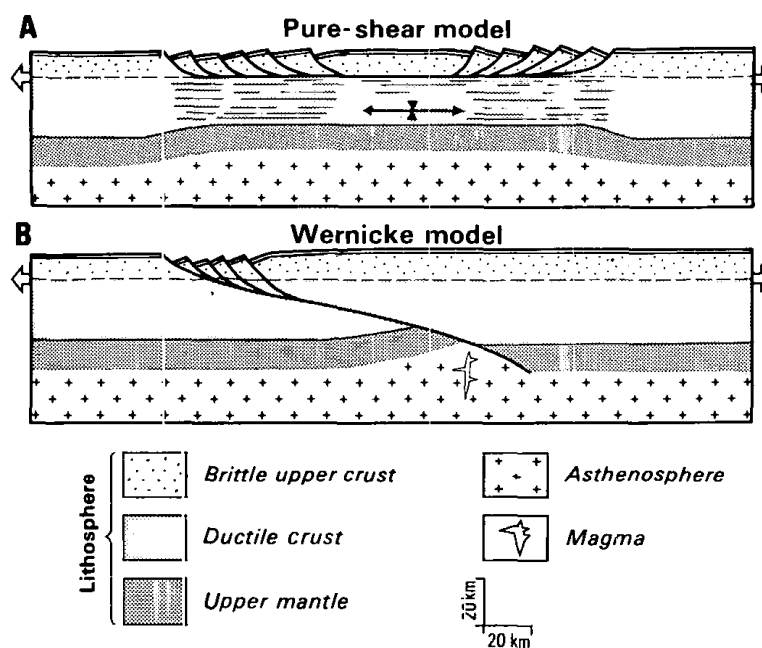
Figure 2. Models for continental extension. Pure-shear model from McKenzie and simple shear model from Wernicke. McKenzie´s model Consist in stretching of continental lithosphere, this led thinning of continental crust and upwelling of asthenosphere. Wernicke´s model proposes a detachment-related zone cutting the whole thickness of the lithosphere. Modified from Lister et al., 1986.

2.1.2.   SEA FLOOR SPREADING

The sea floor spreading rates can vary from 10 up to 180 mm/year, and this is a determinant factor that controls the morphology of a spreading center (Macdonald, 1982). Mapping of the Mid Ocean Ridges shows a discontinuity in their structure, separated by several transform faults (Macdonald, 2001). The distance between the spreading ridges are constant, as there is no movement between the sections. Macdonald divides the morphology of spreading ridges in three categories: slow, intermediate and fast (see figure 3). A fourth category, the ultraslow, was proposed by Dick et al. in 2003. According to Dick et al. the ultraslow spreading is defined when sea floor spreading rates are between 12 mm/year up to 20 mm/yr. According to MacDonald, Slow spreading ridge rates are between 10 – 50 mm/year; Intermediate spreading ridge are between 50-90 mm/year; and fast spreading ridge are faster than 90 mm/yr.
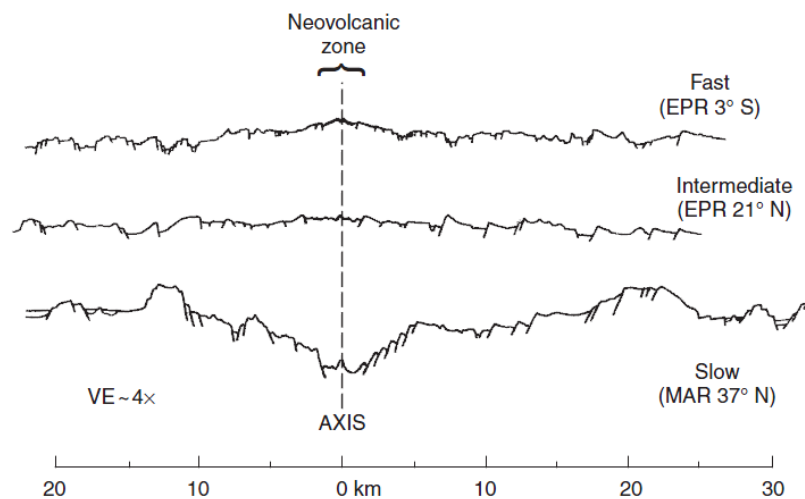
Figure 3.Examples of topography for fast, intermediate and slow spreading ridge with Neovolcanic zone in the center. MAR: Mid Atlantic Ridge. EPR: East Pacific Rise. From Macdonald, 2001.

2.1.3. SHEAR MARGIN AND STRUCTURES

Modern passive margins present along their length, transform segments known as continent-ocean shear or transform margins (Lorenzo and Vera, 1992). Models of continent-ocean transform margins usually distinguish an early stage in which continent-continent shearing is emphasized as the dominant process controlling the tectonic structural development of an elongated, narrow region. Continue the seafloor spreading; the transform fault will eventually finish (Lorenzo and Vera, 1992).

A shear margin typically follow these stages (see figure 4): (1)Rift: shearing of continental crusts and complex rifting (2)Drift: continent-ocean shearing, development of an active transform boundary between ocean and continental crust (3) Shear margin becomes in a passive margin formed along the inactive fracture zone that separates oceanic and continental crusts (Bird, 2001).

During the shear margin regime is expected a particular structural development. Strike slip faults, graben, horst and transpressional and transtensional structures are some structural elements developed during this regime (Fossen, 2010). Strike-slip deformation occurs in areas where one crustal block moves laterally with respect to an adjacent block, creating a shear contact between them.

Transpression and transtension occurs when there are simultaneously combination between strike-slip shear movements and shortening (or extension) perpendicular to it (see figure 5); that means local extension or compression in some areas along the strike-slip fault (Fossen, 2010).

Usually these transtension or transpression creates limited areas where the extensional regime or contraccional regime is clearly dominant inside the main strike-slip movement. Positive flower structures and negative flower structures are associated with the transpression and transtension respectively (Fossen, 2010).

Uplift and subsidence are also predicted for the McKenzie stretching model (McKenzie, 1978). During the shear regime stage, rapid uplift and sedimentation can occur, leading rise to considerable lateral variation in facies within the basins.
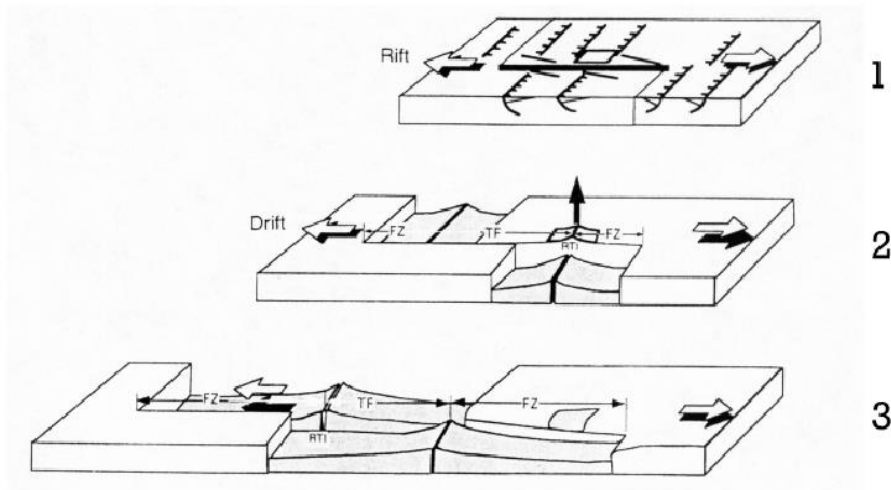
Figure 4. Three-stage model for shear margin formation. (1) Rift: continent-continent shearing; (2) Drift: continent-ocean shearing; (3) Passive margin: continent-ocean fracture zone. From Bird, 2001.
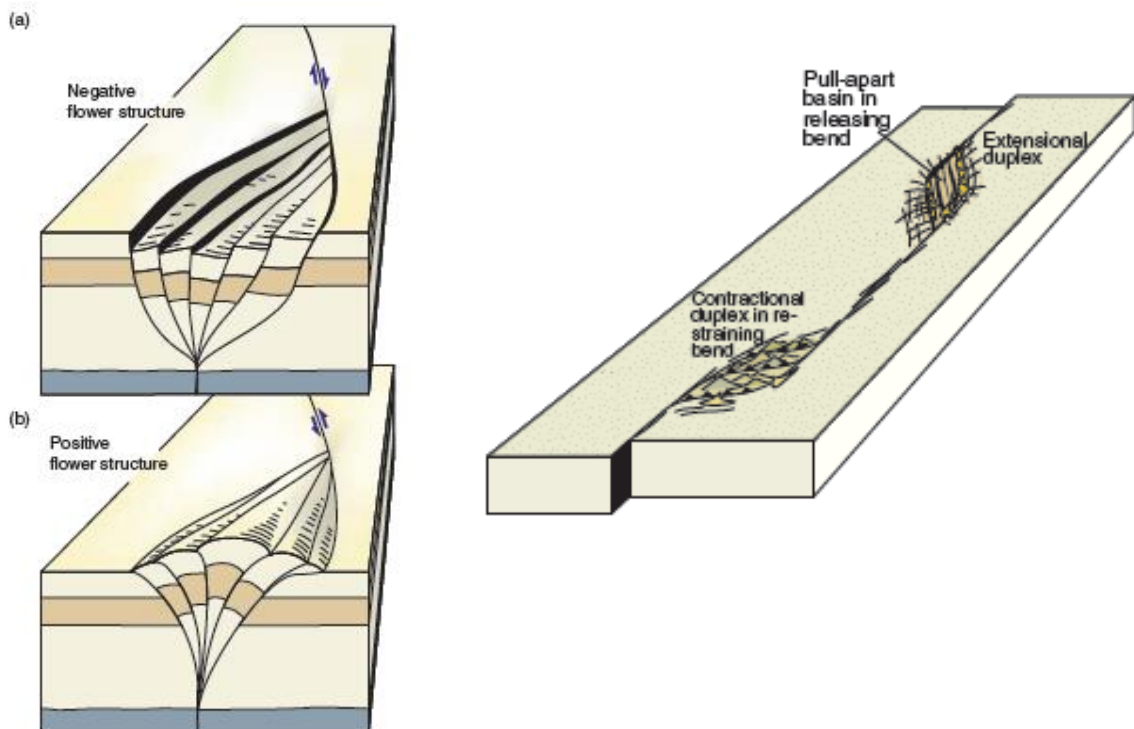
Figure 5. (left) Negative and positive flower structures caused by transtension and transtension respectively. (right) Strike-slip fault scheme showing transpressional features (contractional duplex) and transtensional features (pull-apart basin). Modified from Fossen, 2010.

2.1.4.   UPLIFT AND EROSION

Tectonic Uplift can be induced by rifting and continental breakup (Dimakis et al., 1998). McKenzie model of pure shear includes subsidence and uplift response (McKenzie, 1978). These tectonic events change the previous isostatic level of the litospheric plate, inducing an upwelling of the plate. This uplifted plate is more exposed to erosion. This erosion and lose of plate material, change the isostatic level and inducing another uplift, creating a secondary uplifted event, see figure 6 (Dimakis et al., 1998).

Several erosion ways could affect an uplifted area. Glacial or fluvial activity can erode all this sub-aerial mass, and deposit this eroded sediment over adjacent basins. Regarding to the relation between volcanism and uplift, volcanic activity could affect uplifting in several ways (Dimakis et al., 1998). The lava extrusion could induce an isostatic subsidence response but is difficult evaluate the overall effects of volcanism on uplifting (Dimakis et al., 1998).

2.1.5.   VOLCANISM

Volcanic seismic facies

The characteristics of the extrusive rocks depend from several factors. Presence of water and topography of the emplacement environment are the most important aspects in the categorization of the volcanic facies (Planke et al., 2000). Five volcanic stages have been proposed, where each stage shows a main volcanic feature or facie depending of the rifting development period:

1. The first stage represents initial volcanic activity or wet sediments environment forming complexes basalt-sediments, poorly imaged (Planke et al., 2000).
2. Effusive sub-aerial volcanism, forming the next seismic facies units: Landward Flows, Lava deltas and Inner flows. (Planke et al., 2000).
3. Sub-aerial flood basalts filled the accommodation space created by the subsided rift basins along the breakup axis. Formation of the Inner Seaward dipping reflectors (Inner SDR). (Berndt et al., 2001; Planke et al., 2000).
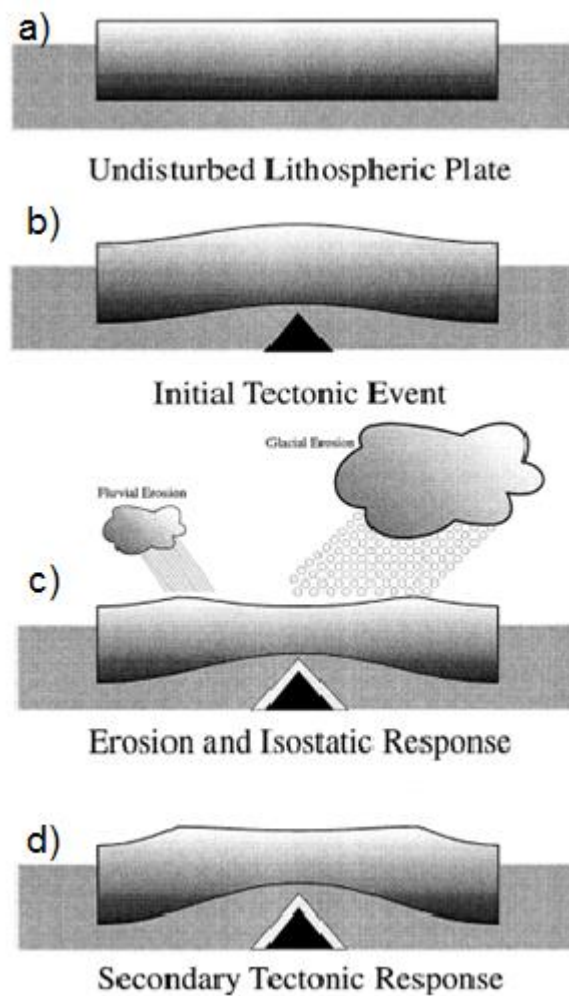
Figure 6. Sketch of relation between tectonic uplift and erosion. (a) Lithospheric plate, without appreciable tectonic influence. (b) Occurs a first tectonic event, altering the isostatic level. (c) Change in the isostatic level and erosion of the upwelling surface (Glacial erosion, fluvial erosion, etc). (d) Isostatic uplift is introduce by previous erosion .Modified from Dimakis et al., 1998.

4. Volanic activity is submerged. Explosive shallow marine volcanism formed deposits called Outer highs (Planke et al., 2000).

5. Volcanic activity submerged deeper. Voluminous deep marine volcanism forming the Outer SDR (Planke et al., 2000).

There are six main extrusive facies identified in volcanic passive margins: Inner Flows, Landward flows, Lava Delta, Inner SDR, Outer SDR, and Outer high (Planke et al., 1999;

Planke et al., 2000). These facies show a particular phase in the rifting volcanic activity, and a differentiated seismic pattern in the seismic images (see table 1).

Seismic Facies Unit	Shape	Boundaries	Internal Pattern	Volcanic facies	Emplacement environment
Landward Flows	Sheet	Top: high amplitude, smooth. Bottom: low amplitude, disrupted.	Subparallel or disrupted. High amplitude.	Flood Basalts	Sub-aerial
Inner Flows	Sheet	Top: high amplitude Bottom: negative polarity, often obscured.	Chaotic or disrupted. subparallel	Massive and fragmented basalts. Volcanoclastic.	Shallow marine
Lava Delta	Bank	Top: high amplitude, reflection truncations Bottom: reflection truncation	Prograding clinoform, disrupted.	Massive and fragmented basalts. Volcanoclastic.	Coastal
Inner SDR	Wedge	Top: High amplitude Bottom: not visible	Divergent-arcute. Disrupted.	Flood basalts	Sub-aerial
Outer SDR	Wedge	Top: High amplitude, smooth Bottom: not visible	Divergent-arcute or planar.	Flood Basalts	Deep marine
Outer High	Mound	Top: High amplitude Bottom: not visible	Chaotic	Volcanoclastic	Shallow marine

Table 1. Dominant features of the main volcanic extrusive facies units. Modified from Planke et al. (2000), Planke and Alvestad (1999) and Berndt et al. (2001).

Lanward Flows: The Landward flows are flood basalts deposited sub-aerially (see figure 7).The top reflector in the seismic image is characterized by a strong, fairly smooth event. The external shape is like sheets and the internal reflections are disrupted or hummocky and subparallel (Planke et al., 2000).

Lava Delta: The Lava delta flows are massive fragmented basalts and volcano-clastic material (Planke et al., 2000). It has high amplitude in the top and truncations in the top and bottom reflections.

Inner Flows: The top reflection shows high amplitude disrupted event, and the base has weak negative polarity difficult to identify. The inner Flows have externally a sheet shape (Planke et al., 2000).

Inner SDR: The inner SDR consist in flood basalt, filling space accommodation created by subsidence (Berndt et al., 2001).The top reflection is strong, and it has a wedge shape (Planke et al., 2000).

Outer high: The Outer highs are build-up volcanoclastic structures in shallow marine enviroments (Berndt et al., 2001). The shape of these extrusive flows is like a mound, with high amplitude top reflection (Planke et al., 2000).

Outer SDR: The Outer SDR are deep marine volcanic flows caused by massive volcanism in the sea floor. Consist of pillows and flood basalts with interbedded sediments. It is characterized by strong reflections on top and a shape-wedge (Planke et al., 2000).
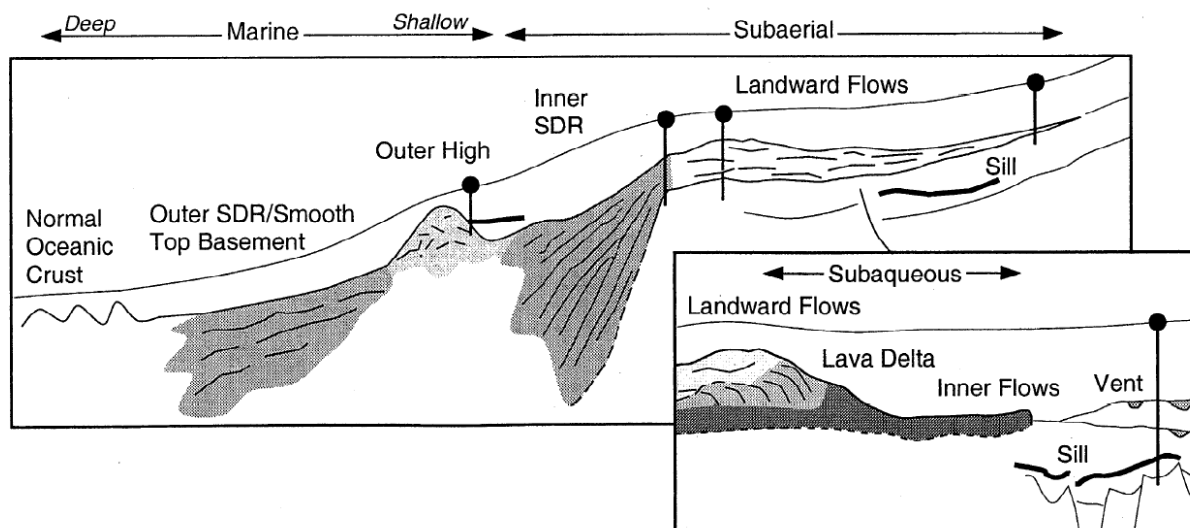
Figure 7.Schematic passive volcanic margin showing the main extrusive seismic sequences. Four main sequences and additional facies appears in the picture: Landward flows and Inner SDR (sub-aerial environment); Outer high, inner flows and lava Flows (shallow marine / subaqueous); Outer SDR (deep marine). (From Planke et al., 2000).

2.2. STRUCTURAL FEATURES AND DEVELOPMENT OF THE SOUTHWESTERN BARENTS SEA MARGIN

2.2.1.   STRUCTURAL DESCRIPTION OF THE WESTERN BARENTS SEA

Basins, highs and fracture zones in the western Barents Sea were formed in response to several phases of regional tectonism inside the North Atlantic- Artic region, concluding with continental separation of Eurasia and Greenland (Faleide et al., 1993a). According to Faleide et al., it is possible classified and describe the main structures of the western Barents Sea in the following way:

Oceanic basin: The Lofoten basin was developed during the Cenozoic sea floor spreading of the Norwegian-Greenlad Sea (Faleide et al., 1993a). Cenozoic uplift and erosion of the continental plate helped the development of oceanic basins and fans along the margin.

Continent-Ocean transition: Along the continent-ocean transition two main structures can be described: Fractures zones (Senja fracture zone in the south and Hornsund fracture zone in the north) and the Vestbakken volcanic province (Faleide et al., 1993a). The Vestbakken Volcanic Province is considered a mixture layer of mafic intrusions and continental crystalline blocks masking the continent, dominantly related to Paleocene-Early Eocene rifting event (Czuba et al., 2011).

Tertiary marginal basins: The Sørvestsnaget basin was developed during cretaceous crustal extension but was affected by major tectonism during Tertiary breakup (Faleide et al., 1993a). Cenozoic uplift probably induced by the continental breakup (Dimakis et al., 1998), caused a complex vertical motion, sedimentation and erosion (Faleide et al., 1993a). About 1km de Paleogene sediments were eroded and deposited in adjacent areas (Faleide et al., 1993a).

Cretaceous basins: Considerable crustal extension and thinning during middle Jurassic to early Cretaceous, led the creation of major cretaceous basins off mid Norway, East Greenland and the South Western Barents Sea (Harstad, Tromsø, Bjørnøya and Sørvestsnaget basins). These basins suffered rapid subsidence and segmentation into sub-basins and highs (Faleide et al., 2008).

Intra-basinal highs: The intra-basinal highs became in positive features inside the cretaceous basin province mainly by late cretaceous and early Tertiary faulting and differential subsidence. Examples: Loppa high, Stappen high, Veslemøy high, etc. (Faleide et al., 1993a).

Cretaceous boundary faults: The eastern boundary faults are mainly extensional in origin and were developed during Early Cretaceous times. Examples: Troms-Finmark Fault Complex and the Bjørnøyrenna Fault Complex. (Faleide et al., 1993a).

Eastern platform regions: The eastern region has acted as a large stable platform since late Paleozoic times. Includes the Finnmark platform, the Hammerfest and eastern Bjørnøya basins, and the Loppa high. Cretaceous tectonism was not a major event in this area (Faleide et al., 1993a).

2.2.2.   EVOLUTION OF THE WESTERN BARENTS SEA MARGIN

The Western Barents Sea margin was formed by early Cenozoic breakup and successive seafloor spreading of the Norwegian-Greenland Sea (Faleide et al., 1984). A succession of rifting events started to appears since Paleozoic and Mesozoic times, creating block-faulted basins like the Bjørnøya basin, Sørvestsnaget basin, etc. (Faleide et al., 1984).

The Western Barents Sea – Svalbard margin could be divided in two large shear segments and a central rifted margin (Faleide et al., 2008). The Senja Fracture Zone (SFZ) represents the southern shear segment described above. This Fracture zone is part of the De Geer mega-shear system, connecting previously the spreading ridge in the Northern Atlantic and the spreading ridge in the Artic (Faleide et al., 2008). The plate motion after the breakup originated a shear system along this previous connection between the Atlantic rift and the Artic rift system.
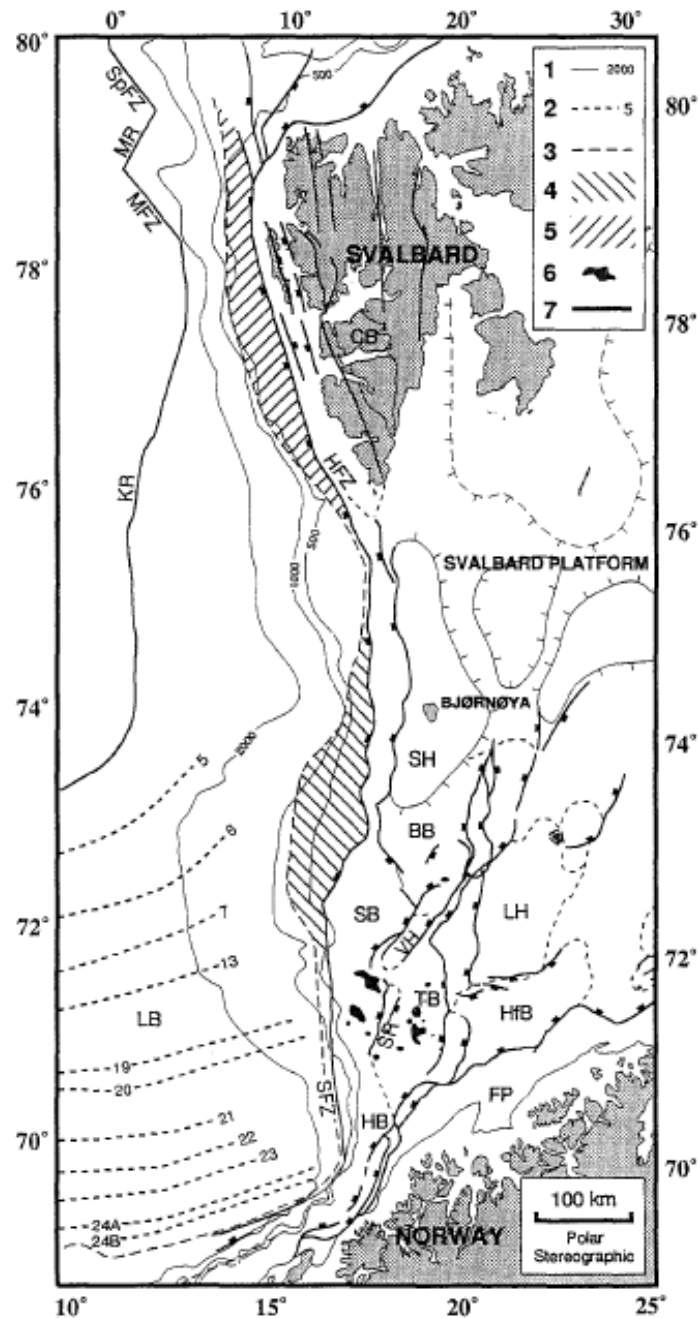
Figure 8. Map showing the main structural features in the western Barents Sea. 1= Bathymetry (m); 2 = magnetic lineations; 3= limit of identified oceanic crust in the seismic sections; 4= Vestbakken volcanic province; 5= Tertiary stretched continental crust; 6= salt ; 7= faults BB = Bjørnøya Basin; CB= Tertiary Central Basin (Spitsbergen); FP= Finnmark Platform; HB= Harstad Basin; HfB= Hammerfest Basin; HFZ= Hornsund Fault Zone; MFZ= Molloy Fracture Zone; MR= Molloy Ridge; SB= Sorvestsnaget Basin; SFZ= Senja Fracture Zone; SH= Stappen High; SR= Senja Ridge; TB= Tromsø Basin; VH= Veslemøy High .From Faleide et al. 1996.

The Vestbakken Volcanic Province is located at the rifted margin segment southwest of Bjørnøya. The continental breakup occurred in the transition between Paleocene and Eocene, originated volcanic activity in the Vestbakken Volcanic Province during Early Eocene. The continental margin north of Bjørnøya could be subdivided into three sheared segments (Faleide et al., 2008). During late Cenozoic the Barents Sea was uplifted and eroded. Several glacial cycles caused the major erosion of the strata, especially in the continental shelf.

Paleozoic to early cretaceous: During the Paleozoic and early Mesozoic times most of the Barents Sea was affected by crustal extension, generating block-faulted basins and high structures (Faleide et al., 1984). Major basins in the western Barents Sea were originated during late Jurassic- early cretaceous rifting: Bjørnøya basin, Sørvestsnaget basin, Tromsø basin, Harstad basin and Hammerfest basin. Basin subsidence coincided with widespread rifting in NE Atlantic and artic rift systems (Faleide et al., 1993a).

Late cretaceous to Eocene: In this final rifting phase started the continental breakup and seafloor spreading. The period after continental breakup was characterized by the change from extensional regime to shear regime (Faleide et al., 2008). The De Geer shear zone is a transcurrent transform system connecting the Atlantic and artic rifting regions, prior to the continental breakup (see figure 9). Pull-apart basins were generated by this change to shear regime.

Eocene to recent times: The continental breakup originated volcanic activity in the Vestbakken Volcanic Province during Early Eocene. After Oligocene, the Barents shelf became tectonically stable (Faleide et al., 2008). Isostatic uplift of the Barents shelf came after continental breakup (see figure 11), probably as a tectonic response (Dimakis et al., 1998). During late Cenozoic the continental margin changes from a shear regime to a passive regime. Several glacial cycles caused major erosion during late Cenozoic times.

2.2.3.   GLACIAL HISTORY IN THE BARENTS SEA

The Western Barents Sea margin is considered a glacial margin that periodically has been affected by grounded ice sheets on the continental shelf (figure 10). According to Faleide et al., 1996, the stratigraphy of the glacigenic sediments of the Western Barents Sea could be divided in three big sedimentary units (GI, GII and GIII), where GI is the oldest, and GIII the youngest. Within these units, seven main reflectors have been identified.
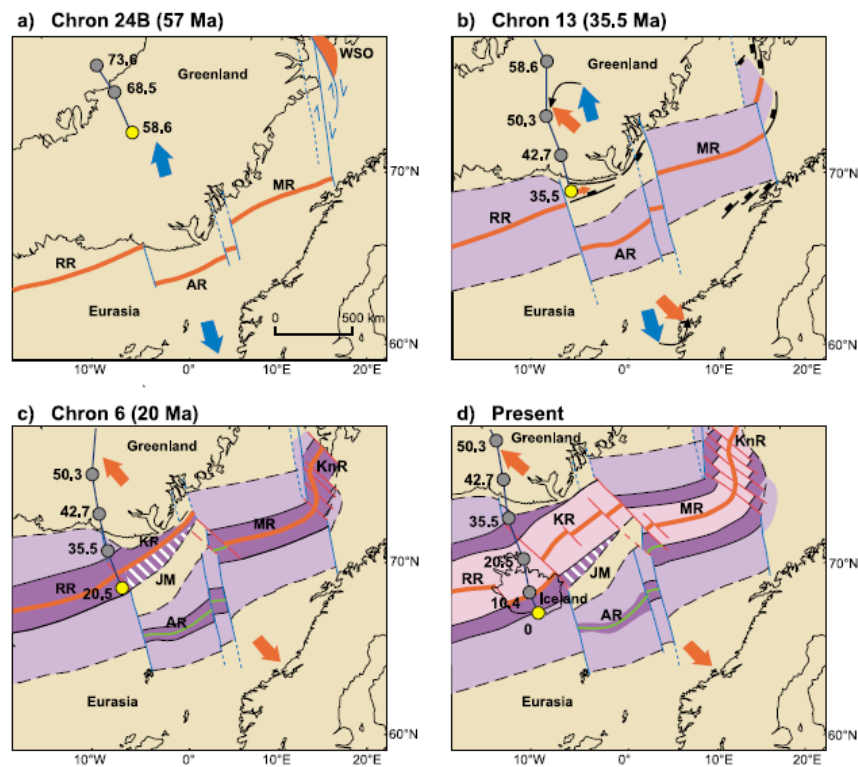
Figure 9. Tectonic of the Norwegian-Greenland Sea. a) Initiation of seafloor spreading. Blue arrows indicated the relative plate motion. De Geer shear zone is indicated in blue lines. b) Main plate reorganization and change in relative motion (from blue to red arrows). c) Separation of the Jan Mayen microcontinent from Greenland by northward movement of the Kolbeinsey Ridge (KR). d) Actual plate configuration. Yellow dots: approx. position of Iceland plume center. Grey dots: previous positions. MR= Mohns Ridge; RR= Reykjanes Ridge; KR=Kolbeinsey Ridge; AR= Aegir Ridge; KnR= Knipovich Ridge; JM= Jan Mayen; WSO= West Spitsbergen orogeny. From Lundin et al, 2002.
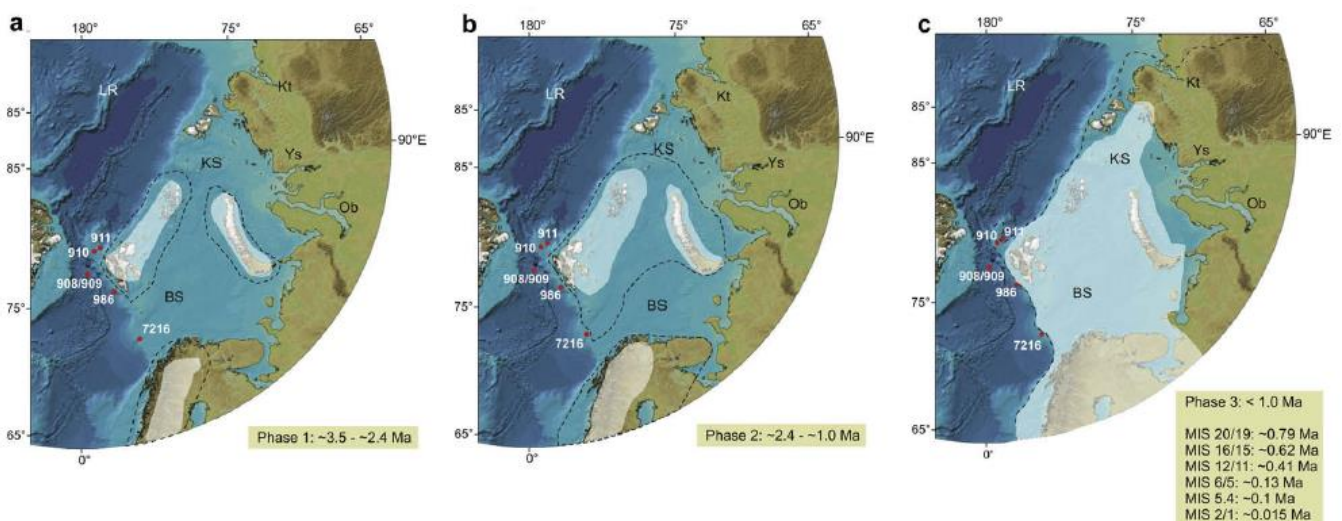
Figure 10. Extension phases of the glaciers during Pliocene-Pleistocene epochs, according to Knies et al. Striped line represents maximum extension, white areas represents minimum extension. Modified from Knies et al., 2009.
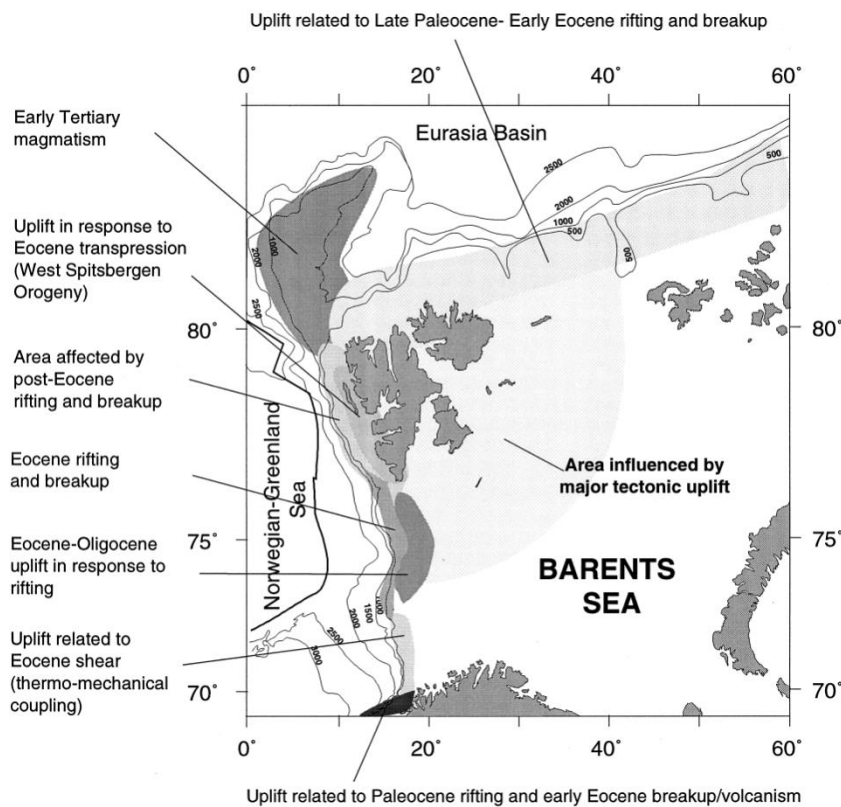
Figure 11. Area influenced by tectonic uplift in the Barents Sea with a description of rifting and breakup stages along the margin. From Dimakis et al., 1998.

The name of these reflectors are R1 through R7, where R1 is the youngest (Faleide et al., 1996, Dimakis et al., 1998). Depositions of glacigenic sediments were dominant since 2.3 Ma ago. The reflector R7 is the base of the western margin trough mouth fans (Faleide et al., 1996).

An initial phase of the glaciation (3.5-2.4 Ma), glaciers would be limited to Svalbard, New Zembla and northern parts of the Barents Sea. The rest of the Barents Sea would be sub-aerially exposed to erosion between 3.5 and 2.4 Ma (Knies et al., 2009)**.** Around 2.7 Ma ago, a period of ice growth on the uplifted Barents Sea beyond the coastline (Knies et al., 2009) is suggested by the glacial intensification in the Atlantic region and a distinct supply of IRD-rich sediments in the Yermak Plateau (2.7 and 2.4 Ma), see Figure 10, part a.

The transition phase (2.4-1.0 Ma) began with a partial fragmentation of the outermost ice margins leading to a more stable position at the coastline. During this phase, a terrestrial glacial build up is inferred by low smectite values along the western Barents Sea and the occurrence of turbidites and debris flows (Knies et al., 2009).
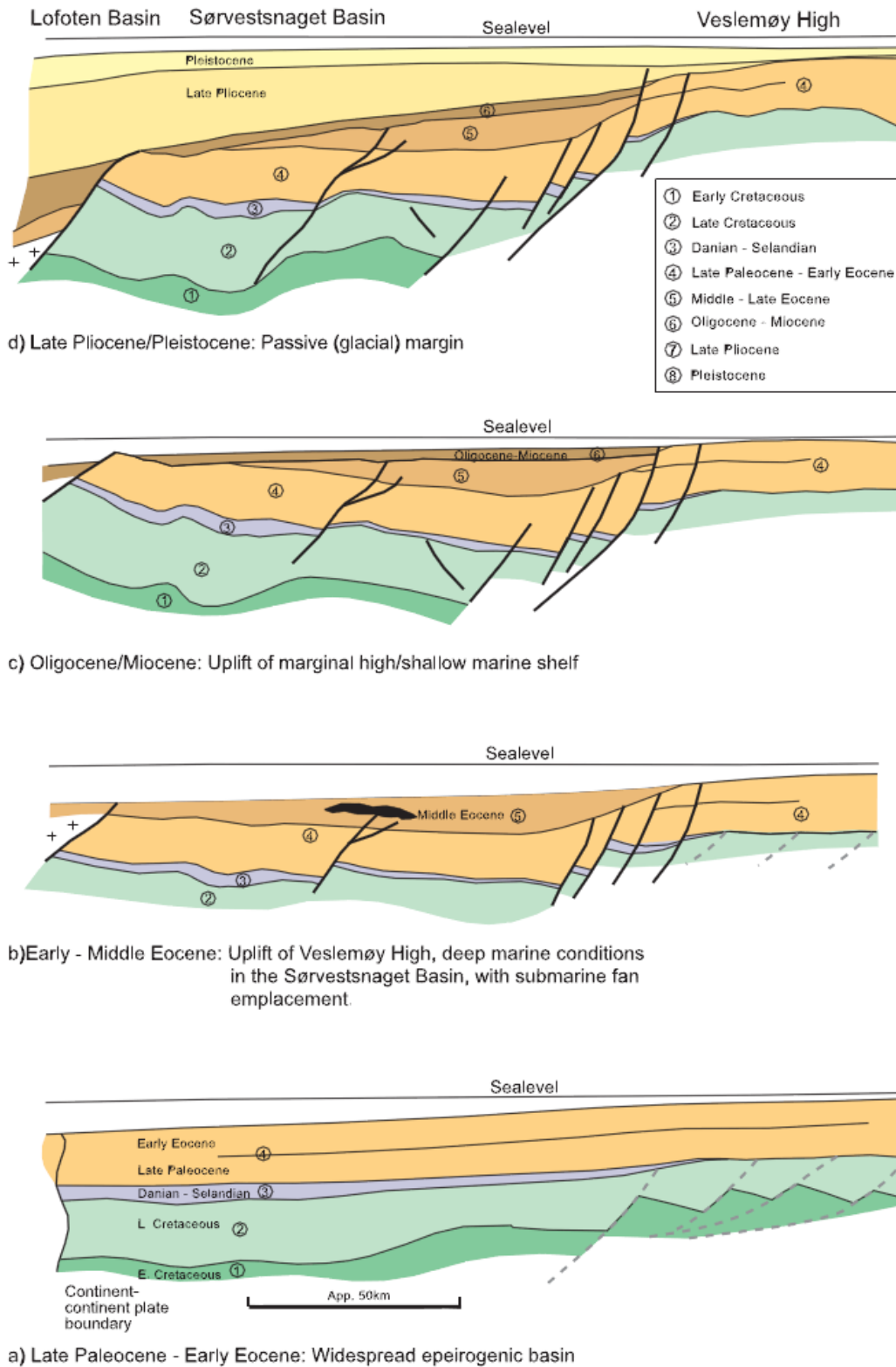
Figure 12. Evolution of the Sørvestsnaget basin and the Veslemøy high. (a) Pre-breakup setting; (b) breakup and beginning of the uplift induced by this tectonic event; (c) Oligocene/Miocene uplift and subsidence in Sørvestsnaget basin. (d) Final stage, passive margin. From Ryseth et al., 2003.

The final phase started around 1.0 Ma, it was characterized by glacial expansion through all the Barents Sea. This glacial activity generated massive erosion, in Svalbard and the Svalbard platform the erosion was between 2-3 kilometers and around 1-2 kilometers in the south of Bjørnøya (Dimakis et al., 1998). These sediments caused by glacial erosion were deposited along the continental margin, creating major fans (see figure 13 and 14) along the margin (Dimakis et al., 1998). Bjørnøya fan and Storfjorden fan are major prograding wedges, where the volume of the glacinetic sediments in each fan have been estimated around 395,000 km^3 (Bjørnøya fan) and 116,000 km^3 (Storfjorden fan) (Dahlgren et al., 2005).
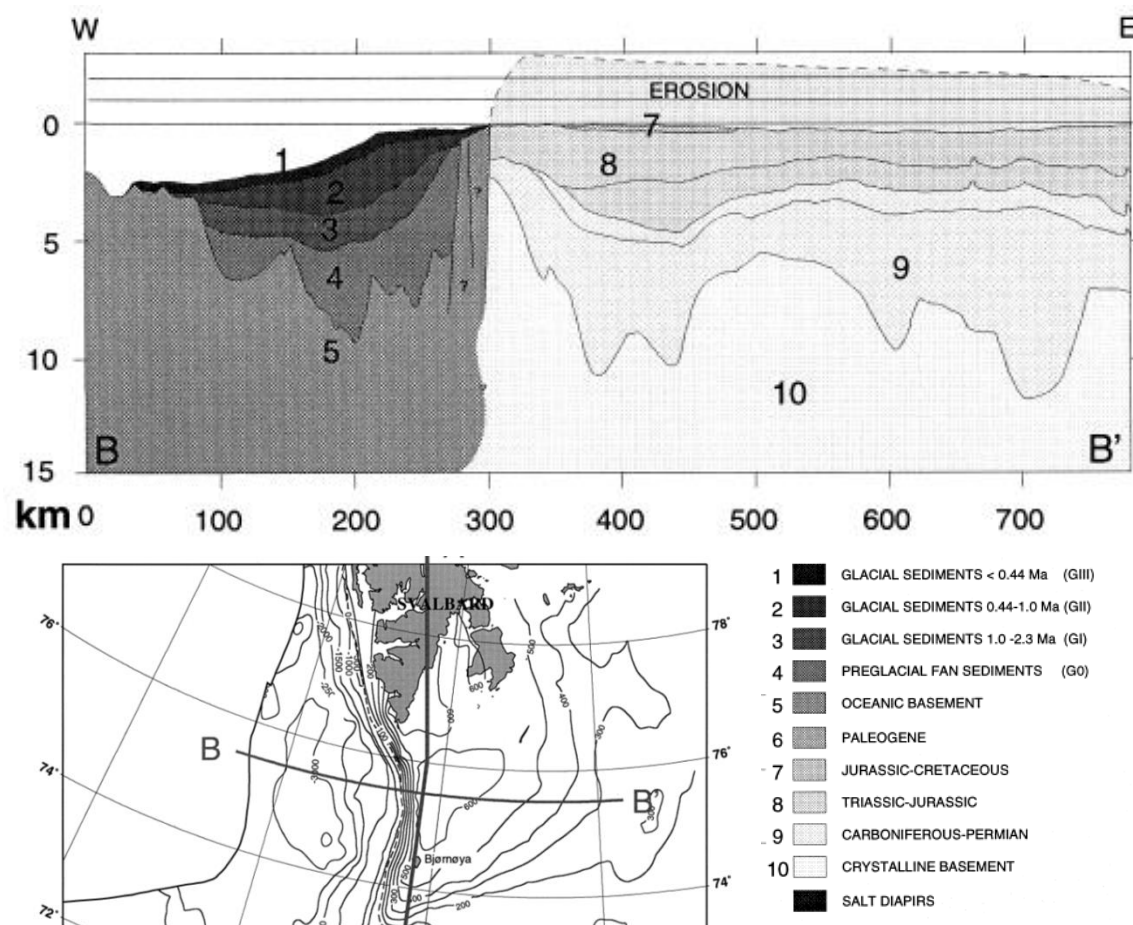
Figure 13. Profile of western Barents Sea margin, north Bjørnøya. The stratigraphy of the glacigenic sediments of the Western Barents Sea could be divided in three big sedimentary units (GI, GII and GIII), where GI is the oldest, and GIII the youngest. Modified from Dimakis et al., 1998.

2.2.4.   CENOZOIC STRATIGRAPHY IN THE WESTERN BARENTS SEA

The Sotbakken Group is dominated by claystone with minor amount of siltstone and carbonate horizons. The basal contact of Sotbakken Group is characterized by an unconformity between the latest Cretaceous and early Paleocene. The age of the Group is suggested to be late Paleocene to early- middle Eocene. Only one formation could be recognized in this group (Norwegian Petroleum Directorate).

The Torsk Formation is composed by light to medium grey non-calcareous claystone, in some cases there are evidence of siltstone and limestone in the formation. Volcanic horizons could be observed in the lower part of the unit. The formation is deposited under open to deep marine shelf environment and the age is suggested to be late Paleocene to Oligocene (Norwegian Petroleum Directorate).

The sediments of these **prograding wedges** along the margin are related to the composition of the hinterland. In the Barents Sea, the hinterland consisted mostly of sedimentary rocks deposited in times before Cenozoic uplift and erosion. The main constituent of these wedges are glacigenic debris flows composed of diamictons, interbedded with slide debris and hemipelagic marine and glacimarine sediments (Dahlgren et al., 2005).

Glacial diamictons consists of a wide range of non-sorted to poorly terrigenous sediments, with glacial erosion origin. In general, the matrix of the glacigenic-diamictons comprises 10–40% sand and the rest are equal amounts of silt and clay (Dahlgren et al., 2005).

The Nordland Group consists of 'sand and clays grade into sandstones and claystones, the sand content increasing upwards. Granite and different metamorphic rocks are found with clay in the upper parts of the group. The clay is grey to greyish green, blocky, non-calcareous, and in some parts silty (Norwegian Petroleum Directorate).
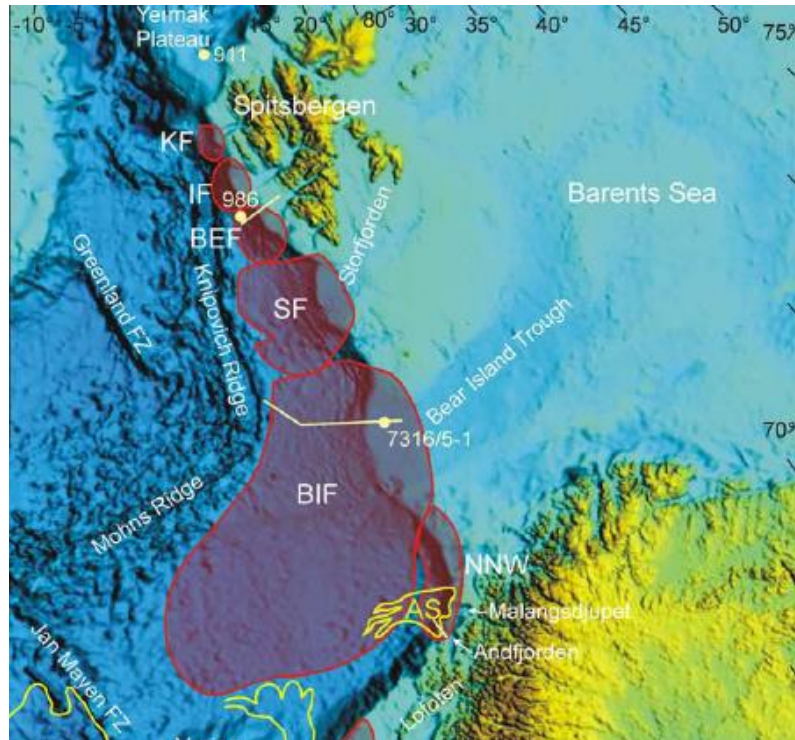
Figure 14. Extension of the sedimentary fans in the western Barents Sea margin. BEF: Bellsund fan. BIF: Bear Island Fan or Bjørnøya fan. IF: Isfjorden fan. KF: Kongsfjorden fan. SF: Storfjorden fan. Modified from Dahlgren et al., 2005.

The Nygrunnen Group consists of greenish to grey claystones with thin limestone intervals in the Tromsø Basin and western parts of the Hammerfest Basin. The Kveit formation is one of the formation presents in this group. It is formed by Greenish-grey to grey shales and shows thin interbreeds of limestone and siltstone (Norwegian Petroleum directorate).
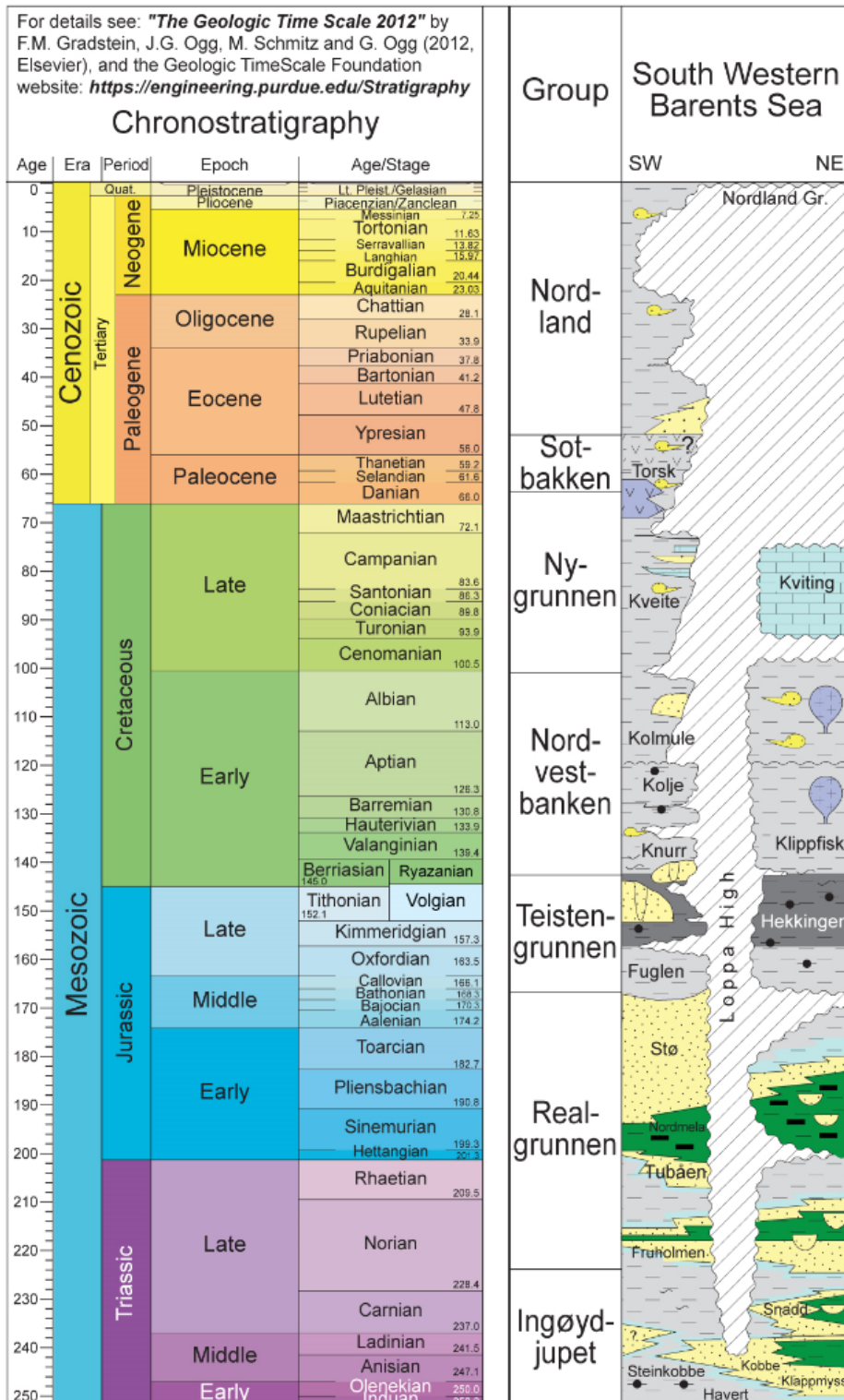
Figure 15.Litoestraigtraphic summary of the South Western Barents Sea. Modified from the Norwegian Stratigraphic Lexicon, Natural history museum – Oslo (Nhm2).

3. DATA AND METHODOLOGY

The data available for this study consisted in 7 seismic lines and 2 wells. Six seismic lines (five E-W direction and one N-S direction) correspond to the seismic acquisition set NPD-BJV2, realized by the Norwegian Petroleum Directorate in 1986 over the Bjørnøya west quadrant (Bjørnøya Vest 2). One seismic line correspond to the seismic acquisition set NPD-BJV1, also realized by the Norwegian Petroleum Directorate in 1986 over the Bjørnøya west quadrant (Bjørnøya Vest 1). There is also a well (7316/5-1) tie to one seismic line and other well (7216/11-1) used for check the uplift estimation.
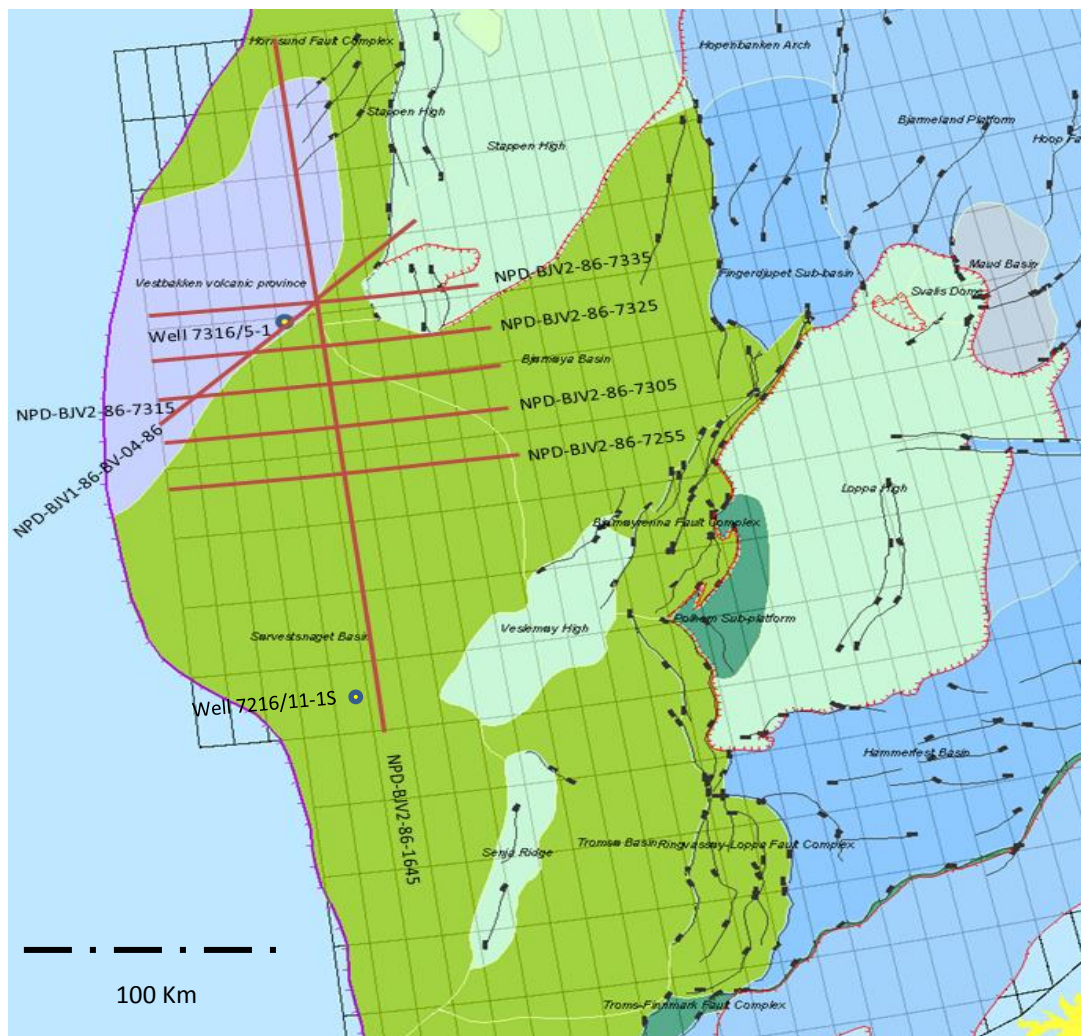
Figure 16.Location of the seismic lines over the main structural features in the western Barents Sea. Seven seismic lines over the Vestbakken volcanic province and the Sørvestsnaget basin were used in this study. Modified from NPD (fact map).

Line	Coordinates (min, max)
NPD-BJV2-86-7255	(72°46'55''N,14°56'53''E),(73°03'9''N,18°33'4''E)
NPD-BJV2-86-7305	(72°56'59''N,14°56'39''E),(73°13'5''N,18°33'7''E)
NPD-BJV2-86-7315	(73°07'3''N,14°56'53''E),(73°23'1''N,18°33'8''E)
NPD-BJV2-86-7325	(73°17'7''N,14°56'51''E),(73°32'9''N,18°33'9''E)
NPD-BJV2-86-7335	(73°27'13''N,14°56'49''E),(73°42'5''N,18°32'40''E)
NPD-BJV2-86-1605	(71°59'5''N,15°40'43''E),(74°33'55''N,17°59'15''E)
NPD-BJV1-86-BV-04-86	(73°06'14''N, 14°53'7''E),(73°53'9''N, 17°48'38''E)

Table 2. Minimum and maximum coordinates of the seismic lines.

3.1. SEISMIC DATA QUALITY

3.1.1.   POLARITY

Check the sea bottom reflection is a good indicator to determinate the phase and the standard polarity used during the seismic acquisition. The American standard consists in obtain a peak (blue) when there is an increase of impedance while the European standard consists in obtain a trough (red) when there is an increase of impedance. According to our data, the seismic study shows a trough in the sea bottom reflection (increase of impedance). Based on this is possible affirm that the European standard have been used (see figure 17).
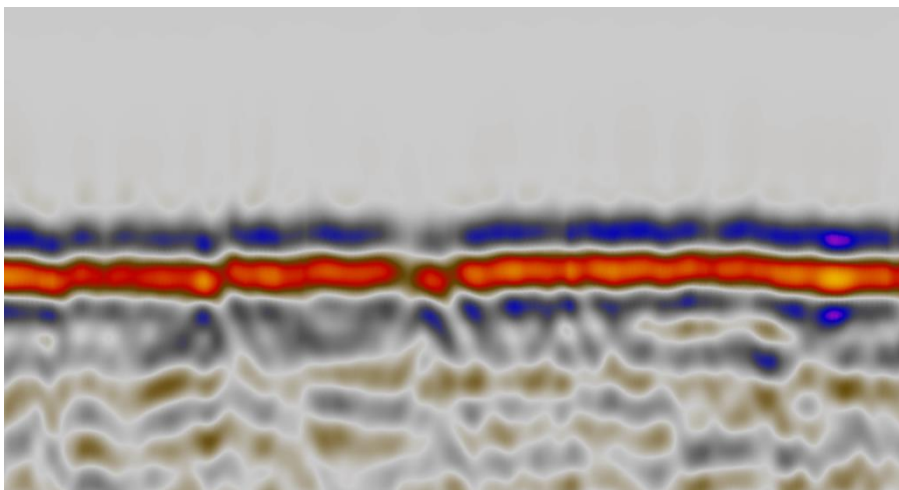
Figure 17.Sea Bottom reflection from one of the seismic lines. Blue sidelobes represent negative amplitude, red peak represent positive amplitude. The seismic shows zero phase and the European standard polarity.

The Zero phase appears in this seismic image, that means two negative sidelobes with a positive amplitude peak in the middle when there is an increase of impedance and is use the European standard (see figure 17, with the sea bottom as example).

3.1.2.   SEISMIC RESOLUTION

With increasing depth the signal frequency will decrease while the velocity and wavelength increase, resulting in poor resolution. The high frequencies are loss in shallower areas, while the lower frequencies reach deeper areas. With increasing depth the sediments are gradually more compacted and therefore the signal velocity increase with depth. The vertical resolution is derived from the wave length and two different layers cannot be differentiated when their thickness is below ¼ of the wavelength. When referring to vertical resolution, it is normally the ¼ wavelength (Brown, 1999).

$$R = \frac{\lambda}{4} \text{ (minimum vertical thickness resolution)}$$

Where λ is the wavelength of the seismic waves and depends of the media velocity (λ= v/f, V=velocity and f= frequency). Assuming a fundamental frequency around 20-50 Hz and the velocity of one layer around 2000 m/s, is possible infer the resolution between 8 m (for 50 Hz) and 25 m (For 20 Hz).

3.2. INTERPRETATION METHODOLOGY

The main objective of this project consist in understand the geological history of the area and built a geological model, focused in the Cenozoic uplift and consequences in the southwestern Barents Sea margin. The methodology applied in this study could be summarized in four stages:

First Stage: Seismic well tie and interpretation of the main line (NPD-BJV1-86-BV-04-86). The correlation of the main lithological packages and the reflectors was possible with the seismic-well tie. The age of the reflectors and seismic packages was possible to determinate with the well correlation and using previous studies from this well.

Second Stage: Correlation of the seismic horizons from the base line with the reflector of the other lines (BJV2 set). Based in the main line, the next step consisted in follow the reflector through all the seismic lines, primary in the lines crossed by the base line.

Third Stage: Building the final Interpretation map and TWT maps. After interpreted the main horizons through all the seismic lines, the next step consisted in build two way travel time maps and the final interpretation map with the main structural features (extension of the Vestbakken Volcanic Province, Location of the main faults and group of faults, location and extension of the basin and sub-basin in the area, main erosional surfaces, etc.).

Four Stage: Estimation of the uplift based in the depth-porosity trends. To have another estimation of the Cenozoic uplift in the area, it was proposed this method that use empirical formulas and the well logs available in this study.

To present the results, it was follow the next format:

1. Observations: description of the main seismic patterns, terminations, discontinuities and other relevant seismic features in the image. Usually was necessary take sub-sections from the main image and then get details of the main characteristics in the seismic line.
2. Interpretation and Geological history, build a geological model based in the interpretation of the seismic lines. Using previous studies in the area, it was suggested a geological history for each line, according to the regional studies and particular features of each line. In the results sections, it was decided show two images: one with the seismic image including main interpreted horizons and faults and other image showing an sketch of the geological model.
3. Presentation of the TWT maps and final interpretation map. Finally it was estimated the uplift using the depth-porosity trends.

3.3. WELL DATA

The Well 7316/5-1 is the only deep well in the Vestbakken Volcanic Province. It was drilled as a wildcat exploration well by Norsk Hydro (operator) in 1986. The well has coordinates 73 ° 31'11.89'' N, 16 °25'59.6'' E and is intersected by the seismic line NPD-BJV1-86-BV-04-

86. Drilling started on the 21st of July 1992 and ended the 5th of October of the same year. The well is located about 150 km southwest of Bjørnøya, over the Vestbakken volcanic province (Norwegian Petroleum Directorate).

The main objective of the well was evaluated the potential of Tertiary prospects at lower Oligocene and upper Eocene levels. The well is 4027 m deep and penetrates the Nordland Group (Pleistocene-Pliocene), the Sotbakken Group (Lower Miocene- Early Eocene) and the Nygrunnen Group (Cretaceous). Other objective in the drilling of this well consisted in undertake a sampling and coring program to improved stratigraphic control in the area (Semple and Bulma, 1993).

A second well, 7216/11-1S was used for check the uplift estimation in the well 7316/5-1. It was drilled as a wildcat exploration well by Norsk Hydro (operator) in 2000. The objective for well 7216/11-1 S consisted in proves the hydrocarbon potential over the Sørvestsnaget basin. Three target horizons were defined in the lower Torsk formation. The well has coordinates 72°0'56.72'' N, 16 °36'22'' E, and drilling started on the 24st of July 2000 and ended the 14th of September 2002 (Norwegian Petroleum Directorate).

Log type	Log top depth [m]	Log bottom depth [m]
CST - TLC	1440	2686
CST - WIRELINE	2570	2750
MDT	1435	1586
MWD MPR - GR RES DIR	386	4239
MWD ORD/CNN - SON DENS POR	2758	4239
PEX DSI SP	999	2752
SWC	1390	2750
VSP	1100	2750

Table 3. Wireline logs in the Well 7216/11-S with the interval measurements. From the Norwegian Petroleum Directorate.

Log type	Log top depth [m]	Log bottom depth [m]
CBL VDL	830	1500
CST GR	467	843
CST GR	562	842
CST GR	885	2900
CST GR	948	2908
CST GR	2974	3290
CST GR	2974	3448
CST GR	3453	4025
DIL LSS GR	876	2933
DIL LSS LDL CNL GR SP AMS	562	638
DIL LSS LDL CNL GR SP AMS	569	873
DLL MSFL LDL CNL NGL AMS	876	1769
DLL MSFL LSS LDL CNL GR SP	2957	4029
FMS4 GR	876	2922
FMS4 GR	2957	4029
LDL CNL NGS	1725	2915
MWD – DPR GR DIR	561	613
MWD – GR RES DIR	473	4027
RFT HP GR	1340	1377
VSP	520	2960
VSP	1900	4020

Table 4. Wireline logs in the Well 7316/5-1 with the interval measurements. From the Norwegian Petroleum Directorate.

3.3.1.   SEISMIC WELL TIE

The seismic well tie is an important tool to correlate seismic reflections with the main geological intervals obtained from well. Using the seismic tie to well is possible have a more precise model and to obtain a better understanding of the entire image. The Seismic Tie to well consists mainly in 3 steps: Seismic-well calibration (with check-shots), generation of the synthetic seismogram (sonic and density logs), and finally integrated the seismic well tie with the real data.

1. Selection of the well and check-shot available for the calibration.
2. Selection of the sonic log (DT) and density log (RHOB) available in the well.
3. Creation of the acoustic impedance curve (AI) using the density log and sonic log.
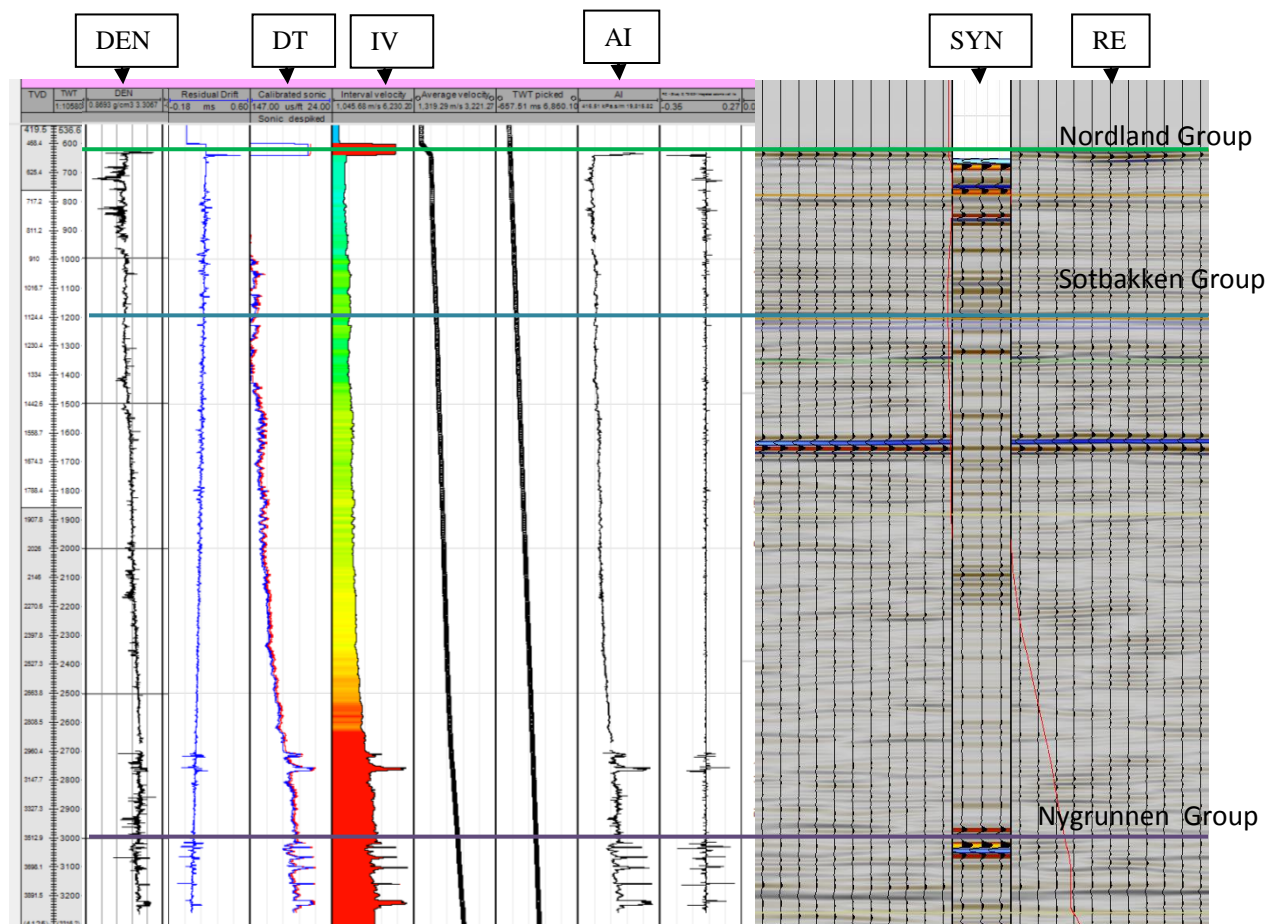
Figure 18. Seismic tie to well 7316/5-1. The three lithological groups founded in the well are marked: Nordland group, Sotbakken group and Nygrunnen group. DEN= density log, DT= Sonic log, IV= Interval Velocity, AI= Acoustic Impedance curve, SYN= Synthetic seismogram, RE= Real seismic data.

Epoch	Group	Top MD (m)
Pleistocene-Pliocene	Nordland Group	475 m (below sea bottom)
Lower Miocene-Early Eocene	Sotbakken Group (Torsk Formation)	948 m
Early Eocene-Cretaceous	Nygrunnen Group (Kveite Formation)	3745 m
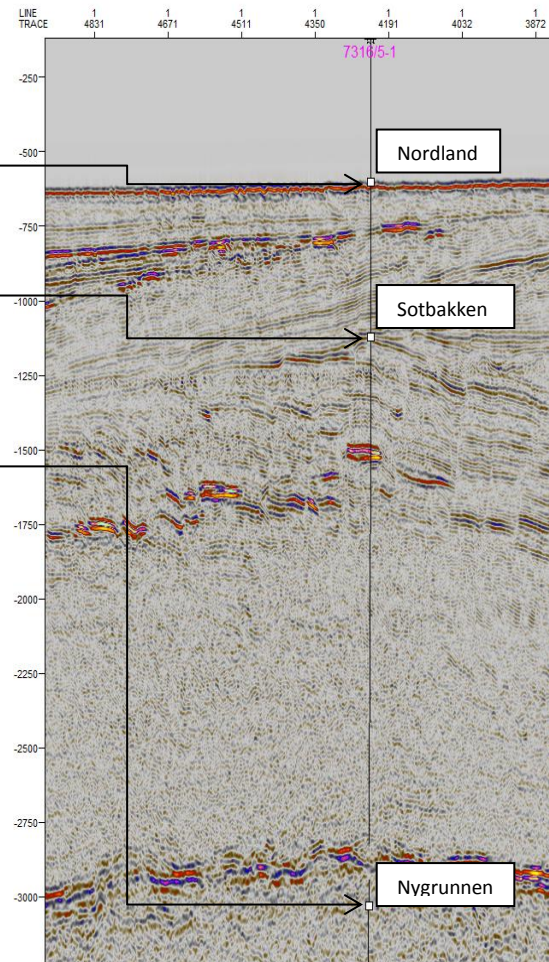
Figure 19.Seismic Tie to well 7316/5-1. The Lithological intervals are based in the well study from Eidvin et al, 1998. With the seismic well tie was possible recognize the reflections related to the top of the main lithological groups.

4. A wavelet is selected to build the synthetic seismogram (Ricker Wavelet) and then this seismogram is displayed together with the seismic image (see figure 18).

5. After some adjustment in the synthetic seismogram, the geological tops were correlated with the reflectors in the seismic. In this step was necessary previous geological information to adjust properly the lithology and age of main reflection.

6. Manual calibration sometimes is necessary to improve the tie between the synthetic seismogram and the real data.

In figure 18 appears the obtained Acoustic Impedance curve (AI), the synthetic seismogram (SYN) and the correlation of the seismic with the tops identified in the well study. Despite the manual adjustment of the synthetic seismogram to improve the seismic-well correlation, there

are still evident differences between both traces. There are different reasons to explain this mismatch between both traces:

1. Deviation of the well 7316/5-1, mainly in the deeper parts (after 1600 m), creating problems in the seismic well correlation.

2. Real data contain "multiple energy" due to rebounds between reflectors within the earth. This creates extra reflections in the seismic images (Ewing, 2001)

3. The formations are anisotropic. In real seismic, the energy does not travel purely vertically, but has a horizontal component which increases at far offsets (Ewing, 2001)

4. Problems in the seismic velocity model, problems in the log-tool measurement, dispersion effect and other several causes can explain the mismatch between both traces (Ewing, 2001).

Epoch	Interval MD (m)
Pleistocene-Pliocene	477-948 m
Lower Miocene	948-960
Lower Miocene-Lower Oligocene	960-982
Lower Oligocene	982-1090
Middle Eocene	1090- 3745
Early Eocene – Paleocene	3745 and below
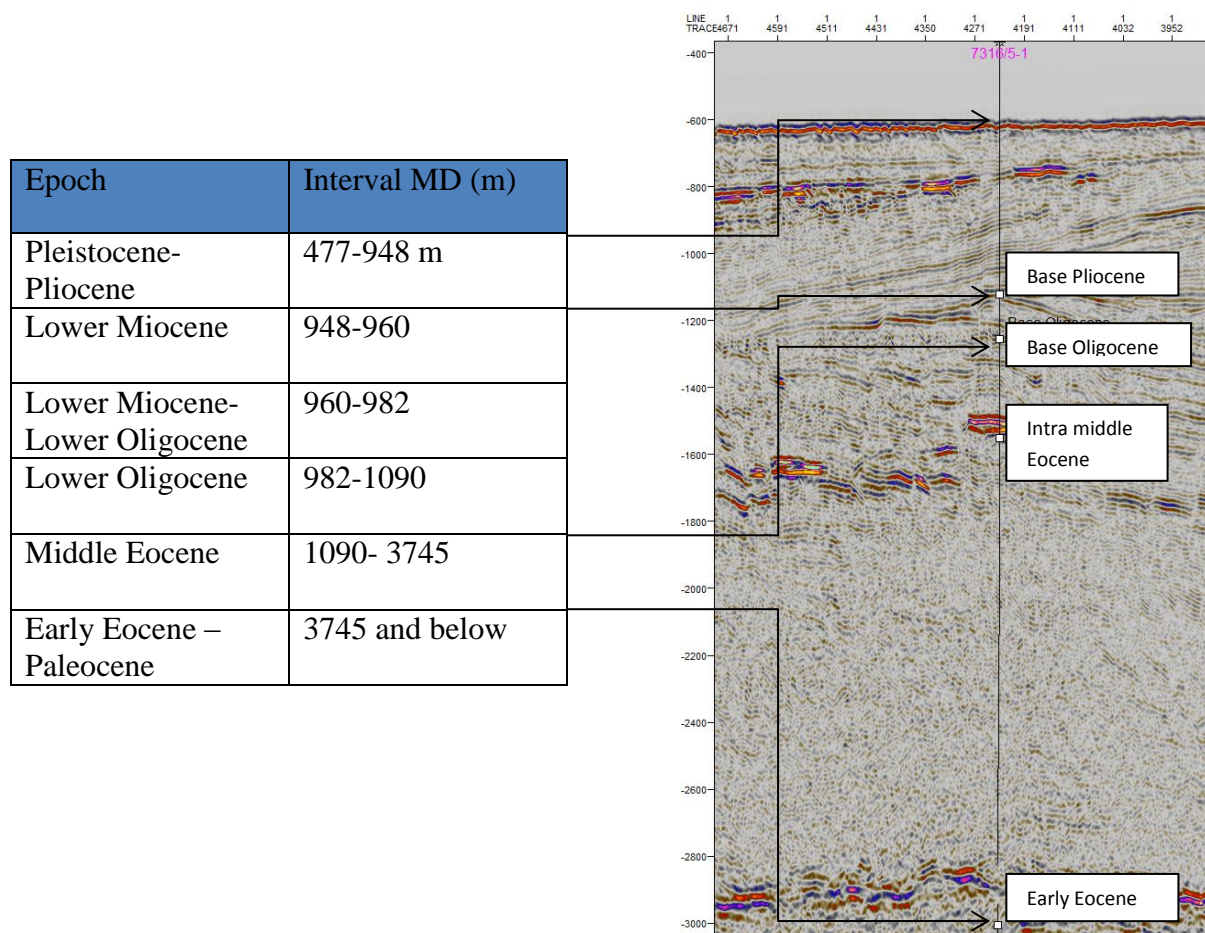
Figure 20. Seismic Tie to well 7316/5-1. The age interval is based in the well study from Eidvin et al., 1998.

Despite these problems, an accurate determination of the main reflections was possible. Previous studies of this well make possible the precise identification of the geological tops and the relation with the reflectors (Eidvin et al., 1998).

3.4. MODELING OF DEPTH-POROSITY TRENDS

3.4.1.   POROSITY DEPTH TRENDS

The decreasing of porosity rates for sands and shales trends is more rapid at shallow depths, and slows at greater depth of burial (Magara, 1980). At deposition, shales tend to have relatively high porosities compared with sands. Sands have depositional porosities around 40% and in shales could be higher than 80 % (Avseth et al., 2005) as shown in Figure 21.This has been observed by other authors who have proposed a different number of compaction curves for sandstones and shales (Magara, 1980; Ramm and Bjørlykee, 1994).

Ramm and Bjørlykke proposed a clay-dependent exponential regression model for porosity versus depth of sands, valid only for mechanical compaction:

$$\varphi = Ae^{-(\alpha+\beta.C1)Z} \text{ (Ramm and Bjørlykke model)}$$

Where φ is porosity, Z is depth, and A, α and β are regression coefficients. A is related to initial porosity at zero burial depth, α is a framework grain stability factor for clean sandstones (C1=0), and β is a factor describing the sensitivity towards increasing clay index. The clay index is defined as the volume content of total clays (V_{C1}) relative to the total volume content of stale framework grains (assuming grain of quartz V_{Qz}):

$$C1 = \frac{V_{C1}}{V_{Qz}} \text{ (clay Index)}$$

There are at least 3 stages in the compaction of shales and sands: Depositional stage, mechanical stage and chemical compaction stage (Avseth et al., 2005, see figure 21). In the estimation of the uplift, only were applied the formulas at intervals into this stage of mechanical compaction.
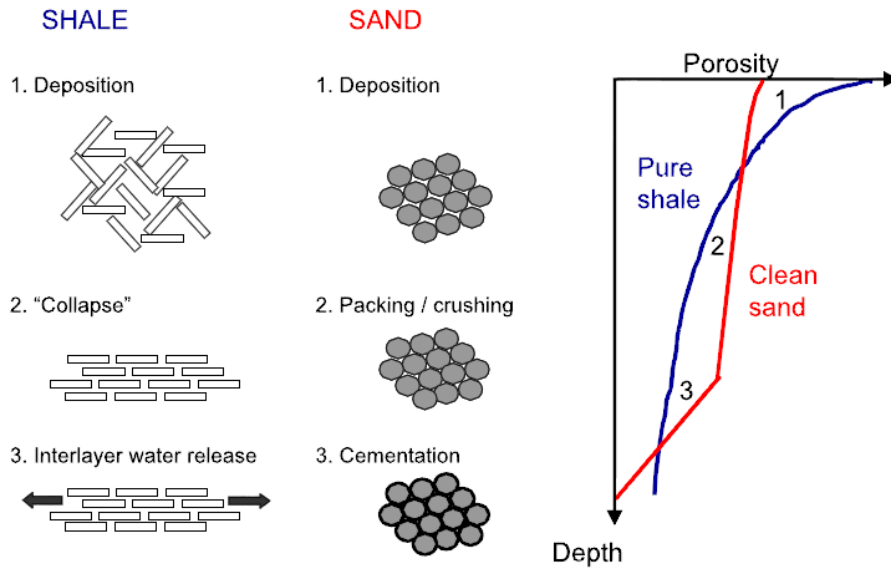
Figure 21.Illustration of porosity-depth trends for sand and shales (From Avseth et al., 2005). (1) Porosity gradient during depositional porosity stage; (2) Porosity gradient during mechanical compaction stage; (3) Porosity gradient during chemical compaction. The interval used for the estimation of the uplift is exclusively in the mechanical compaction stage (2).

3.4.2.   UPLIFT ESTIMATION USING DEPTH-POROSITY TRENDS

Using empirical porosity-depth curves from North Sea (Avseth et al., 2005), it was possible create an empirical gradient of the porosity versus depth. In other hand, using the available well data, it was possible create a porosity curve obtained from the density log and estimating the matrix and fluid density (2.65 g/cc for matrix and 1.00 g/cc for fluid).

These empirical formulas from Avseth et al. (2005) are based in the models of Ramm and Bjørlykke (1994). According to Avseth et al. (2005) the general trend of porosity for shales and sandstones in the North Sea are estimated by the next formula:

$$\varphi = 45e^{-(0.10+(0.27x0.1))Z} \text{ (formula for sandstones porosity)}$$

$$\varphi = 60e^{-(0.01+(0.22x2.0))Z} \text{ (formula for shale porosity)}$$

The Sands were calibrated with clean Heimdal formation sands at 2150-2160 m, and is supposed a critical porosity of A=45. Shales were calibrated with Lisa formation at 2140-2154m, and the critical porosity is A=60 (Avseth et al., 2005).The main assumption is that the shales or sandstones show porosities from bigger depths (higher compaction) because these

rocks were moved from depth areas to shallower during the uplift event. For that reason it was necessary change the value of Z to adjust the empirical curve from the density-porosity curve. The empirical gradient trend is close with the gradient trend given by the density porosity, for that reason was assumed that the parameters used by Avseth et al. (2005) are enough similar to use in this study (supposing the same regression coefficients α, β, and C1). The uplift estimation was applied in the available wells (7316/5-1 and 7216/11-1S), but getting different results due to the difference in the geological features between them.
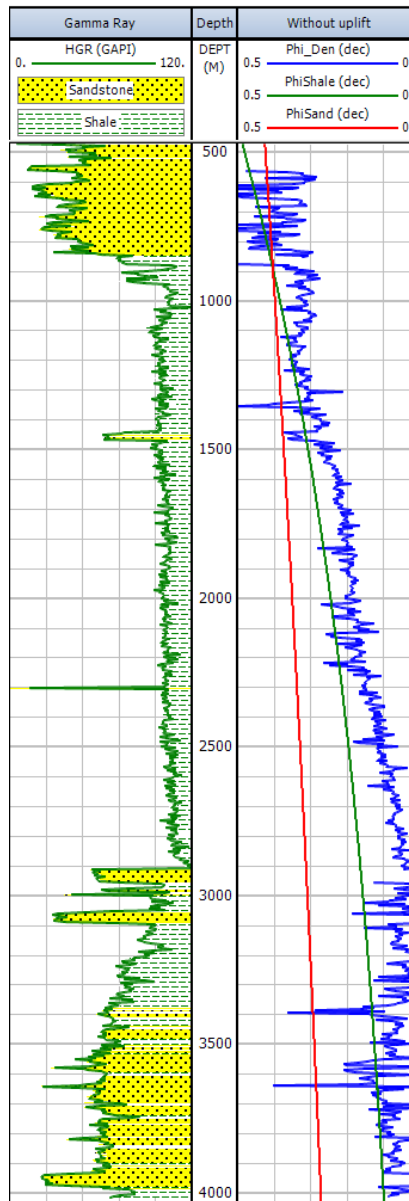
Figure 22.The Gamma Ray log shows the areas with dominant Shale and Sand formations. With blue line is represent the porosity-density curve, with red line the sand empirical porosity trend and with green line the shale empirical porosity trend.

4. RESULTS

In this chapter, it will be shown the most relevant sections of the seismic lines, their interpretations and proposed geological models. NPD-BJV1-86-BV-04-86 (The seismic line with SW-NE direction, see figure 23) was the first interpreted line, because it was tie with the only available well in the area (VVP). Based in this seismic line and detailed studies from this well, it was possible mark the main horizons and have an estimate age. These horizons were correlated with the rest of the seismic lines, primarily with the lines crossing this main line. Some horizons were not possible to follow through the other lines, and was necessary interpret these horizons visually, based in seismic patterns and terminations. It could be risky, but is part of the interpretation work.

The first step to study the main seismic line (NPD-BJV1-86-BV-04-86) was observed and described all the relevant seismic features, summarized in one table. The second step consisted in interpret the horizons and then built the geological model. Finally, is shown a table with a brief geological evolution according to the seismic image and well data. For the other seismic lines, the procedure was more or less the same: Observations, interpretation and geological model. It was no considered necessary repeat the tables, because there is a concordance with the main seismic line. Seismic patterns are more or less the same in all the seismic lines, and the geological history is common for all the area.

The geological history from the main seismic line will be the base to understand the other lines and the entire area. This seismic line is tie to the well 7316/5-1, which has been studied by other authors that have made a detailed description from this data.

The seismic lines extend over large distances and not all the seismic image has the same data quality. To solve this problem, only sections of these lines were shown and interpreted (see figure 23). These sections show the main features and the available information of the seismic lines. For more detailed features, it was necessary create subsections of the seismic lines, these are marked in the non-interpret image of the seismic profile.

The main focus of this thesis is looking for evidence of the late Cenozoic uplift along the southwestern Barents Sea margin. For this reason, it was necessary a detailed understanding of the geological events through the seismic images, since Paleocene times until Pleistocene

times. Find and describe main erosive truncations and other uplift generated structures, was the main purpose of this work.

A second well was used to check the estimated uplift value obtained by the first well. The well 7216/11-1S is over the Sørvestsnaget basin, located almost 100 km away from the studied area. This well is over a thicker section in the Bjørnøya fan (prograding wedge), and only the pre-glacial strata was founded in the deeper intervals of the well. This well was not intersected by any of the seismic lines, and for that reason was not possible applies the seismic well tie.
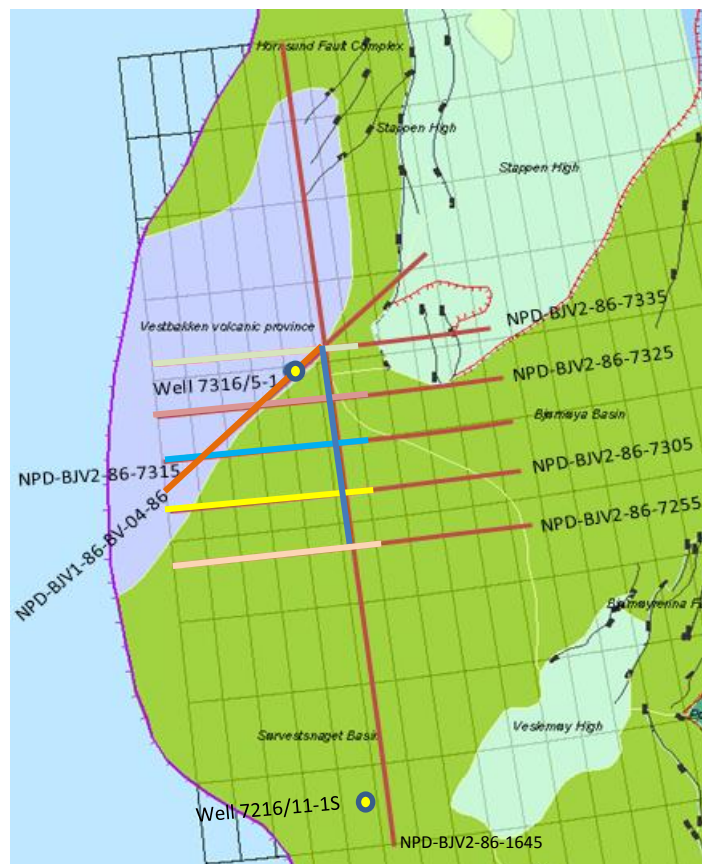
Figure 23. The colored sections inside the seismic lines, represents the detailed interpretation sections. The seismic lines and interpreted models present in the figures of this chapter were built based in these colored sections. Modified from NPD (Norwegian Petroleum Directorate, 2014).

4.1. NPD-BJV1-86-BV-04-86

The line NPD-BJV1-86-BV-04-86 is the only seismic line with SW-NE direction. This Line cross other four seismic lines (NPD-BJV2-86-1645, NPD-BJV2-86-7335, NPD-BJV2-7325, and NPD-BJV2-86-7315) and is tie to one well (well 7316/5-1). It could be considered the mainline, essential to interpret and build a regional model of this area. This is the main seismic line because is tie to a detailed studied well. The well 7316/5-1 and related studies give us the possibility of dating several reflectors and also built a proper history of the geological events during the Cenozoic, especially related to the uplift and erosion that affected a big portion of the southwestern Barents Sea margin.

The seismic line has a length of 110 km and was mainly interpreted 75 km (focused in the area with better resolution and the Vestbakken Volcanic Province, see figure 23 with the colored section). According to the structural maps of the area, this line is mainly over the Vestbakken Volcanic Province (see figure 23).

4.1.1. OBSERVATIONS

The seismic line NPD-BJV1-86-BV-04-86 (figure 26) shows a medium resolution. It is possible observe better resolution in shallower areas in comparison with deeper areas (mostly noisy). Three main characteristics distinguish this seismic line:

1. High Amplitude Reflectors (HAR) in deeper areas of the image, tilting to the west (sub-section 1, figure 24). These set of strong reflections create a mask over the underlayed strata. Beneath these high amplitude reflectors, the seismic shows a chaotic pattern with poor seismic resolution. HAR are possible to see in almost all the seismic lines, and it is associated with the Vestbakken Volcanic Province.

   The High Amplitude Reflections (HAR) show a reflection signature as two negatives amplitude sidelobes, with a positive amplitude peak in the middle like the sea bottom. This signature indicates a strong positive change of amplitude, because there is a

change from sedimentary rocks (lower acoustic impedance) to extrusive rocks (higher acoustic impedance).
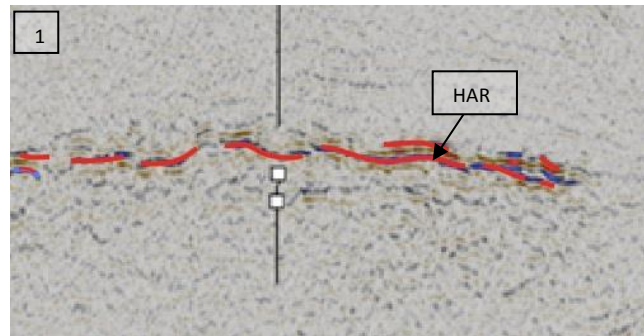
Figure 24. Sub-section 1 of the seismic line NPD-BJV1-86-BV-04-86 showing the high amplitude reflectors (HAR, marked with red lines), associated to extrusive activity.

2. A divergent pattern with a main discontinuity in the eastern side (sub-sections 2 and 3, Figure 25 and 26). This area shows several discontinuities in the reflections, probably associated with a fault setting. The divergent pattern in the east shows the location of the Western sub-basin and the main discontinuity marks the Eastern boundary fault. Between The HAR and the divergent patterns there are chaotic reflectors with really poor resolution that creates uncertainties in the interpretation.
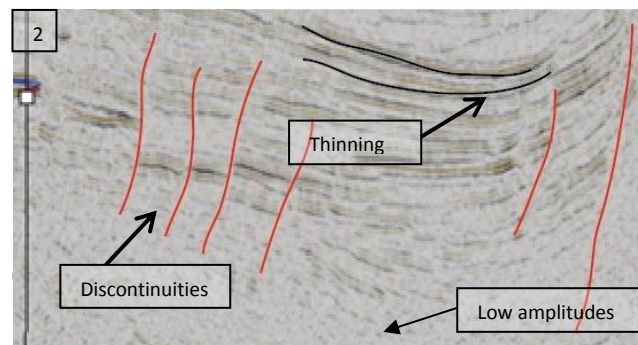
Figure 25. Sub-section 2 of the seismic line NPD-BJV1-86-BV-04-86. It is possible observe the divergent pattern from the western sub-basin, and associated discontinuities. This thinning in the packages is an evidence of subsidence and deformation due to faulting activity.
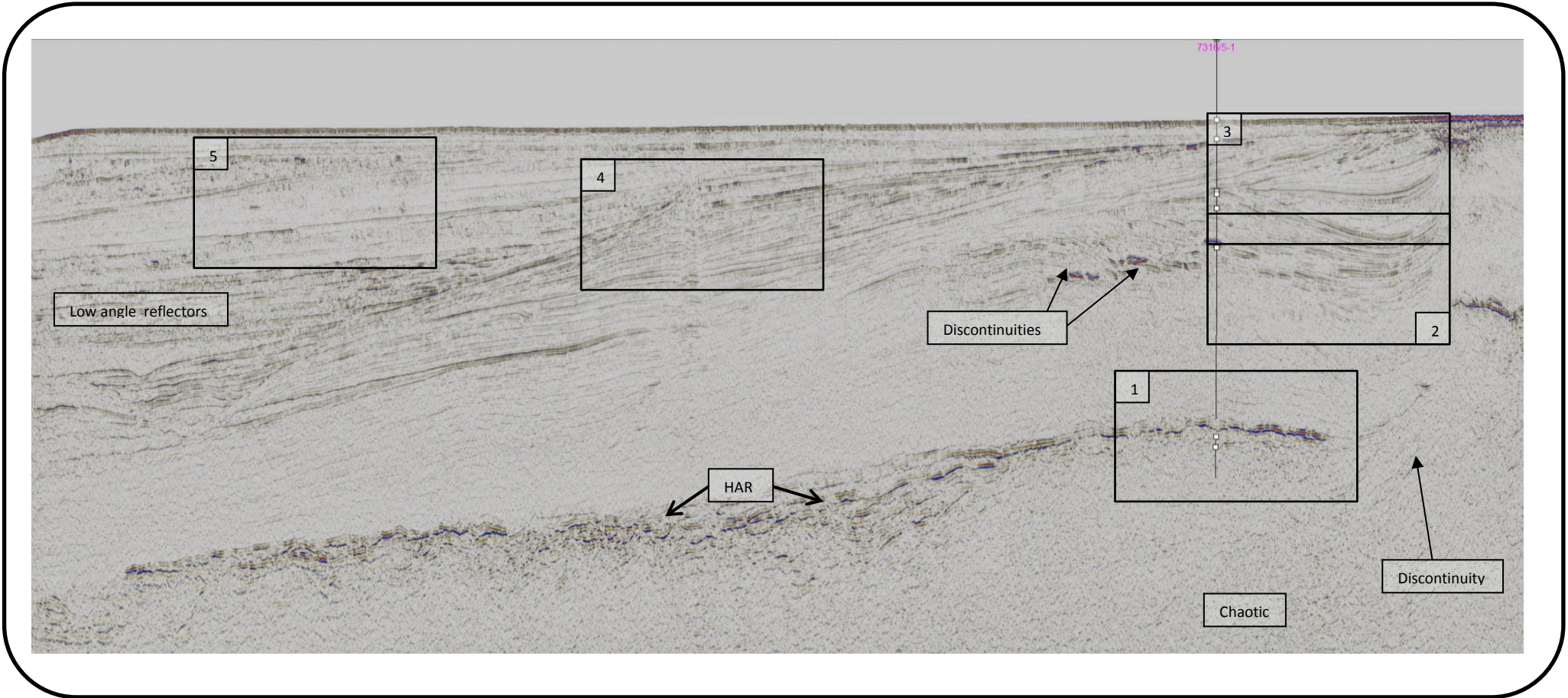
Figure 26. Seismic Line NPD-BJV1-86-BV-04-86 with initial observation and displayed subsections.

3. An area with parallel and subparallel reflections creates a large wedge with the deepest part on west (upper section of the Bjørnøya fan, see figure 26, subsections 4 and 5). Several terminations mark the different boundaries of the strata, mainly truncations (see figure 27).
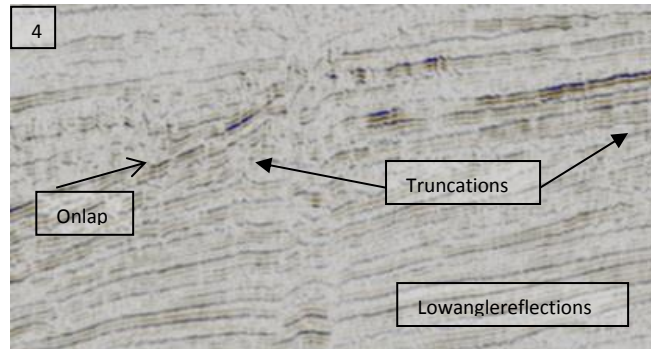
Figure 27. Sub section 4 of the seismic line NPD-BJV1-86-BV-04-86. Some truncations are distinct in the image. These truncations could be associated with the cycles of uplift and glacial erosion during Pleistocene-Pliocene times.

Some discontinuities are also visible in the wedge, probably as consequence of a minor faulting accommodation event. Truncations were the key to understand the several cycles of uplift and glacial erosion.

Tables 4 and 5 show a seismic description of the main packages, based in their seismic patterns and using the proposed ages from the well 7316/5-1. This table summarizes the main seismic features of the image.
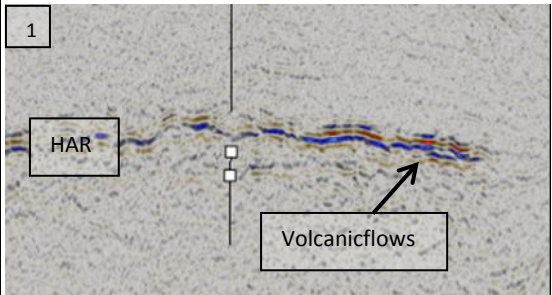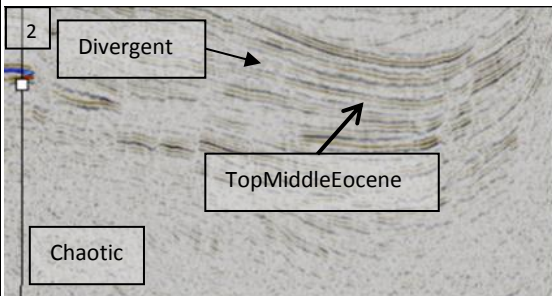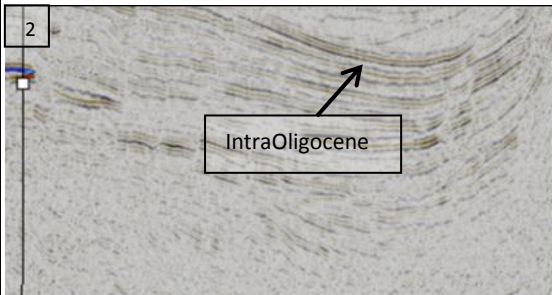
Age	Seismic pattern	Interpreted reflections	Amplitude and continuity of top horizon	Other features	Sub-section example from seismic line
Lower Eocene-Upper Paleocene	Chaotic, irregular dipping. Generally continue, with some discontinuities. Strong reflections on top.	Top of the horizon (Then Interpreted like volcanic flows)	Between low amplitude and high amplitude (caused by volcanic flows)	Strong amplitude due to volcanic flows. Masking of the strata under this reflector.	
Middle Eocene	Chaotic pattern with low amplitudes in the base, divergent pattern in top. Variable dipping (From 0^0 until 15^0)	Top and base of the Middle Eocene strata and three intra middle Eocene reflectors.	Medium amplitude, Medium continuity of top reflection.	Reflectors in the top show some discontinuities, also thinning to the east. Major discontinuity in the east part.	
Lower Oligocene	Divergent pattern. Variable dipping (From 0^0 until 15^0)	Top and base of the Lower Oligocene strata and one intra middle lower Oligocene reflector.	Medium amplitude, Medium continuity of top reflection.	Reflectors in the top show some discontinuities, also thinning to the east. Major discontinuity in the east part. Major truncation to the west.	

Table 5. Observation table from the seismic line NPD-BJV1-86-BV-04-86. Description from Upper Paleocene until Lower Oligocene strata.
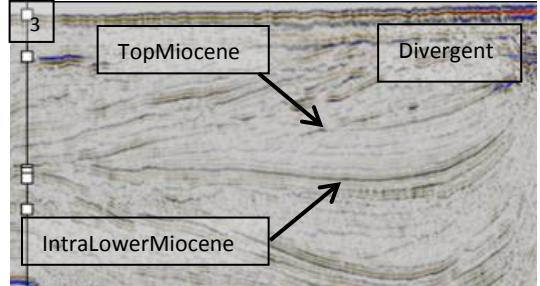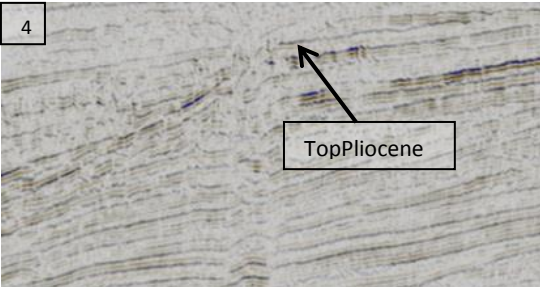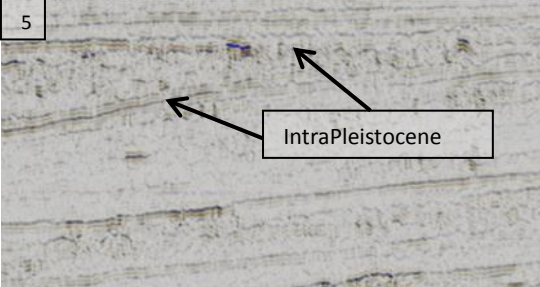
Age	Seismic pattern	Interpreted reflections	Amplitude and continuity of top horizon	Other features	Sub-section example from seismic line
Lower Miocene	Divergent pattern. Variable dipping (From 0^0 until 15^0)	Top and base of the Miocene strata and one Intra Lower Miocene reflector.	Low amplitude, low continuity of top reflector.	Major discontinuity in the east part. It is suggested Syn-deposition during Miocene times. Major truncation on top of the Miocene strata.	
Pliocene	Parallel-subparallel pattern. Variable dipping (From 0^0 until 30^0)	Top and base of the Pliocene strata and five intra Pliocene reflections.	Medium amplitude, high continuity of the top reflector.	Several truncations define the erosional cycles during the Pliocene.	
Pleistocene	Parallel-subparallel pattern. Variable dipping (From 0^0 until 30^0)	Top and base of the Pleistocene strata (Quaternary) and 2 intra Pleistocene reflections.	- Sea bottom-	Several truncations define the erosional cycles during the Pleistocene times.	

Table 6. Observation table of the seismic line NPD-BJV1-86-BV-04-86. Description from Lower Miocene until Pleistocene strata.

4.1.2.   INTERPRETATION AND GEOLOGICAL HISTORY

Upper Paleocene – Lower Eocene

Only the top reflector was interpreted in these strata (High Amplitude Reflector, HAR).The top of the Upper Paleocene-Lower Eocene can be easily distinguished in the seismic line like a strong volcanic reflector. Using the well correlation, it has been prove that these strong reflections are caused by extrusive rocks. These volcanic rocks were originated during Paleocene-Eocene times, when rifting affected the area. Several authors have described this rifting event that led the formation of the Vestbakken Volcanic Province (Faleide et al., 1993; Faleide et al., 2008; Eldholm et al., 1989; Gabrielsen et al., 1990; Planke et al., 1999).

The volcanic reflector (HAR) presents a shift in the eastern part, close to the Eastern boundary fault. This shift was probably consequence of fault activity after the extrusion, during the fault activity periods through Eocene until Miocene times. Evidence of this activity is the thinning and syn-deposition of the Miocene strata. In the southwestern part the HAR presents an inclination, probably due to subsidence after deposition of thick Middle-Eocene Pleistocene strata.

Under this layer is not possible distinguish clear reflection patterns, probably caused by the masking effect created by the extrusive rocks. HAR is the only recognizable feature in the eastern part of the eastern boundary fault.

Middle Eocene

Three Intra middle Eocene horizons were interpreted, including the top of the middle Eocene strata (IME 1, IME 2, IME 3, and BO, base Oligocene, see figures 28 and 29).The Base Oligocene is marked with help of the well 7316/5-1. The reflector IME 3 is difficult to identified, but it marks the boundary between low amplitude reflectors in the lower part and the medium amplitude reflectors with divergent pattern in the upper part.

The Reflectors IME 2 and IME 1 show strong amplitudes inside the package, and some terminations in the western part (IME 1, figure 25). In the eastern part, these reflectors present some shifts due to fault activity, during late Eocene times to Oligocene times and reactivation during Miocene time.

A thick Middle Eocene package was deposited after the volcanic activity. In the well 7316/5-1 these strata were located between 1067 and 1577 meters. In this period of time, the entire margin was dominated by a shear margin setting (Faleide et al., 2008). The western sub-basin close to the eastern boundary fault subsided rapidly, probably receiving material from east (Eidvin et al., 1998). The seismic pattern close to the fault area indicates subsidence during this period of time, where important quantities of material were deposited.

These thick Middle Eocene strata probably represents the distal facies of prograding wedges (Eidvin et al., 1998).Sequences from this age were created during transtensional effects (leaky Transform model) and evidence of this is the subsidence in the seismic images (see Table 6 and subsection 2, Figure 28).

Due to the poor data quality in the east part of the eastern boundary fault, it is difficult follow the reflectors from this time. In the previous case was possible with the HAR, because it was a clear and really strong reflection, easy to follow after the boundary fault.

Upper Eocene – Upper Oligocene

The interpreted reflectors were the Base Oligocene, one Intra-lower Oligocene and other Intra Oligocene reflector. All these three reflections were correlated with the well 7316/5-1. These three reflectors present shifts caused by the faulting activity, and thinning to the east due to subsidence and syn-deposition (differential in compaction) close to Lower Miocene times.

The Upper Eocene sediments are absent in the well 7316/5-1 and one of the proposed theories for this absence is based in uplift and inversion of the west downthrown flank (western sub-basin, Eidvin et al., 1998). The sediments were eroded or non-deposited due to this tectonic event. It could be a period of transpression along this area in the South Western Barents sea margin.

After this period of transpression, it is proposed gentle subsidence during early Oligocene time. This gentle subsidence was accompanied by westerly tilting of the sub-basin. Extension (Middle Oligocene- Upper Oligocene) after the compressional event could explain faulting of the Middle Eocene and Oligocene strata. The lower Oligocene strata were located between 960 until 1090 m in the well 7316/5-1.Upper Oligocene sediments are not proved in the well but it is suggested a sequence severely condensed (Eidvin et al., 1998).

According to Faleide et al. (2008), since Oligocene times the southwestern Barents Sea becomes in a passive margin. Also, Early Oligocene rifting reactivates faults in the

Vestbakken Volcanic Province (Faleide et al., 2008) and could explain some of the fault setting in the west flank or western sub-basin (see Table 7 and sub-section 3, Figure 28).

Early Miocene

Only one Intra lower Miocene reflector (or base Miocene) was interpreted. The Intra Lower Miocene reflector shows a clear subsidence pattern, probably caused by activity of the eastern boundary fault during this time.

Lower Miocene strata appear in the interval between 948 until 960 meters in the well 7316/5-1. There are no evidence of late Miocene strata in the well. It is proposed Early Miocene Subsidence along the downthrown flank of the eastern boundary fault (Eidvin et al., 1998). Some syn-deposition of lower Miocene strata was observed in the seismic line; it was probably originated during reactivation of the Eastern boundary fault and eventual subsidence of the west flank (see Table 6, and subsection 4, Figure 28).

According to some authors, thick Miocene strata were deposited, but these were mainly eroded by a Late Miocene-Pliocene pre-glacial tectonic uplift (Faleide et al., 2008). Other theories suggest a condensed Miocene section that was eroded by the tectonic uplift during Miocene-Pleistocene transition. This condensed section was originated during the transpression and activation of some Oligocene faults (Eidvin et al., 1998).

At this time sea-floor spreading activity would have been well established. The Intra-Lower Miocene reflector is an indicator of transgression across the high at this time by (Eidvin et al., 1998).

Miocene to Pliocene

During Miocene to Pliocene times there was a regional uplift of the Barents Sea shelf, affecting the Vestbakken Volcanic Province. This tectonic uplift probably originated as consequence of heat transmission, leading entire areas to become sub-aerial and then affected by erosion.

Easterly tilting was facilitated by subsidence of the hanging wall along the eastern boundary fault. Uplift involved an easterly tilt component, aided by reactivated movement along the hanging wall in the eastern boundary fault. Some Oligocene fault reactivation is proposed as consequence of this major tectonic event (Eidvin et al., 1998).

After this initial tectonic uplift, isostatic uplift and several phases of glacial erosion affected this area during all the Pliocene and Pleistocene times. Initial tectonic uplift was followed by intensive glacial erosion, compensated by isostatic uplift, which induce the maintenance of an elevated glaciated terrain. Glacial erosion could be considered the main erosional factor; from 1/2 up to 2/3 of the Cenozoic erosion was glacial in origin (Dimakis et al., 1998).

Pleistocene-Pliocene

The Pleistocene-Pliocene strata are formed by a major depositional wedge along the South-Western Barents Sea Margin (upper section of the Bjørnøya fan). This wedge was originated by a succession of uplift and erosional events during these times. This progradational wedge lead subsidence along this area. In the well section, this interval appears between 477 until 948 m, but the sedimentary wedge continue in depth to the west.

The first tectonic uplift and erosional event was compensated by isostatic uplift. According to Fiedler and Faleide (1996) the entire shelf became sub-aerial after the tectonic uplift. Erosion of this sub-aerial shelf led deposition of material along the margins, and filling of sedimentary basins on the southern Barents Sea shelf. The material eroded in this primary tectonic uplift event (Fiedler and Faleide, 1996, called 'pre-glacial' sediments) were deposited in deeper west areas along the margin, for that reason this material is not clear visible in the seismic image.

A second episode during latest Tertiary and Quaternary age was characterized by glacial erosion, probably together with a secondary uplift response. This last event transported erosional products to the present margins (Rasmussen and Fjeldskaar, 1996). These glacial sequences created the sedimentary wedge that is visible in this seismic image.

This history of uplift and erosion is marked by the Base Pliocene surface (BP, figures 28 and 29) .The Base Pliocene also define the boundary for the subsequent glacial domination period (Fieldler and Faleide 1996). It can be distinguish at least 6 intra-Pliocene surfaces and 5 of this surfaces shows clear erosional truncation of the reflectors (IP1, IP2, IP 3, IP 4, IP 5, Figures 28 and 29) and probably these 6 surfaces are related to different glacial phases. It is possible distinguish at least three recent and distinct Quaternary erosional cycles in the seismic, showing erosional truncations (Reflectors BP, IQ1 and IQ2, Figures 28 and 29). Glacio-Isostatic tectonic cycles could explain these erosive surfaces.

According to Fiedler and Faleide (1996) the Pliocene-Pleistocene wedge could be divided in 3 main sequences, GI, GII and GIII (see figure 29). The ages of these packages have been coarsely estimated: GIII from 0.44 Ma to recent times; GII from 1.0- 0.44 Ma; and GI from 2.3 – 1.0 Ma (Fiedler and Faleide, 1996). Each sequence is related to the three main phases in the glacial erosion of the south western Barents Sea margin.

The base of sequence GI represents the onset of extensive continental shelf glaciation, about 2.3 Ma. Then it was easily eroded because in that time the area should become sub aerial by the uplift event. The base of sequence GII marks the onset of large scale mass movements in the Bjørnøya Fan and is tentatively related to an intensification of the glaciation 1.0 Ma. Sequence GIII corresponds to the sediments above the base quaternary and it has been dated around 0.44 Ma (Fieldler and Faleide, 1996).
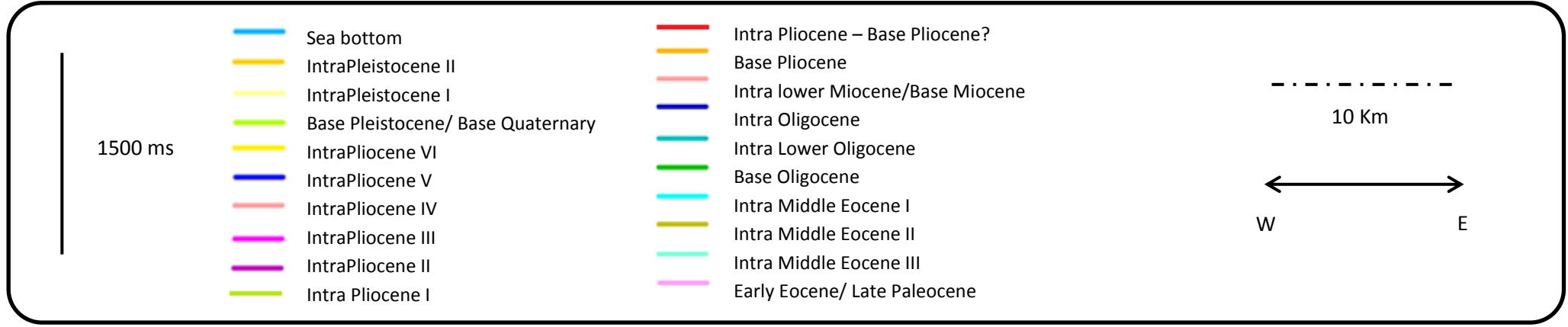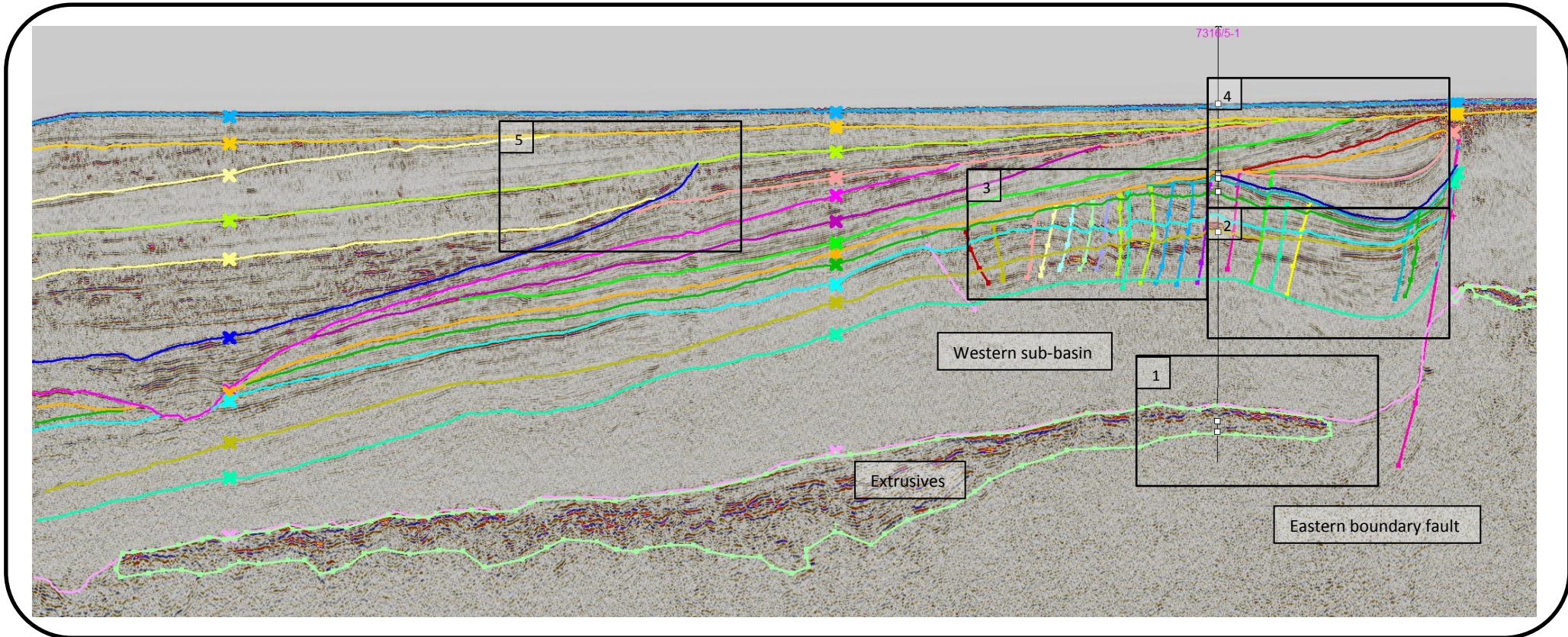
Figure 28. Interpreted horizons and other main features in the seismic line NPD-BJV1-86-BV-04-86.
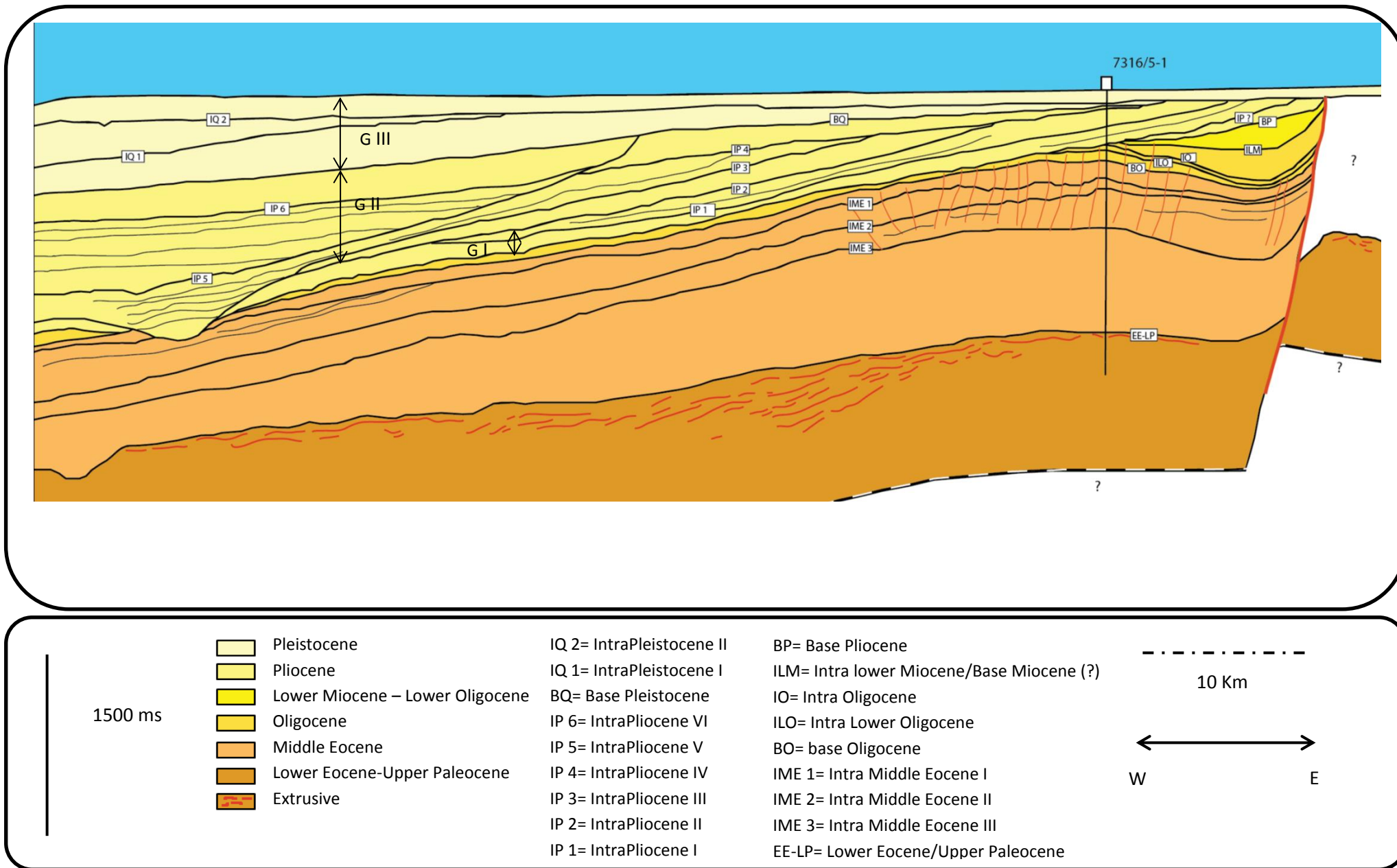
Figure 29. Geological model from the seismic line NPD-BJV1-86-BV-04-86. GI, GII, and GIII are the main sequences defined by Fiedler and Faleide (1996).   49
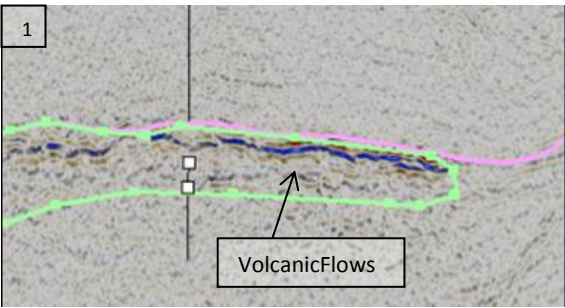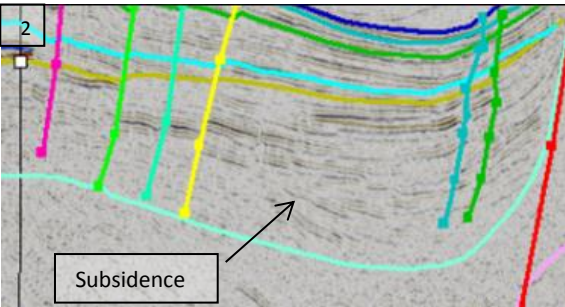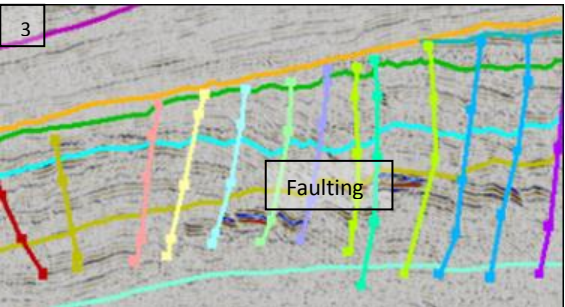
Age	Main geological events	Sub-section example from Seismic line
Lower Eocene-Upper Paleocene (Breakup and rifting)	(a) Volcanic flows due to rifting and continental breakup during Paleocene-early Eocene transition (Faleide et al., 2008).	
MiddleEocene (Shear margin setting/ transtension)	(a) Sub-basin in the west of the eastern boundary fault subsided rapidly, probably receiving material from east (Eidvin et al., 1998). (b) It probably represents the distal facies of prograding wedges (Eidvind et al., 1998).Deep marine conditions persisted in the SW Barents Sea, with deposition of significant sandy submarine fans during Middle Eocene (Ryseth et al., 2003). (c) Sequences from this age were created during transtensional effects (Leaky Transform model)	
Upper Eocene-UpperOligocene (Shear margin setting/ transpression/ beginning of the passive margin stage)	(a) Upper Middle-Eocene, Upper Eocene strata is not in the well section. This is caused probably by Uplift and inversion of the hanging wall. The sediments were consequently raised above the wave base, resulting in a period of erosion or non-deposition (Eidvin et al, 1998). Transpression during Late Eocene-Earliest Oligocene could explain the inversion. (b) Appears locally to have been a period of gentle subsidence accompanied by westerly tilting of the sub-basin after this transpressive event. (Eidvin et al., 1998). (c) Extension and subsidence (Middle Oligocene- Upper Oligocene) after the compressional event could explain faulting of the Middle Eocene and Oligocene strata.	

Table 7. Main geological events described in the line NPD-BJV1-86-BV-04-86. Description from the Upper Paleocene until Upper Oligocene strata.
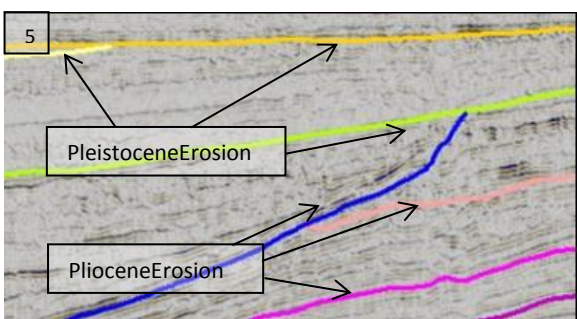
Age	Main geological events	Sub-section examples from Seismic line
Upper Oligocene to Late Miocene (Passive Margin)	(a) Upper Oligocene sediments are not proved in the well. It is suggested a sequence severely condensed. (b) Early Miocene Subsidence along the downthrown flank of the eastern boundary fault (Eidvin et al., 1998). (c) At this time sea-floor spreading activity would have been well established (Eidvin et al., 1998). (d) Deposition of thick Miocene strata, now remove by uplift/erosion. Indication of transgression across the high at this time by the Intra-Lower Miocene reflector (Eidvin et al., 1998). (e) It is suggested syn-deposition of lower Miocene strata during reactivation of the Eastern boundary fault.	
Miocene to Pliocene	(a) Net Regional uplift of the Vestbakken Province, presumably together with much of the present western Barents Sea area (Eidvin et al, 1998). (b) Reactivation of some Oligocene faults (Eidvin et al., 1998). (c) Easterly tilting was facilitated by subsidence of the hanging wall along the eastern boundary fault (Eidvin et al., 1998). (d) Uplift involved an easterly tilt component, aided by reactivated movement along the hanging wall of the eastern boundary fault (Eidvin et al., 1998). (e) Isostatic uplift response after the tectonic uplift and erosion (Fiedler and Faleide, 1996). Creation of the base Pliocene erosional surface.	
Pleistocene-Pliocene	(a) Initiation of cyclic progradation of the Plio-pleistocene wedges on the unconformity surface (Base wedge). Succession of glacial-erosion events. Evidence of the westerly tilting. It is possible distinguish at least three recent and distinct Quaternary erosional cycles and other three major Pliocene erosional truncations. Glacio-isostatic tectonic cycles could explain these erosive surfaces. (b) Plio-Pleistocene uplift and glacial erosion of the Barents Shelf and deposition of large volume of glacial deposits in submarine fans along the margin occasioned regional tilt of the margin (Dimakis et al., 1998).	

Table 8. Main geological events described in the line NPD-BJV1-86-BV-04-86. Description from the Upper Oligocene until Pleistocene strata.
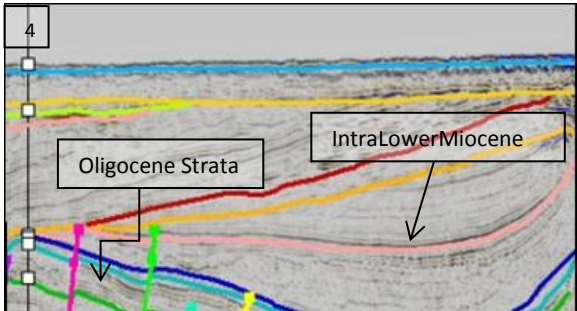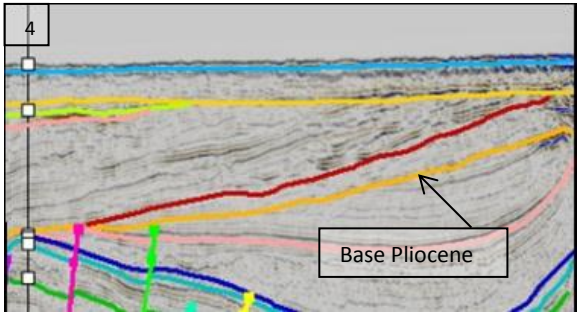
4.2. NPD-BJV2-86-7355

The line NPD-BJV2-86-7355 is the most northern seismic line with east-west direction studied in this thesis. It cross other 2 seismic lines: NPD-BJV2-86-1645 (with south-north direction) and the line NPD-BJV1-86-BV-04-86 (with southwest-northeast direction, and considered the main line).

The seismic line has a length of 110 km and were mainly interpreted 75 km (focused in the area with better resolution in the western part of the eastern boundary fault, see figure 23 with the colored section). According to the structural maps of the area, this seismic line is mainly over the Vestbakken Volcanic Province (see figure 23).

The interpretation of this line has a close history with the line NPD-BJV1-86-BV-04, because it is relatively close. Main features like the eastern boundary fault and the western sub-basin were interpreted in this seismic line.

4.2.1. OBSERVATIONS

At first sight, the line NPD-BJV2-86-7355 looks similar to the previous line: the High Amplitude Reflectors (HAR) in depth areas, a major discontinuity in the east part, and the big sedimentary wedge into the west. Four subsections were selected from the seismic image for obtain a better understanding from the observations. The resolution could be considered medium, with an improvement in the upper areas (ex. subsection 4, figure 32)

1. The high amplitude reflectors (HAR) are present in the deeper part of the seismic line. There is a shift between two sections of these HAR (see figure 30). Like in the previous seismic line, the areas under these high amplitude reflectors show a chaotic pattern, probably by the masking effect of these reflectors. Above HAR, it is possible observe low amplitude reflectors with a more coherent pattern.
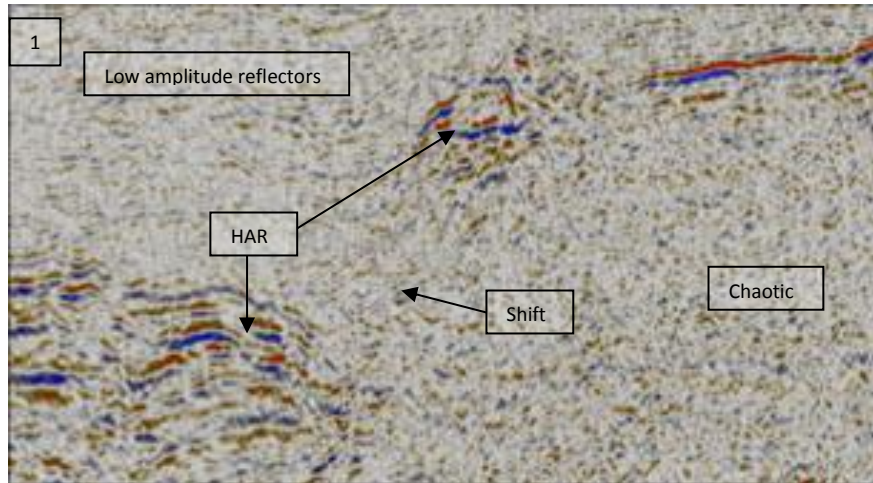
Figure 30. Subsection 1 from the seismic line NPD-BJV2-86-7355 (see figure 33). Like in the previous seismic line, the HAR appears but shifted in two sections. This feature could be interpreted as fault activity after the volcanic extrusion.

2. Two packages with divergent patterns were observed in the east part. These packages are separated by a major discontinuity. In the east part, the eastern discontinuity is also visible like in the previous line. Under these packages there are low amplitude reflectors. These packages show a major top truncation tilted to the west.
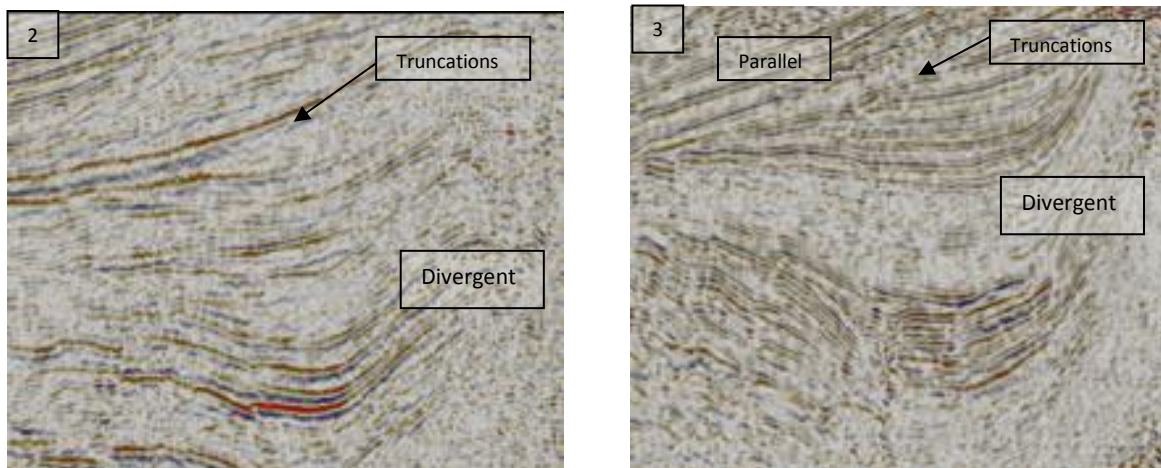
Figure 31. Subsections 2 and 3 from the seismic line NPD-BJV2-86-7355 (see figure 33). This divergent shape is associated with faulting activity (the previous interpreted eastern boundary fault, and the central east fault, interpreted in this line). Due to this discontinuity in the middle, the western sub-basin could be separated in two parts (HAR are also shifted).

3. The western area is dominated by the large sedimentary wedge. It present several truncations, and parallel to subparallel low angle reflections. Some discontinuities are

visibles, but these have smaller dimensions in comparison with the previous described discontinuities.
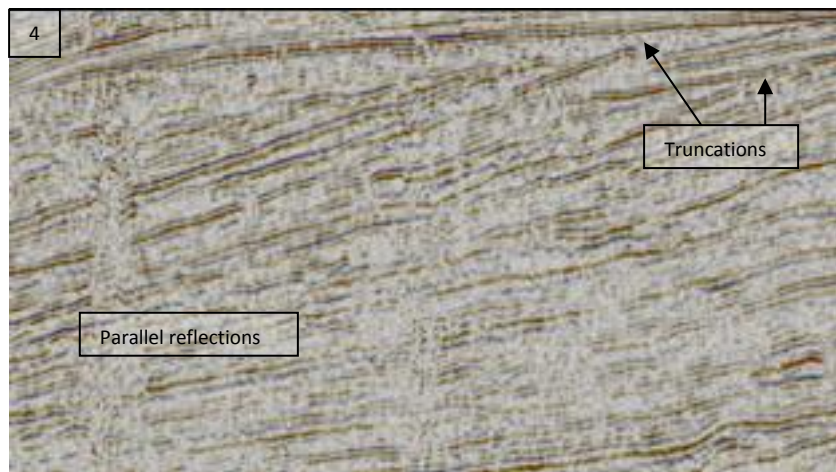
Figure 32. Subsection 4 from the seismic line NPD-BJV2-86-7355 (see figure 33). Truncations mark the boundary between the different packages inside the depositional wedge. These truncations were interpreted as part of the uplift and erosional glaciation cycle during Pleistocene-Pliocene times.
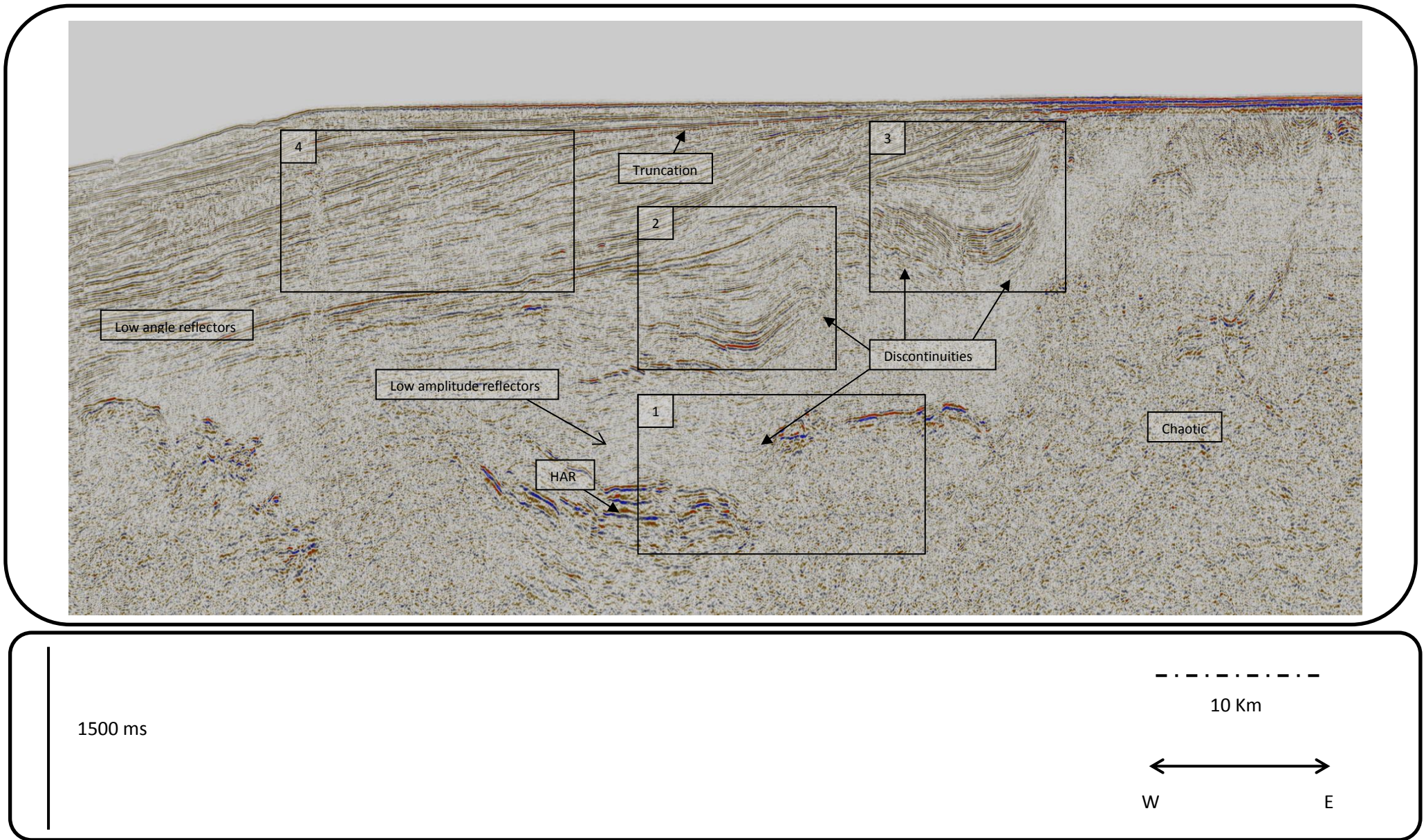
Figure 33. Seismic Line NPD-BJV2-86-7335 with initial observation and displayed subsections.

4.2.2.　　INTERPRETATION AND GEOLOGICAL HISTORY

Upper Paleocene – Lower Eocene

The High Amplitude Reflectors (HAR) were interpreted as the top of the Upper Paleocene-Lower Eocene strata. The HAR were interpreted specifically like volcanic rocks originated during the rifting and continental breakup of the Norwegian-Greenland Sea during Late Paleocene to Early Eocene times. Under these volcanic layers, it was not possible interpreted deeper reflectors due to the masking effect.

The HAR shows a major shift that divided it in two sections (see subsection 1, figure 30). This shift was generated as consequence of fault activity of the central east fault (see figure 34 and 35) after the volcanic extrusion.

Middle Eocene – Lower Oligocene

In this package were interpreted one intra middle Eocene horizon and one Intra Oligocene horizon. Some of the interpreted horizons in the previous line do not cross the present studied line and the interpretation was mainly based in the comparison of the seismic patterns between both lines.

One main difference between the features of this line and the previous line is the clear presence of what was denominated like the 'central east fault'. This fault was probably active since Middle Eocene times (after the volcanic activity, late Paleocene-early Eocene times) until Miocene tines (before the Miocene-Pliocene uplift). The central east fault could be considered directly associated to the eastern boundary fault, controlling both the movement of the hanging walls in the western sub-basin.

Transtension during middle Eocene could be the origin of the Central-East fault, probably created just before of the eastern boundary fault. This divided sub-basin was affected by the middle Eocene subsidence proposed by Eidvin et al. (1998).

After a period of Transpression during Eocene-Oligocene transition, it is proposed a gentle subsidence during the early Oligocene times. This gentle subsidence was accompanied by westerly tilting of the sub-basin. Extension (Middle Oligocene- Upper Oligocene) after the compressional event could explain faulting of the Middle Eocene and Oligocene strata. These faults could be also explained by the Early Oligocene fault reactivation (Faleide et al., 2008).

Early Miocene – Late Miocene

Only one Intra Miocene (or base Miocene?) reflection was interpreted in this package. This Intra Miocene reflector was also interpreted in both flanks of the western sub-basin (subsections 2 and 3, figure 33). Like in the previous history, some proposed syn-deposition of lower Miocene strata is observed in the seismic line. It was probably originated during reactivation of the main faults, the Eastern boundary fault and Central east boundary fault, and eventual subsidence of the two flanks.

According to some authors, thick Miocene strata were deposited, but it was mainly eroded by a Late Miocene-Pliocene Uplift (Faleide et al., 2008). Other theories suggest a condensed Miocene section that was also eroded by the Miocene-Pliocene tectonic uplift. This condensed section was originated during the transpression and activation of some Oligocene faults (Eidvin et al., 1998).

Miocene to Pliocene

The Base Pliocene marks the evidence of the major tectonic uplift and erosion during these times. Initial tectonic uplift is followed by intensive glacial erosion, compensated by isostatic uplift, which induce the maintenance of an elevated and glaciated terrain (Dimakis et al., 1998). Easterly tilting was facilitated by subsidence of the hanging walls along the eastern boundary fault and the central eastern fault. Some Oligocene fault reactivation is proposed as consequence of this major tectonic event (Eidvin et al., 1998).

Pleistocene-Pliocene

The First tectonic uplift and subsequent uplift rebound and glacial erosion is marked by the Base Pliocene surface (BP, figures 34 and 35). It can be distinguished at least 4 intra-Pliocene surfaces that shows a clear erosional truncation of the reflectors (IP 2, IP 3, IP 4, IP 5, Figures 34 and 35). These surfaces are related to uplift and glacial events. It is possible distinguish at least two recent and distinct Quaternary erosional cycles in the seismic. Also they show erosional truncations (reflectors BP and IQ2, Figures 34 and 35). Glacio-Isostatic tectonic cycles could also explain these erosive surfaces.
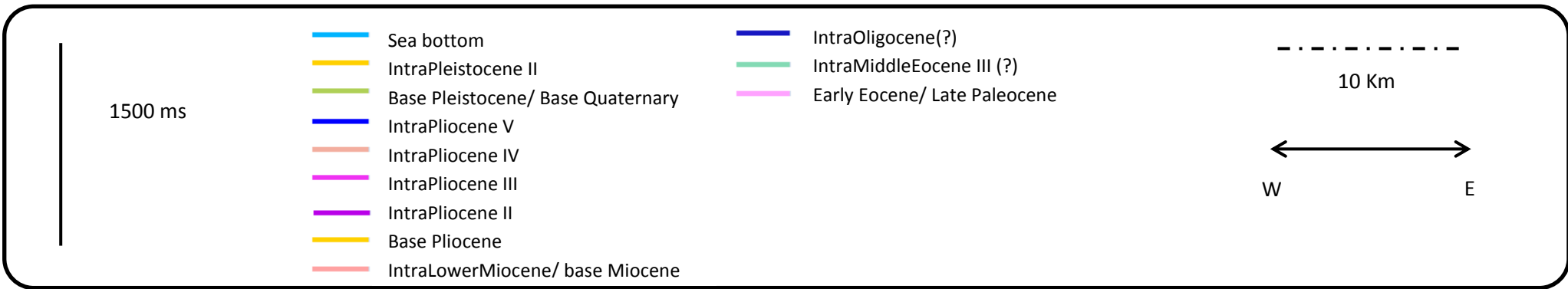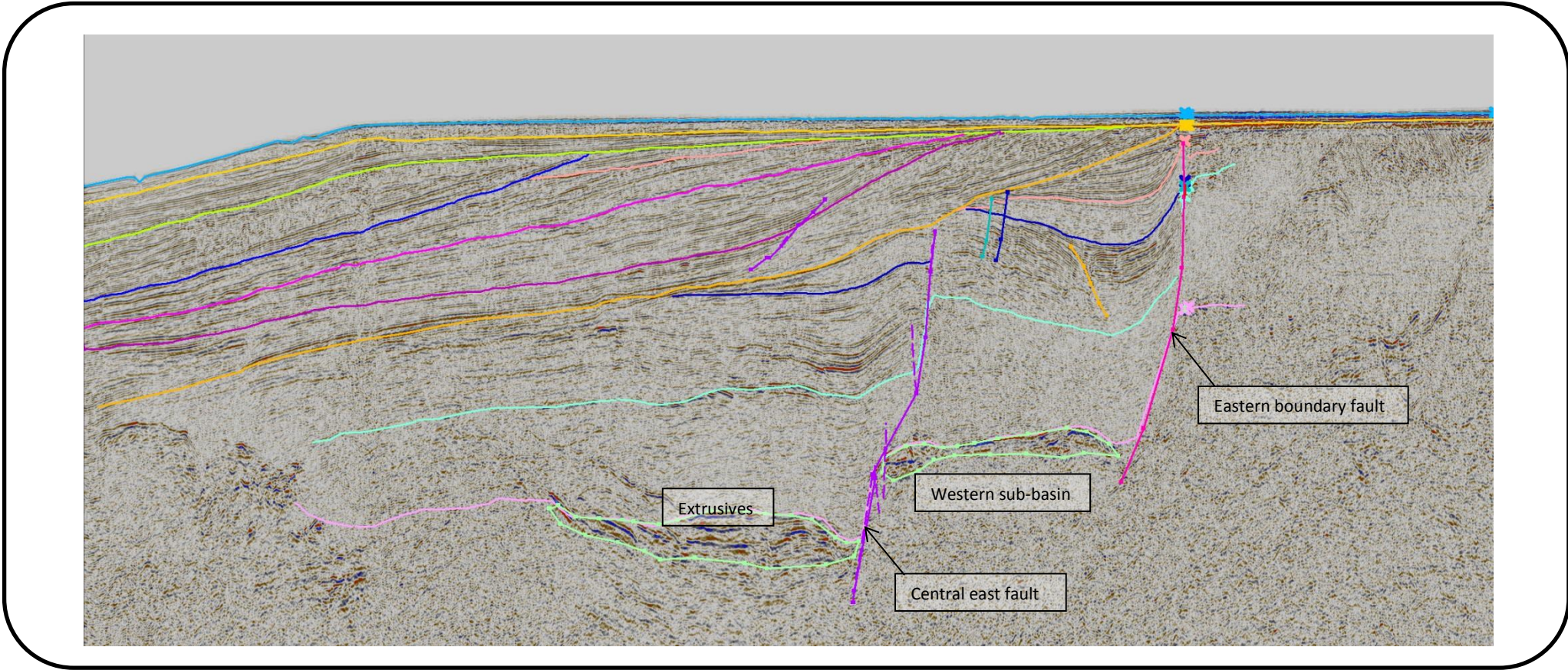
Figure 34. Interpreted horizons and other main features in the seismic line NPD-BJV2-7335.
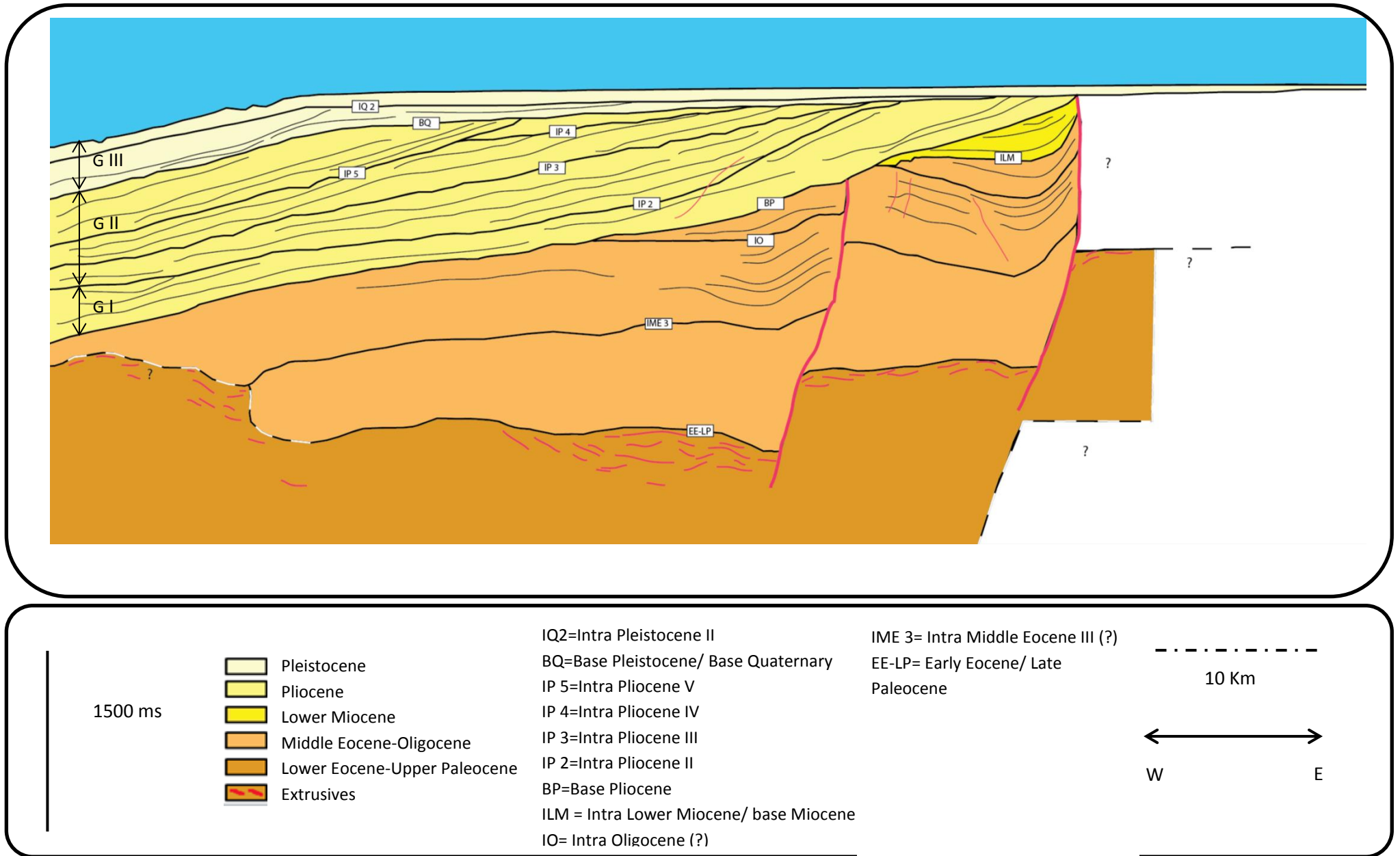
Figure 35. Geological model from the seismic line NPD-BJV2-7335.

4.3. NPD-BJV2-86-7325

The line NPD-BJV2-86-7325 is one of the five seismic lines that have east-west direction. It cross other 2 seismic lines: NPD-BJV2-86-1645 (with south-north direction) and the line NPD-BJV1-86-BV-04-86 (with southwest-northeast direction, and considered the base line).

The seismic line has a length of 110 km and were mainly interpreted 75 km (focused in the area with better resolution in the western part of the eastern boundary fault, see figure 23 with the colored section). According to the structural maps of the area, this seismic line is over the Vestbakken Volcanic Province and the Sørvestsnaget basin (see figure 23).

The interpretation of this line has a close history with the line NPD-BJV1-86-BV-04, because they are relatively close. Main features like the eastern boundary fault and the western sub-basin appear in this this seismic line.

4.3.1.   OBSERVATIONS

Like in the previous 2 lines, the main features are more or less visible in this seismic line. For a better description and understanding of the seismic image, three representative subsections were selected (see figure 39).

1. The High Amplitude Reflectors (HAR) mark the boundary of the Vestbakken Volcanic Province. The HAR have the tendency to finish closer to the west in comparison with the previous parallel line. This tendency continuous, until the HAR disappear in the most southern seismic line. The areas under these high amplitude reflectors show a chaotic pattern, mainly by the masking effect of these reflectors. Above HAR, it is possible observe low amplitude reflectors with a more coherent pattern. In general terms HAR shows a tilting to the west, this feature is shared with the rest of the lines over the Vestbakken Volcanic Province.
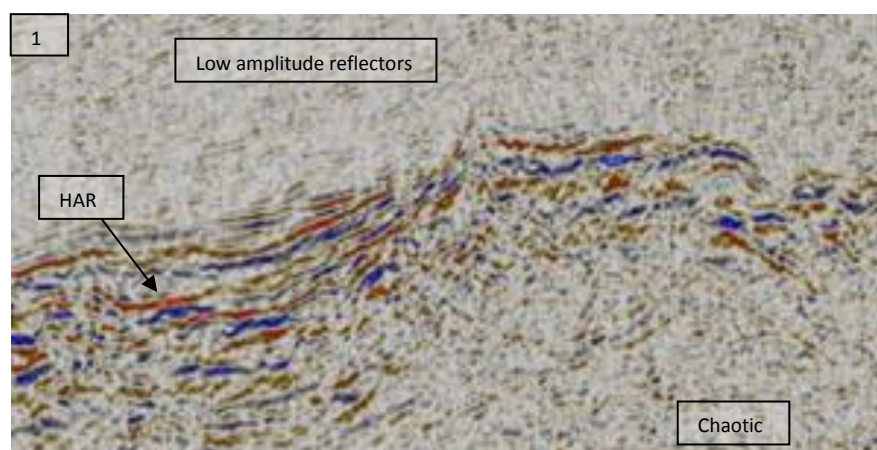
Figure 36. Subsection 1 from the seismic line NPD-BJV2-86-7355 (see figure 39). Like in the previous seismic line, the HAR appears with some inclination to the west direction.

2. One package with divergent pattern was observed in the west part of the major eastern discontinuity. Over this package there are tilting reflections with low angle parallel patterns. Between this package with divergent seismic pattern there is a clear truncation, later interpreted as the base Pliocene truncation. In the west part of this divergent pattern, there are several discontinuities (see figure 37) like in the base line.
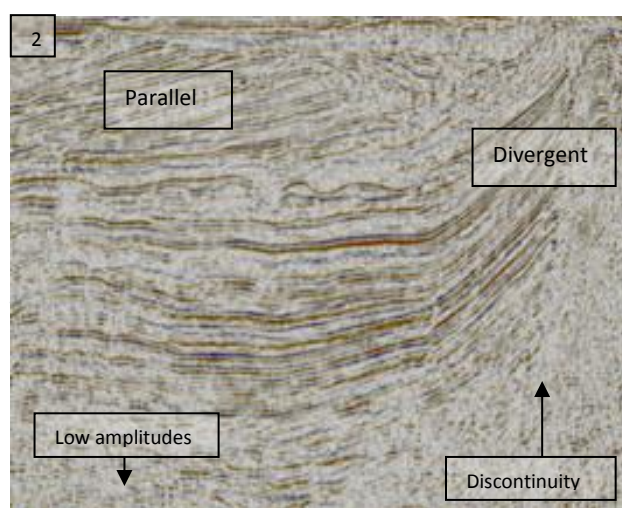
Figure 37. Subsection 2 from the seismic line NPD-BJV2-86-7325. The divergent shape is associated with the fault activity of the eastern boundary fault. The parallel reflections and the divergent reflections are separated by a major truncation surface. This truncation, caused by the Miocene-Pliocene tectonic uplift is a major feature possible to see in all the seismic lines.

3. The western area is dominated by the Bjørnøya fan (see subsection 3 and figure 38). It shows several truncations, and parallel to subparallel low angle reflections. In general terms this wedge shows a tilting to the west, this feature is shared with the rest of the lines where the wedge is present.
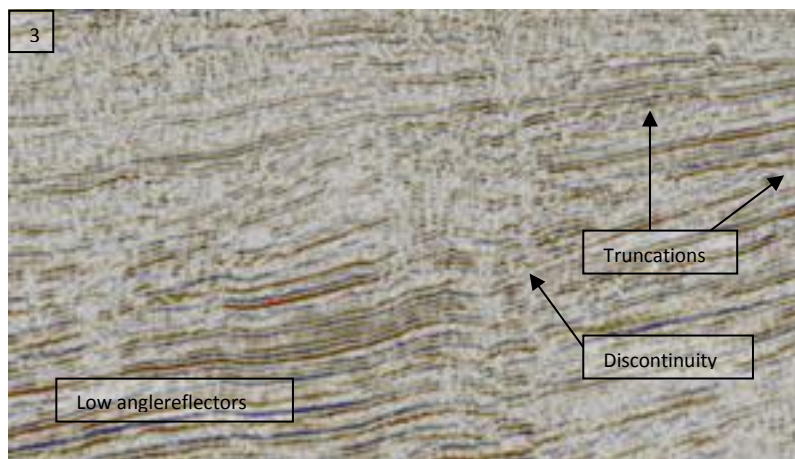
Figure 38. Subsection 3 from the seismic line NPD-BJV2-86-7325. Some truncations are visible in the image, and then interpreted as part of the uplift-erosional cycles. Discontinuities in the reflections are also visible; these were interpreted as accommodation faults.
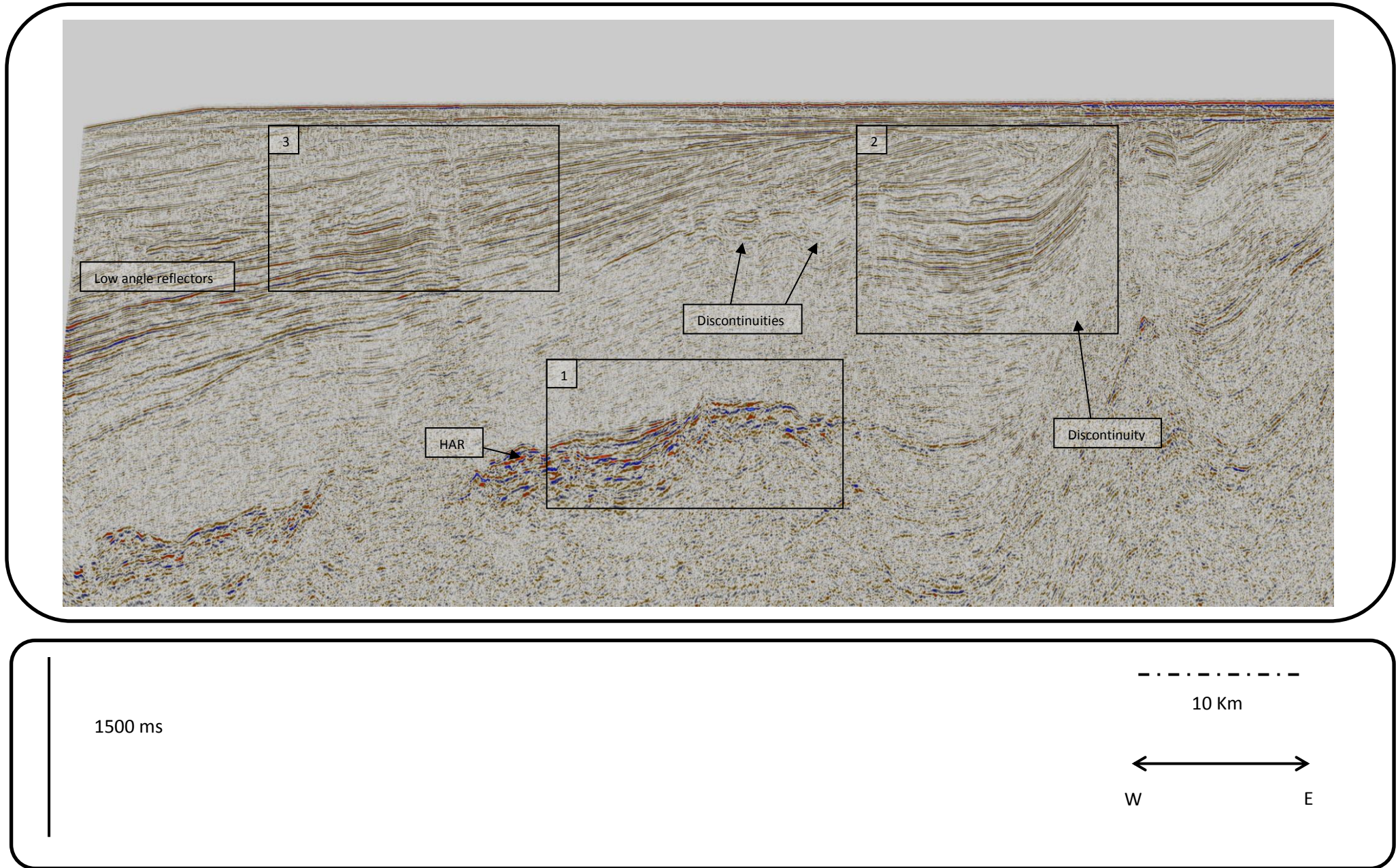
Figure 39. Seismic Line NPD-BJV2-7325 with initial observation and displayed subsections.

4.3.2.   INTERPRETATION AND GEOLOGICAL HISTORY

Upper Paleocene – Lower Eocene

Like in the previous lines, only the top of the Upper Paleocene-Lower Eocene strata was interpreted (HAR). These high amplitude reflections are caused by volcanic rocks. These extrusive rocks were originated during the rifting and continental breakup of the Norwegian-Greenland Sea during Paleocene-Eocene transition (Faleide et al., 2008). Under this volcanic intrusion, interpretation was no possible due to the masking effect.

Middle Eocene

It was possible interpreted three intra middle Eocene horizons (IME 1, IME 2, IME 3, see figure 40 and 41). The interpretation was based crossing and following the horizons interpreted in the base line and comparing the seismic patterns and features with the studied line.

In comparison with the previous line (NPD-BJV2-86-7335) is not possible see the central east fault. Instead of this, it was interpreted a faulted setting like in the line NPD-BJV1-86-BV-04-86 (base line) affecting the Middle Eocene strata (see figure 39) and probably originated during Oligocene times.

Early Oligocene – Late Miocene

In these strata, it was no possible interpreted intra-horizons (Intra Oligocene or Intra/Base Miocene) only the base Oligocene and the top of the Miocene strata (base Pliocene wedge). After a period of transpression during Eocene-Oligocene transition, it was proposed a gentle subsidence during the early Oligocene. This gentle subsidence was accompanied by westerly tilting of the flank (western sub-basin). Extension (Middle Oligocene- Upper Oligocene) after the compressional event could explain faulting in the Middle Eocene and some of the Oligocene strata. These faults could be also explained by the Early Oligocene fault reactivation (Faleide et al., 2008).

Similar with the history of the previous lines, some proposed syn-deposition of lower Miocene strata is observed in the seismic line; it was probably originated during reactivation of the Eastern boundary fault, and eventual subsidence of the western flank.

According to some authors, thick Miocene strata were deposited, but it was mainly eroded by a Late Miocene-Pliocene Uplift (Faleide et al., 2008). Other theories suggest a condensed Miocene section that was also eroded by the tectonic uplift. This condensed section was originated during the transpression and activation of some Oligocene faults (Eidvin et al., 1998).

Miocene to Pliocene

After the initial tectonic uplift and erosion, uplift rebound was induced and glacial erosion affected this area during Pliocene and Pleistocene times. An evidence of this event is the clear base Pliocene truncation, which appears in all the seismic lines. Initial tectonic uplift was followed by intensive glacial erosion, compensated by isostatic uplift, which induce the maintenance of an elevated and glaciated terrain (Dimakis et al., 1998). Easterly tilting was facilitated by subsidence of the hanging wall along the eastern boundary fault. Some Oligocene fault reactivation is proposed as consequence of this major tectonic event (Eidvin et al., 1998).

Pleistocene-Pliocene

It can be distinguished at least 5 intra-Pliocene surfaces that indicated a clear erosional truncation (IP1, IP 2, IP 3, IP 4, IP 5, Figures 40 and 41). These intra-Pliocene erosional surfaces should be related to uplift events and glacial cycles. It is possible distinguish at least two recent and distinct Quaternary erosional cycles in the seismic (Base Quaternary and Intra quaternary II, IQ 2).
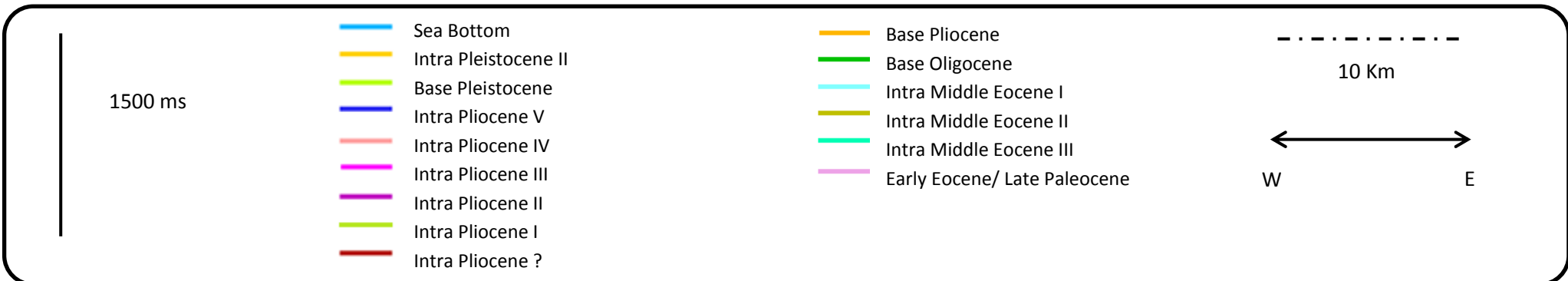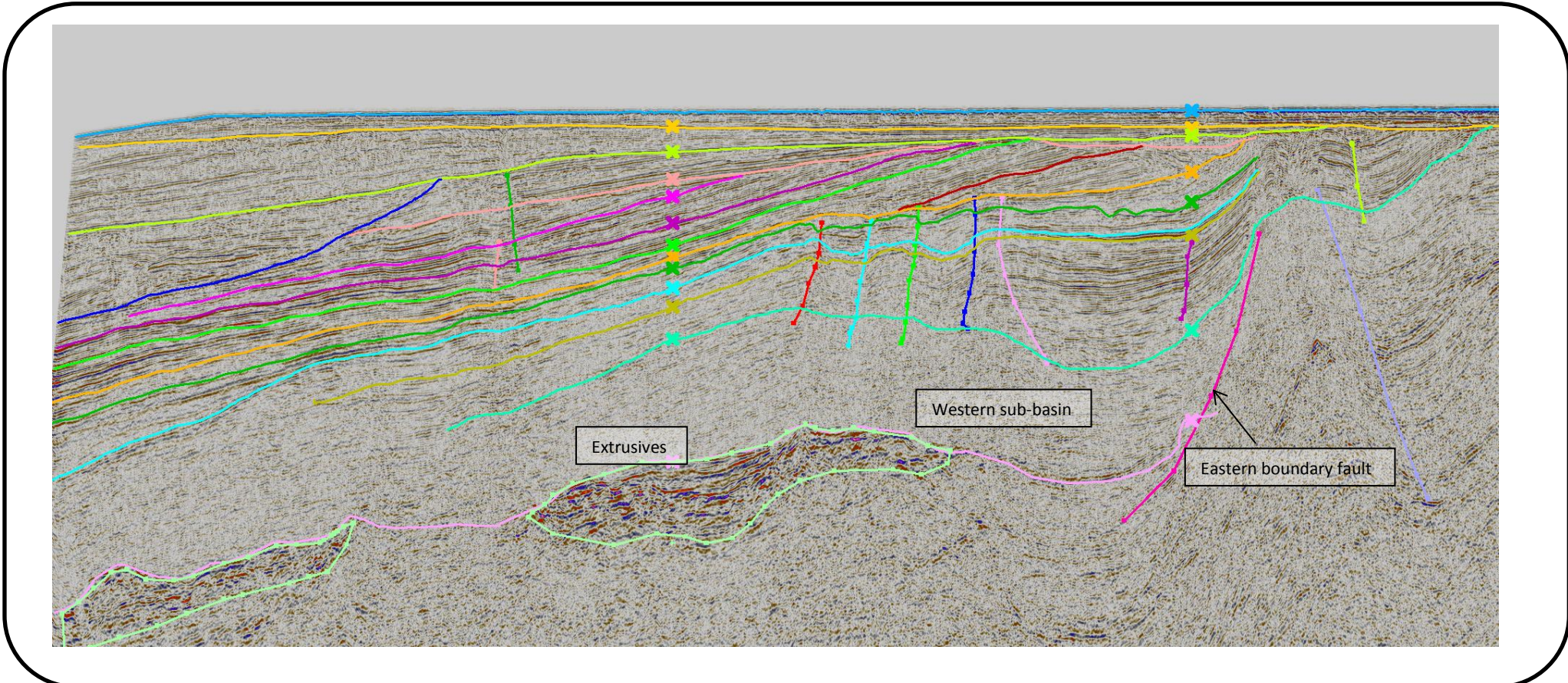
Figure 40. Interpreted horizons and other main features in the seismic line NPD-BJV2-7325.
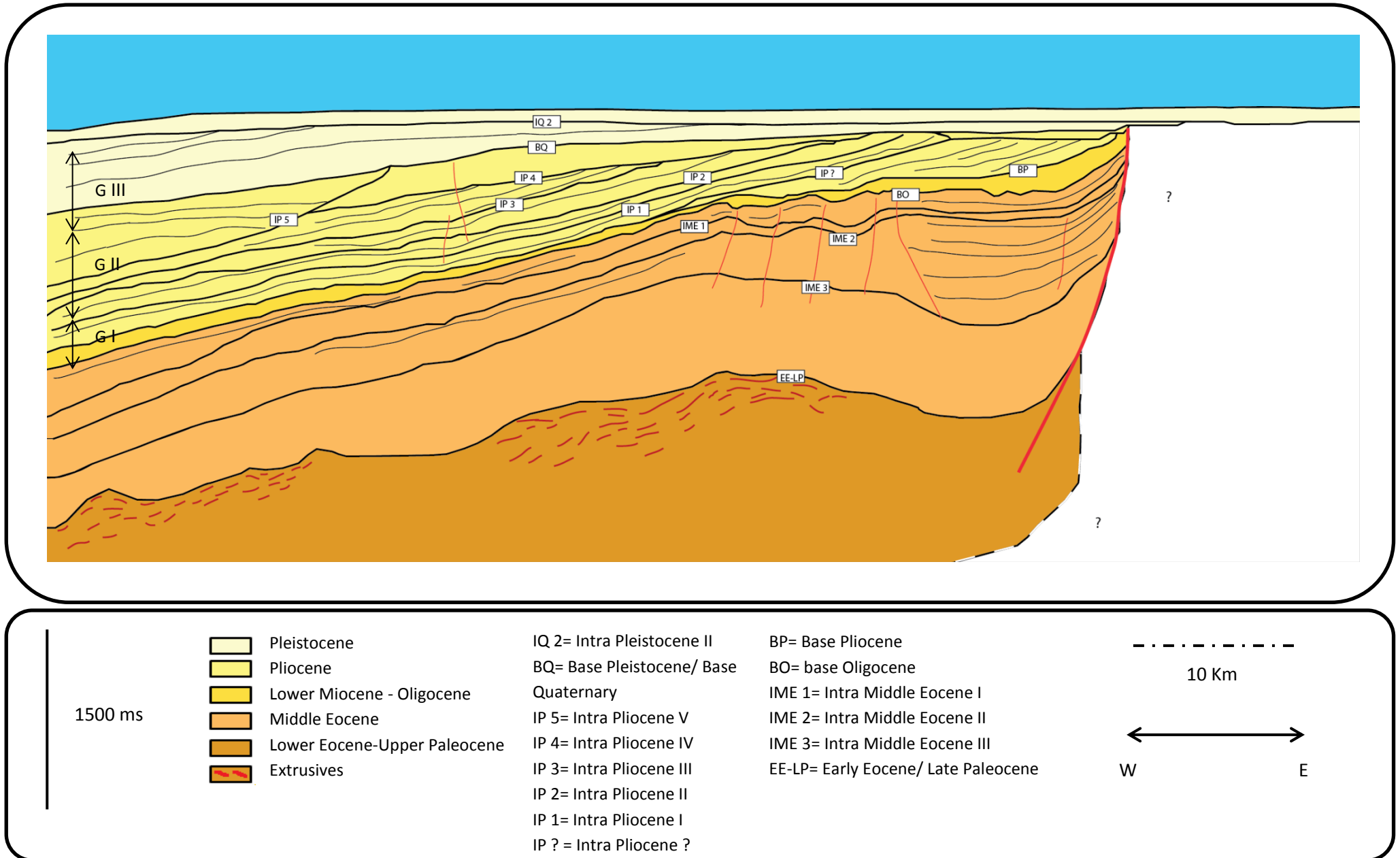
Figure 41. Geological model from the seismic line NPD-BJV2-7325

4.4. NPD-BJV2-86-7315

The line NPD-BJV2-86-7325 is one of the five seismic lines that have east-west direction. It cross other 2 seismic lines: NPD-BJV2-86-1645 (with south-north direction) and the line NPD-BJV1-86-BV-04-86 (with southwest-northeast direction, and considered the base line).

The seismic line has a length of 110 km and were mainly interpreted 75 km (focused in the area with better resolution in the western part of the eastern boundary fault, see figure 23 with the colored section). According to the structural maps of the area, this seismic line is over the Vestbakken Volcanic Province and the Sørvestsnaget basin (see figure 23).

The interpretation of this line has a close history with the line NPD-BJV1-86-BV-04. Main features like the eastern boundary fault and the western sub-basin also appears in this this seismic line. The central east fault (see seismic line NPD-BJV2-7335) does not appear clearly in this image, instead of this, appears a faulted setting with a major central fault plane.

4.4.1.   OBSERVATIONS

Like in the previous lines, the main features appear in this image: The high amplitude reflectors, the eastern boundary fault and the faulting setting in the western sub-basin. For a better description and understanding of the seismic image, three representative subsections were selected (see figure 45).

1. The high amplitude reflectors (HAR) are the main feature in the Vestbakken Volcanic Province. Areas under these high amplitude reflectors show a chaotic pattern, mainly by the masking effect of these reflectors and also by the loss of resolution in depth. Above HAR, it is possible observe low amplitude reflectors with a more coherent pattern. In general terms, HAR shows a tilting to the west; this feature is shared with the rest of the lines over the Vestbakken Volcanic Province.
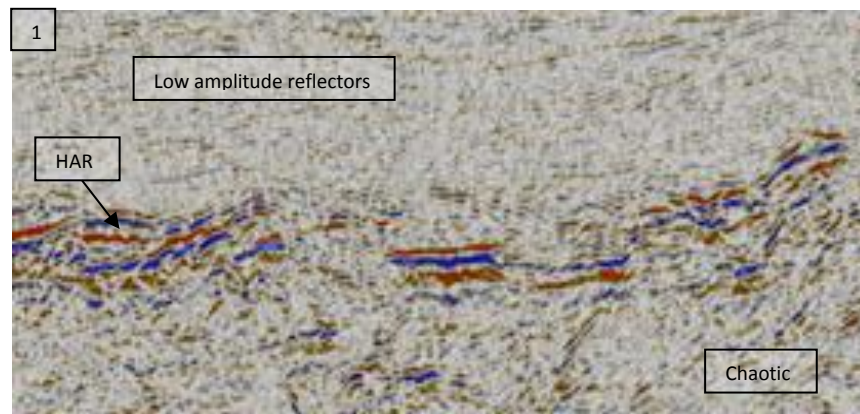
Figure 42. Subsection 1 from the seismic line NPD-BJV2-86-7325 (see figure 45). Like in the previous seismic line, the HAR appears with a characteristic seismic pattern and with a general tilting to the west.

2. One package with divergent pattern was observed in the west part of the major eastern discontinuity. Over this package there are reflections with low angle parallel patterns. Between these two packages with different seismic pattern there is a clear truncation, later interpreted as the base Pliocene truncation. In the west part of this divergent pattern, there are several discontinuities (see figure 43) like in the base line.
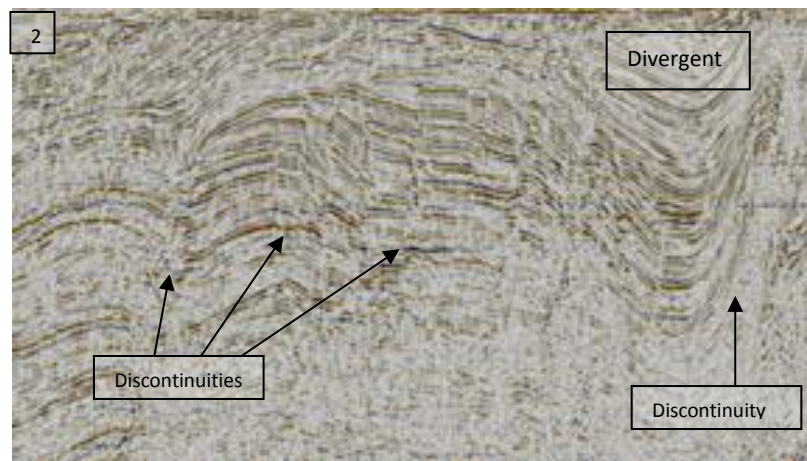
Figure 43. Subsection 2 from the seismic line NPD-BJV2-86-7325. The divergent shape is associated with the fault activity of the eastern boundary fault. The parallel reflections and the divergent reflections are separated by a major truncation. This truncation, caused by the Miocene-Pliocene tectonic uplift is a major feature possible to see in all the seismic lines.

3. The western area is dominated by a large wedge (see subsection 3, figure 44). It shows several truncations, and parallel to subparallel low angle reflections. In general terms, this wedge shows a tilting to the west; this feature is shared with the rest of the lines where the wedge is present.
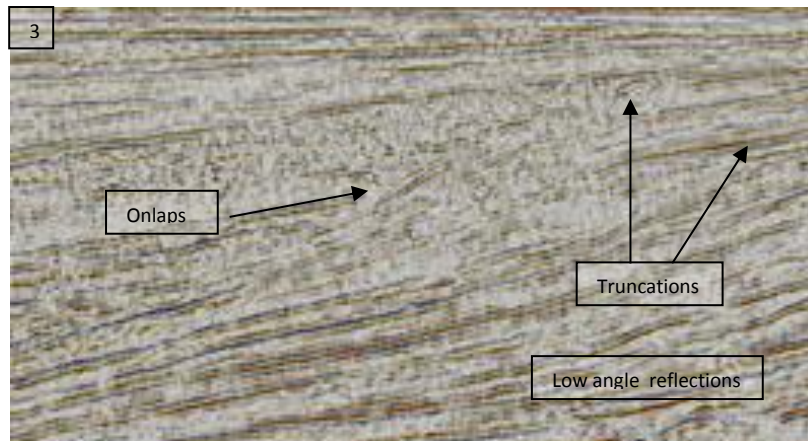
Figure 44. Subsection 3 from the seismic line NPD-BJV2-86-7325. Some truncations are visible in the image, and then interpreted as part of the uplift-erosional cycles. Discontinuities in the reflections are also visible; these were interpreted like accommodation faults.
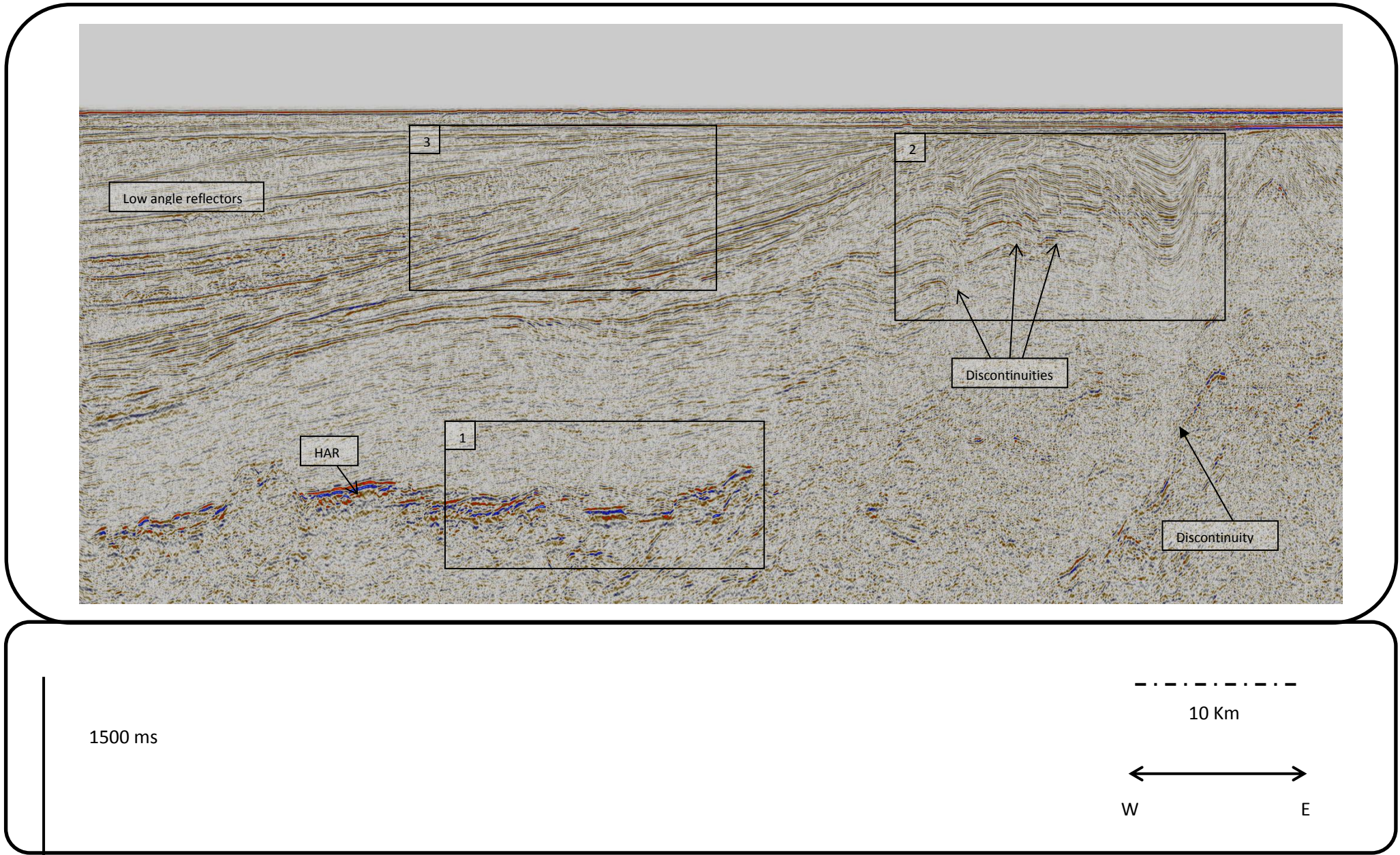
Figure 45. Seismic Line NPD-BJV2-7315 with initial observations and displayed subsections.

4.4.2.   INTERPRETATION AND GEOLOGICAL HISTORY

Upper Paleocene – Lower Eocene

Only the top of the Upper Paleocene-Lower Eocene strata was interpreted. These high amplitude reflections are caused by volcanic rocks of the Vestbakken Volcanic Province. These extrusive rocks were originated during the rifting and continental breakup of the Norwegian-Greenland Sea during Paleocene-Eocene transition (Faleide et al., 1993a; Faleide et al., 2008). Under this volcanic intrusion, interpretation was no possible due to the masking effect.

The volcanic rock shows a general tilting to the west in almost all the lines. This is probably consequence of the deposition and subsidence of the big depositional wedge over the volcanic province.

Middle Eocene

Three middle Eocene horizons were interpreted. The interpretation was based crossing and following the horizons interpreted in the base line and comparing the seismic patterns and features from both lines.

In comparison with the seismic line NPD-BJV2-86-7335 is not possible see the central east fault clearly. Instead of this, it was interpreted a faulted setting like in the line NPD-BJV1-86-BV-04-86 (base line) and the line NPD-BJV2-86-7325, but with a main fault in the middle (central-east fault?). This fault setting affected the Middle Eocene strata and the interpreted Oligocene strata (see figure 46).

Early Oligocene – Late Miocene

It was no possible interpreted intra-horizons in these strata, (Intra Oligocene or Intra/Base Miocene) only the base Oligocene and the top of the Miocene strata (base Pliocene wedge). These strata are characterized by a clear divergent pattern, probably as consequence of the syn-deposition accumulation during the activation of the eastern boundary fault and eventual subsidence of the west flank (western sub-basin).

It has been proposed subsidence during the early Oligocene after a period of transpression during Eocene-Oligocene transition. This subsidence was accompanied by westerly tilting of the western sub-basin. Extension (Middle Oligocene- Upper Oligocene) after the

compressional event could explain faulting in the Middle Eocene and some of the Oligocene strata. The fault generation could be also explained by the Early Oligocene fault reactivation (Faleide et al., 2008).

According to some authors, thick Miocene strata were deposited but it was mainly eroded by a Late Miocene-Pliocene Uplift (Faleide et al., 2008). A second theory suggests a condensed Miocene section that was also eroded by the tectonic uplift. This condensed section was probably originated during the transpression and activation of some Oligocene faults (Eidvin et al., 1998).

Miocene to Pliocene

Several episodes of uplift and erosion affected this area through all the Pliocene-Pleistocene times, starting with the main tectonic uplift during Miocene to Pliocene times (Faleide et al., 2008). A clear evidence of this event is the base Pliocene truncation, which appears in all the seismic line. Initial tectonic uplift was followed by intensive glacial erosion, compensated by isostatic uplift that maintained an elevated and glaciated terrain (Dimakis et al., 1998). Easterly tilting was facilitated by subsidence of the hanging wall along the eastern boundary fault. Some Oligocene fault reactivation is proposed as consequence of this major tectonic event (Eidvin et al., 1998).

Pleistocene-Pliocene

It can be distinguish at least 5 intra-Pliocene surfaces, and four of them indicated a clear erosional truncation (IP 1, IP 2, IP 3, IP 4, IP 5, Figures 46 and 47). These intra-Pliocene erosional surfaces should be related to uplift events and glacial cycles. The Base Pliocene mark the erosive surface created by the proposed tectonic uplift and successive erosion during late Miocene times (BP, figures 46 and 47). It is possible distinguish at least three recent and distinct Quaternary erosional cycles in the seismic (Base quaternary, IQ 1 and IQ 2). Glacio-Isostatic tectonic cycles could explain these erosive surfaces, uplift and then glacial erosion.
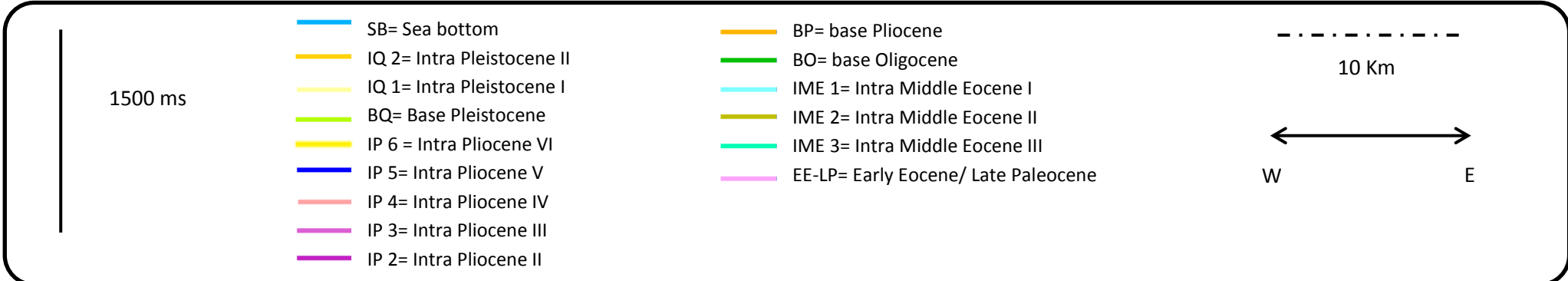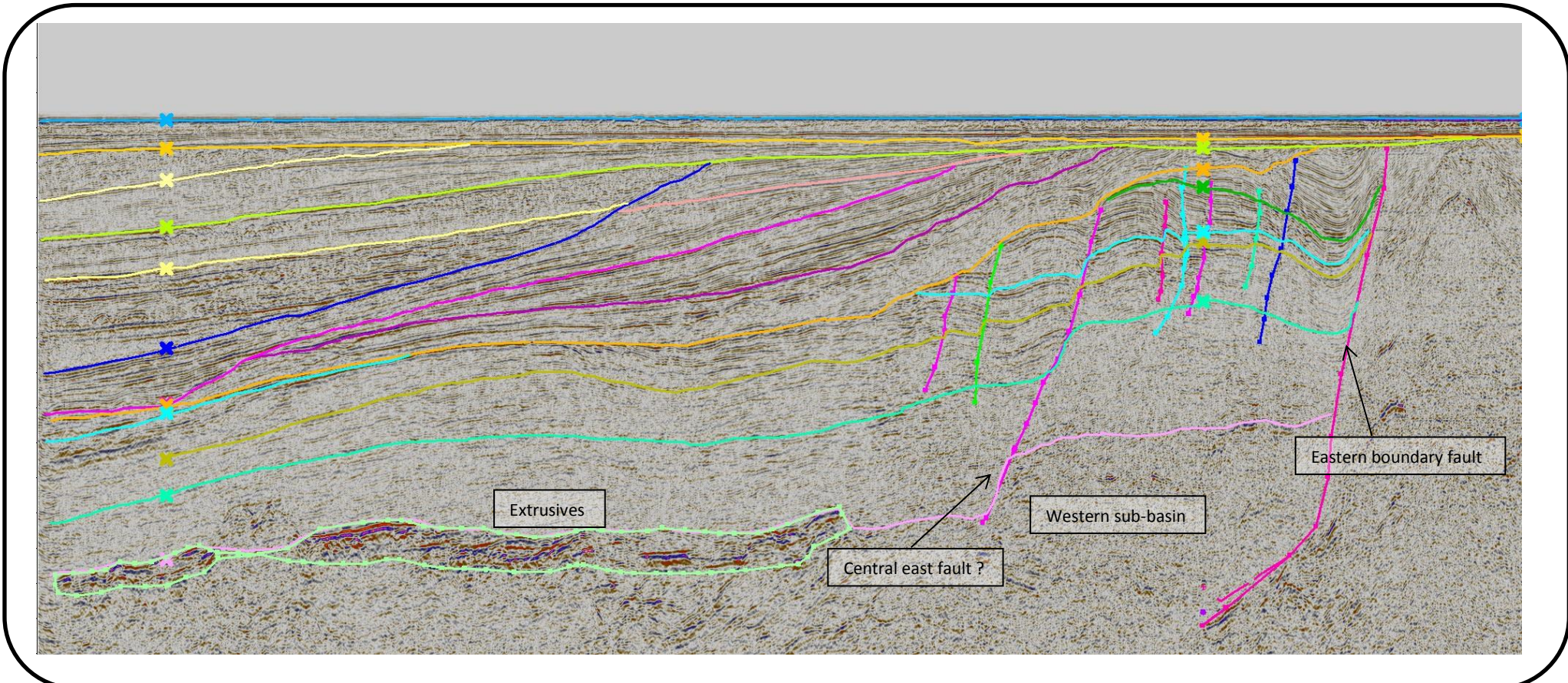
Figure 46. Interpreted horizons and other main features in the seismic line NPD-BJV2-7315.
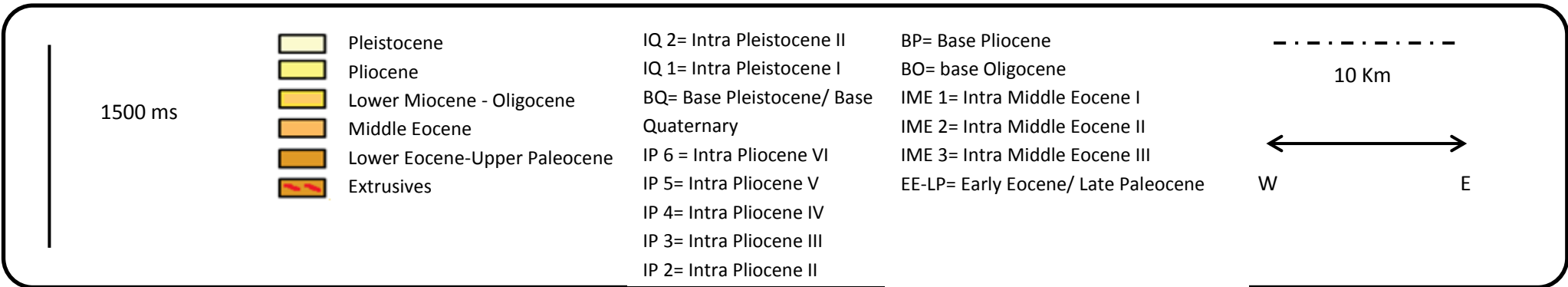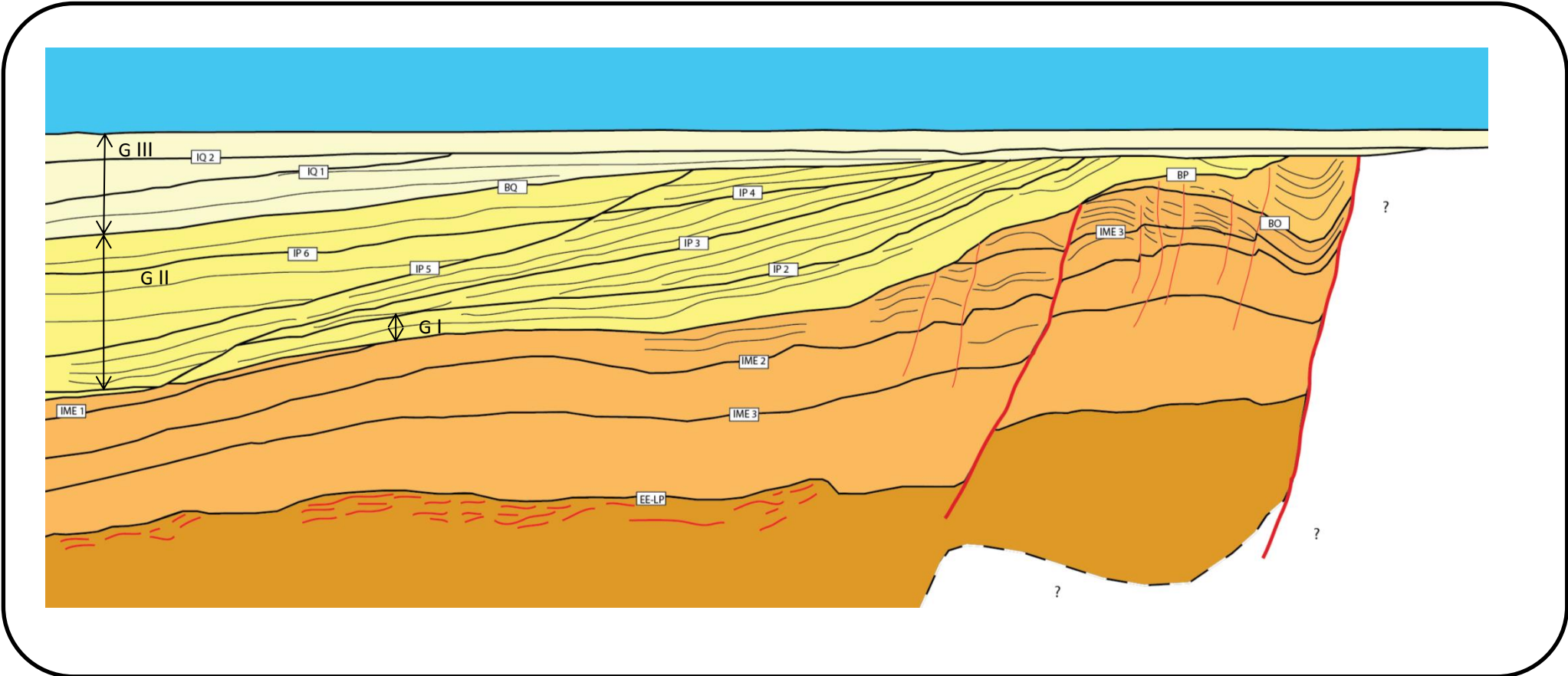
Figure 47. Geological model from the seismic line NPD-BJV2-7315

4.5. NPD-BJV1-86-7305

The line NPD-BJV2-86-7305 is one of the five seismic lines that have east-west direction. It only crosses other seismic lines: NPD-BJV2-86-1645 (with south-north direction). This line does not cross the base line, making more imprecise the interpretation and the age of the main horizons.

The seismic line has a length of 110 km and were mainly interpreted 75 km (focused in the area with better resolution in the western part, see figure 23 with the colored section). According to the structural maps of the area, this seismic line is mainly over the Sørvestsnaget basin and only the extreme western section is over the Vestbakken Volcanic Province (see figure 23).

The interpretation of this line should have a close history with the four previous seismic lines, but it has some main differences. The eastern boundary fault does not appear clearly; instead of that, the eastern part of the image is characterized by a setting of normal faults. There is a sub-basin and folding of the HAR in the western part of the interpreted Eocene-Miocene strata, only visible in this seismic line.

4.5.1.   OBSERVATIONS

This seismic image could be divided in two main areas, the west area whit more clear reflections in depth and the east part with clear reflections only in the shallow areas. Like in the previous lines, it was decided take subsections from the main image. The main reason for this consisted in have a better description and understanding of the seismic line (see figure 51).

1. The High Amplitude Reflectors (HAR) are also present in this seismic line, precisely in the extreme western part (see figure 52). The areas under these high amplitude reflectors show a chaotic pattern, mainly by the masking effect of these reflectors. Above HAR, it is possible observe low amplitude reflectors with a more coherent pattern. In general terms, HAR shows a tilting to the west, and it is possible distinguish a 'high' and a ´lower´ part (see figure 51).
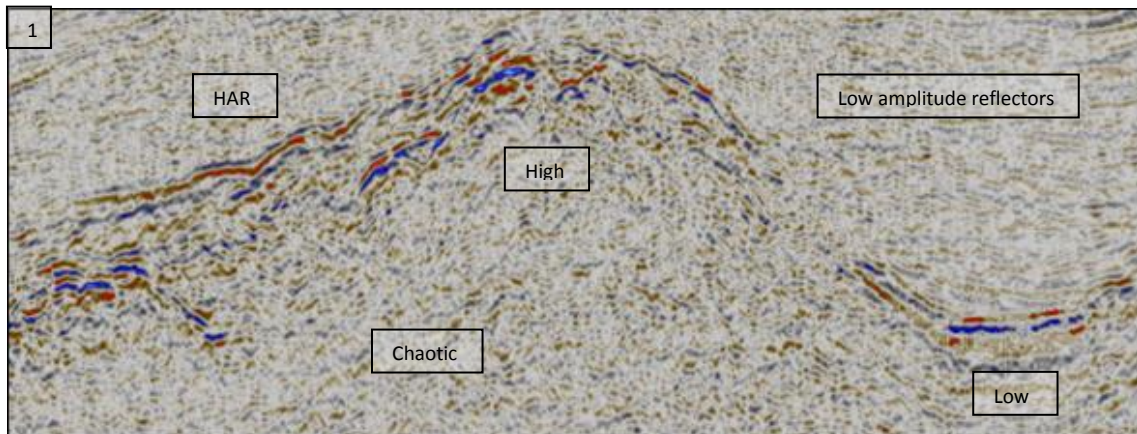
Figure 48. Subsection 1 from the seismic line NPD-BJV2-86-7355 (see figure 52). HAR are present like in the previous seismic line, but appears folded. This feature could be interpreted as subsidence of the reflectors originated by a fault activity in the upper part of the strata.

2. The eastern part of the image does not show a clear discontinuity, interpreted in the previous lines like the 'Eastern boundary fault'. In this case, there is setting of discontinuities, interpreted later as a group of faults. The area under these discontinuous reflectors shows a chaotic pattern, due to the missing of resolution in depth. Above these discontinuous reflectors, it is possible observe low amplitude reflectors with a more coherent pattern.
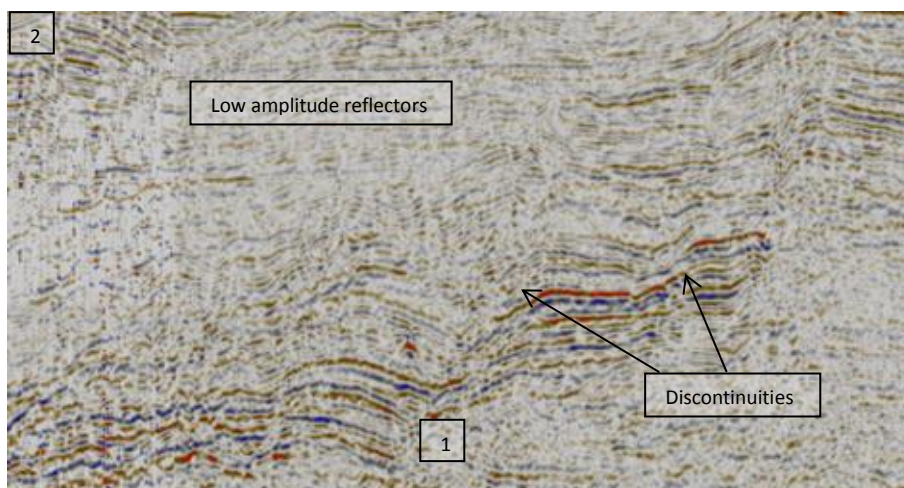
Figure 49. Subsection 2 from the seismic line NPD-BJV2-86-7305. The setting of discontinuous reflectors is associated with faulting activity in the eastern area. It is consistent with the previous images, but there is not a clear and unique main discontinuity (the eastern boundary fault).

3. There is a particular reflection feature displayed in the subsection 3 (figure 50). It shows a divergent pattern, a main discontinuity in the west part and other discontinuities through all the reflectors. In the top of these reflectors is possible see a main truncation (interpreted as Base Pliocene).
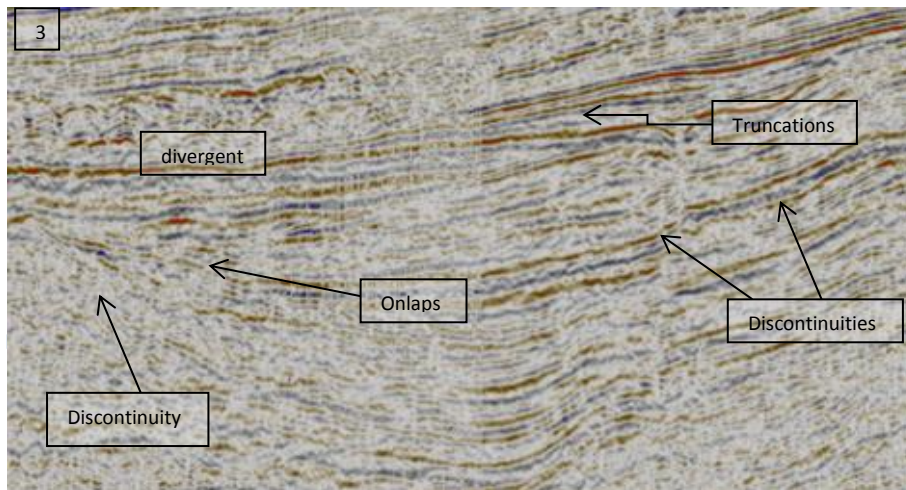
Figure 50. Subsection 3 from the seismic line NPD-BJV2-86-7305. Some divergent patterns were observed and then interpreted as consequence of the fault movement. The discontinuity in the western part of the image was then interpreted as the potential fault that caused this divergent pattern in the reflectors (sub-basin).

4. The western area is dominated by the Bjørnøya fan (see subsection 3 and figure 52). It shows several truncations, and parallel to subparallel low angle reflections. This wedge shows a tilting to the west; this feature is shared with the rest of the lines where the wedge is present
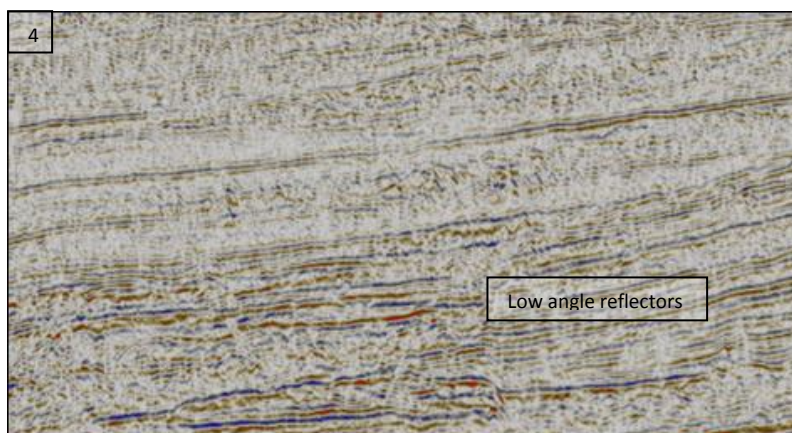
Figure 51. Subsection 3 from the seismic line NPD-BJV2-86-7325. Some truncations are visible in the image, and then interpreted as part of the uplift-erosional cycles. Discontinuities in the reflections are also visible; these were interpreted as accommodation faults.
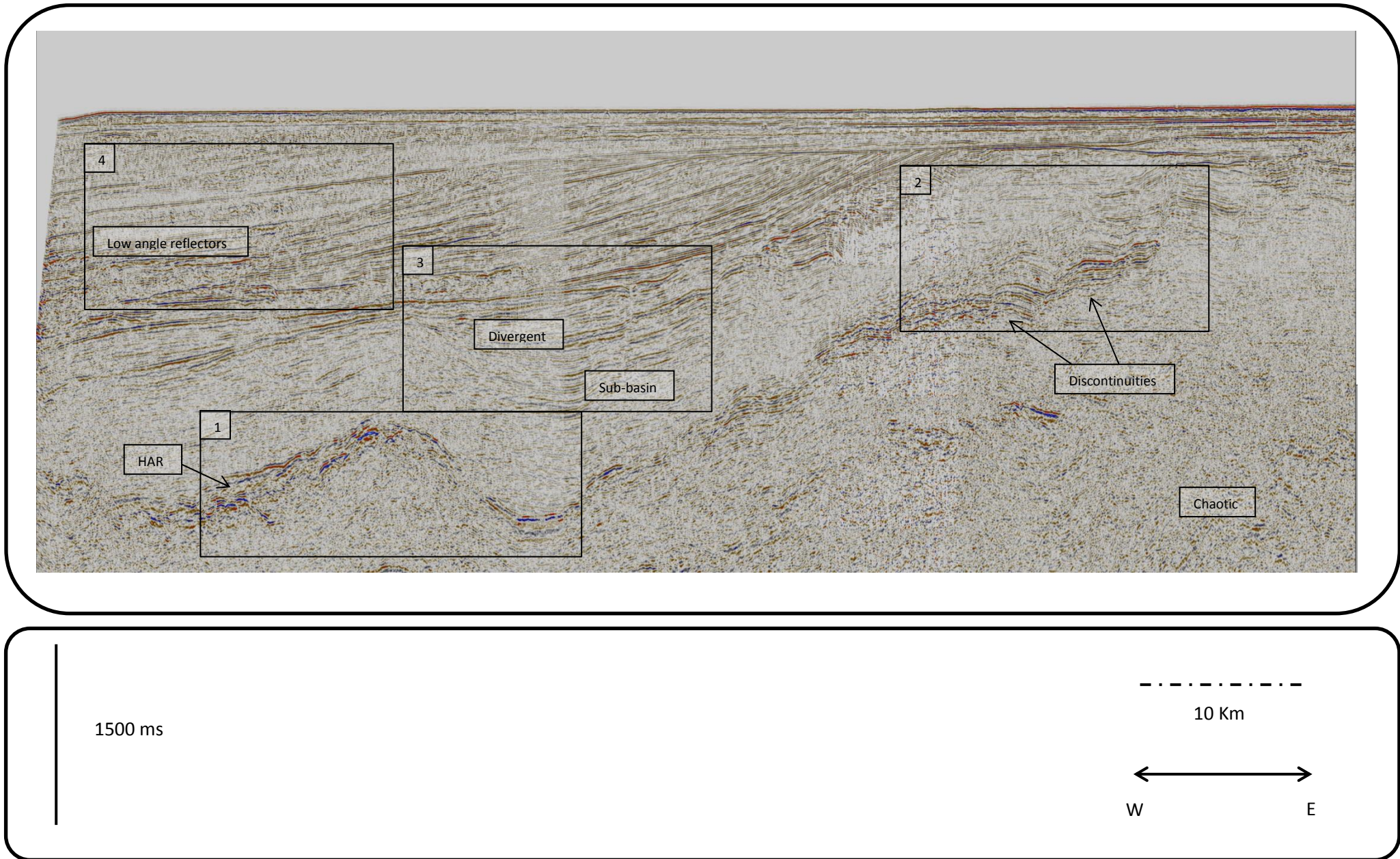
Figure 52. Seismic Line NPD-BJV2-7305 with initial observations and displayed subsections.

4.5.2.   INTERPRETATION AND GEOLOGICAL HISTORY

Upper Paleocene – Lower Eocene

Only the top of the Upper Paleocene-Lower Eocene strata was interpreted, the high amplitude reflections caused by the volcanic rocks (visible in the western areas, see image 52). These extrusive rocks were originated during the rifting and continental breakup of the Norwegian-Greenland Sea during Paleocene-Eocene transition.

The High Amplitude Reflectors caused by the volcanic activity (HAR) show a folding shape, probably caused by some transpressive event during Oligocene time that led faulting and subsidence of the upper strata (Middle Eocene).

In comparison with the previous seismic line (NPD-BJV2-86-7335), it is not possible see the eastern boundary fault. Instead of this, it was interpreted a faulted setting that affected the Middle Eocene strata and the Upper Paleocene-Eocene strata. The origin of these faults is probably related to the continental breakup of the Norwegian-Greenland sea and the shear margin stage that dominated the entire area (trantensional effects could explain this normal faulting).

Middle Eocene- Late Miocene

In these strata only were possible interpreted one intra middle Eocene horizons. The interpretation was mainly based following seismic patterns, because the base line does not cross it and the North-South line (NPD-BJV2-86-1645) cross it far away in the eastern part.

The main characteristic of these strata is the description of one sub-basin (see subsection 3, where appears a divergent seismic pattern) shaped by the folding of the Middle Eocene strata. This sub-basin was probably originated due to fault generation in the western part. The divergent pattern in this sub-basin could be described as syn-deposition during the fault activity. The origin of this fault could be explained by the Early Oligocene fault reactivation (Faleide et al., 1998). But the absence of a precise age in the reflectors of these strata makes difficult the suggestion of a particular regional event to explain the generation of this sub-basin (see section 3, Figure 50 and 52).

According to some authors, thick Miocene strata were deposited, but it was mainly eroded by a Late Miocene-Pliocene Uplift (Faleide et al., 2008). A second theory suggests a condensed Miocene section that was also eroded by the tectonic uplift. This condensed section was originated during the transpression and activation of some Oligocene faults (Eidvin et al., 1998). Probably this sub-basin (see section 3) was mainly filled with Oligocene-Miocene sediments.

Miocene to Pliocene

The Base Pliocene marks the evidence of the major tectonic uplift during these times. After this initial tectonic uplift, a several episodes of uplift and erosion affected this area through all the Pliocene and Pleistocene times. Initial tectonic uplift is followed by intensive glacial erosion, compensated by isostatic uplift (Dimakis et al., 1998). Easterly tilting was facilitated by subsidence of the hanging wall along the eastern boundary fault and the central eastern fault. Some Oligocene fault reactivation is proposed as consequence of this major tectonic event (Eidvin et al., 1998).

Pleistocene-Pliocene

The Base Pliocene mark the erosive surface created by the proposed tectonic uplift and successive erosion during late Miocene times (BP, figures 53 and 54). It can be distinguished at least four intra-Pliocene surfaces that indicated a clear erosional truncation of the reflectors (IP 2,IP 3, IP 4, IP 5, Figures 53 and 54). Glacio-Isostatic tectonic cycles could also explain these erosive surfaces. These intra-Pliocene erosional surfaces should be related to uplift events and glacial cycles. It is possible distinguish at least three recent and distinct Quaternary erosional cycles are presents in the seismic (Base Quaternary, IQ 1 and IQ 2).
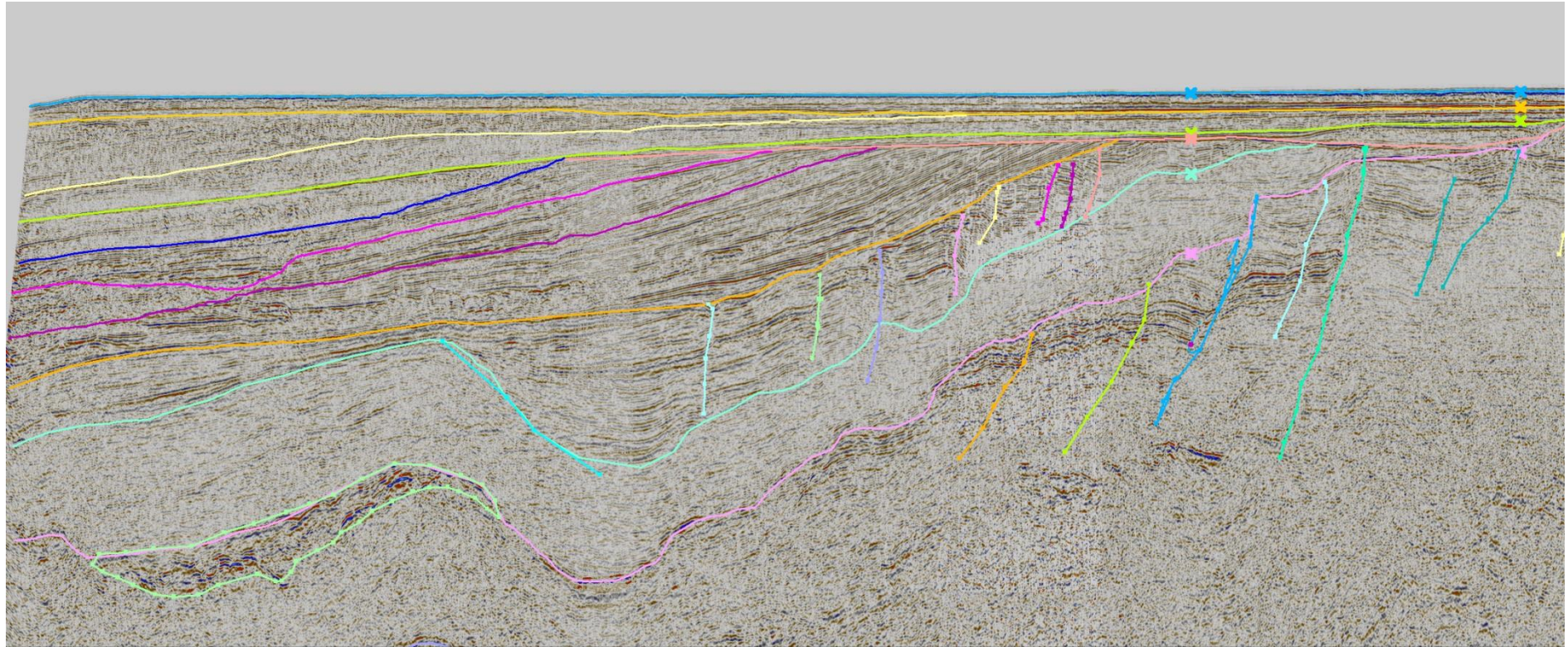
— Sea bottom	— Base Pliocene
— Intra Pleistocene I	— Intra Middle Eocene
— Intra Pleistocene II	— EE-LP= Early Eocene/ Late Paleocene
— Base Pleistocene/ Base Quaternary	
— Intra Pliocene V	
— Intra Pliocene IV	
— Intra Pliocene III	
— Intra Pliocene II	

1500 ms

10 Km

W   E
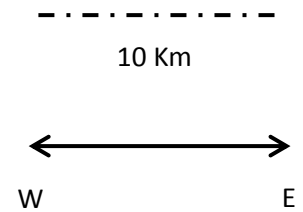
Figure 53. Seismic Line NPD-BJV2-7305 with initial observations and displayed subsections.
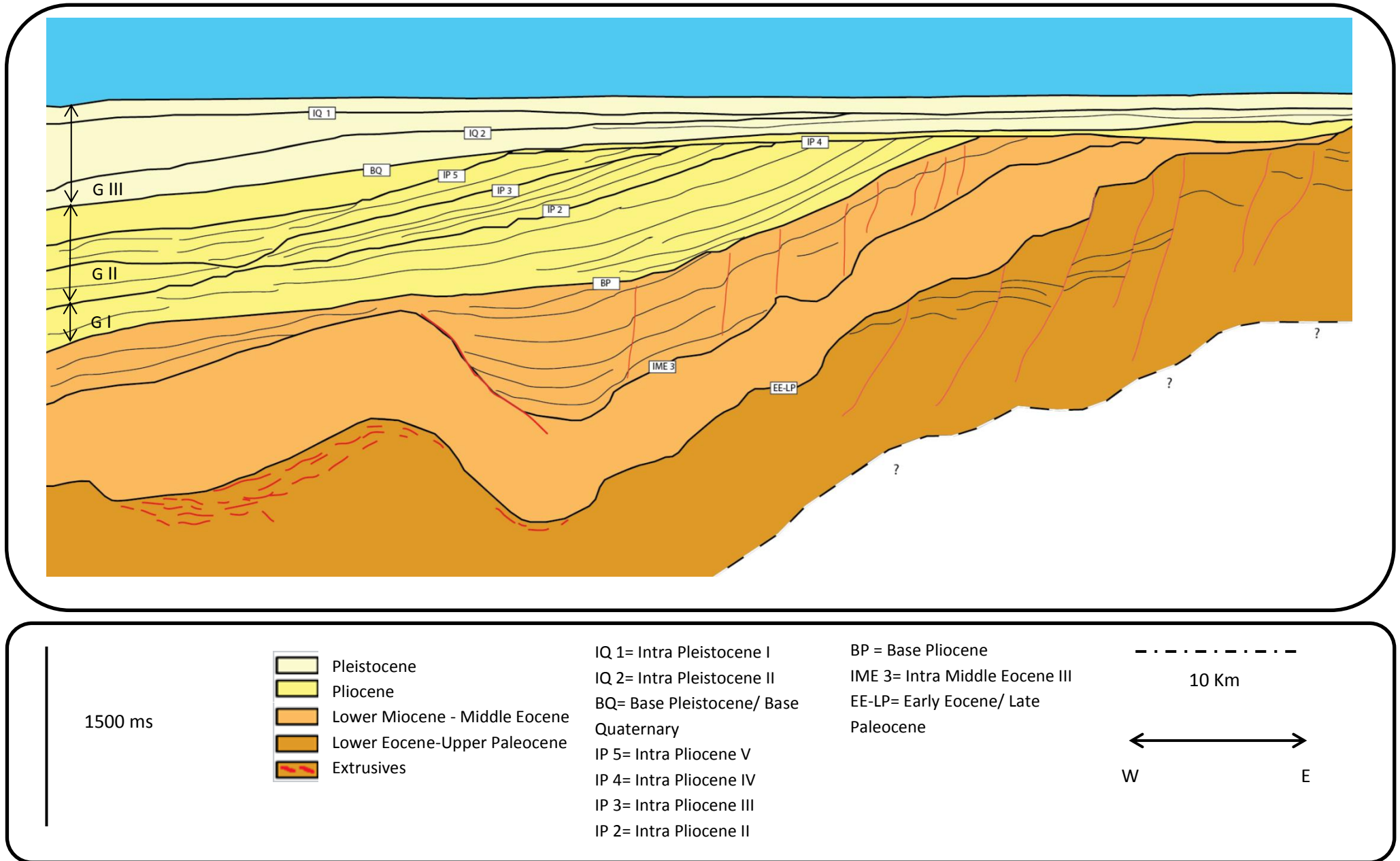
Figure 54. Geological model from the seismic line NPD-BJV2-7305

4.6. NPD-BJV2-86-7255

The line NPD-BJV2-86-7255 is the most southern line that has east-west direction. It only crosses other seismic lines: NPD-BJV2-86-1645 (with south-north direction). This line does not cross the base line, making imprecise the interpretation and the age of the main horizons.

The seismic line has a length of 110 km and were mainly interpreted 75 km (focused in the area with better resolution in the western part, see figure 23 with the colored section). According to the structural maps of the area, this seismic line is entirely over the Sørvestsnaget basin. It is the only line that does not have extension over the Vestbakken Volcanic Province (see figure 23).

The interpretation of this line should have a close history with the rest of the seismic lines, but it has several differences. Like in the previous seismic line (NPD-BJV2-86-7305) the eastern boundary fault does not appear, the western sub-basin is not possible to interpreted, and also it is the only seismic line where the volcanic reflectors does not appears.

4.6.1.   OBSERVATIONS

The Upper part of the seismic line is dominated by clear low angle reflections. In depth, the patterns become less clear and the resolution decrease. Two subsections were selected in the seismic line NPD-BJV2-86-7255 for a better understanding and description of the seismic image.

1. In the eastern part of the image there is setting of discontinuities, interpreted later as a group of faults. The areas under these discontinuous reflectors show a chaotic pattern, due to the missing of resolution in depth. Above these discontinuous reflectors, it is possible observe low amplitude reflectors with a more coherent pattern.
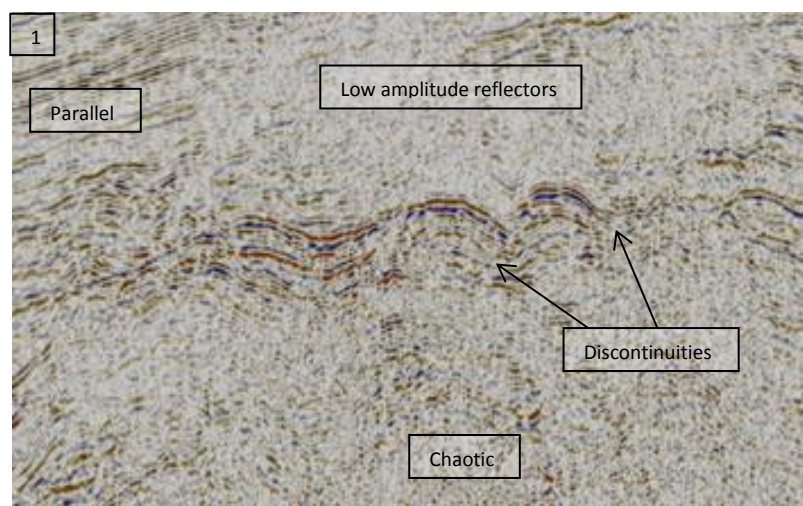
Figure 55. Subsection 1 from the seismic line NPD-BJV2-86-7255. In the eastern part of the image, it is possible observe some discontinuities in the reflectors. These discontinuities were then interpreted as a set of faults in the Upper Paleocene- Early Eocene strata.

2. Dominating the western part, the large depositional wedge is also present in this seismic line. It shows low angle reflectors, and some truncations marks the boundaries between the packages of the reflectors. Some discontinuities in the reflectors are visible in this package.
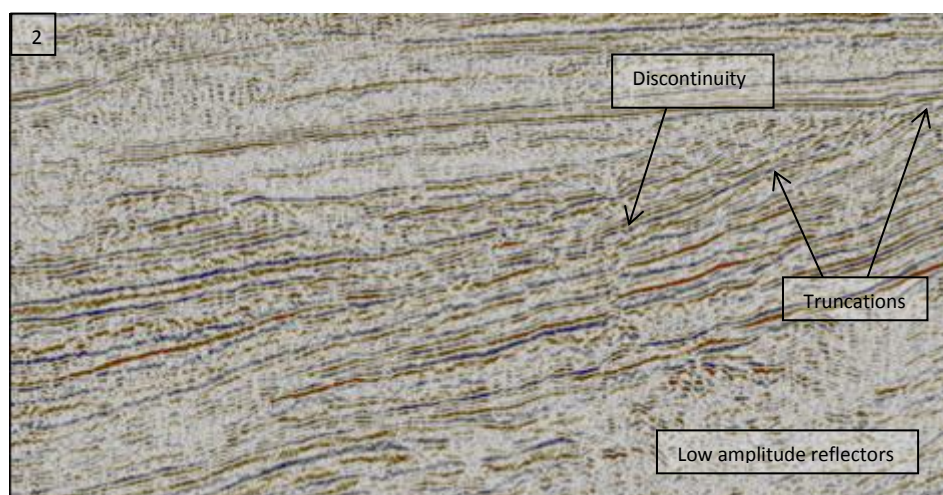
Figure 56. Subsection 2 from the seismic line NPD-BJV2-86-7255. Some truncations are visible in the image, and then interpreted as part of the uplift and erosional cycles. Discontinuities in the reflections are also visible; these were interpreted as accommodation faults.
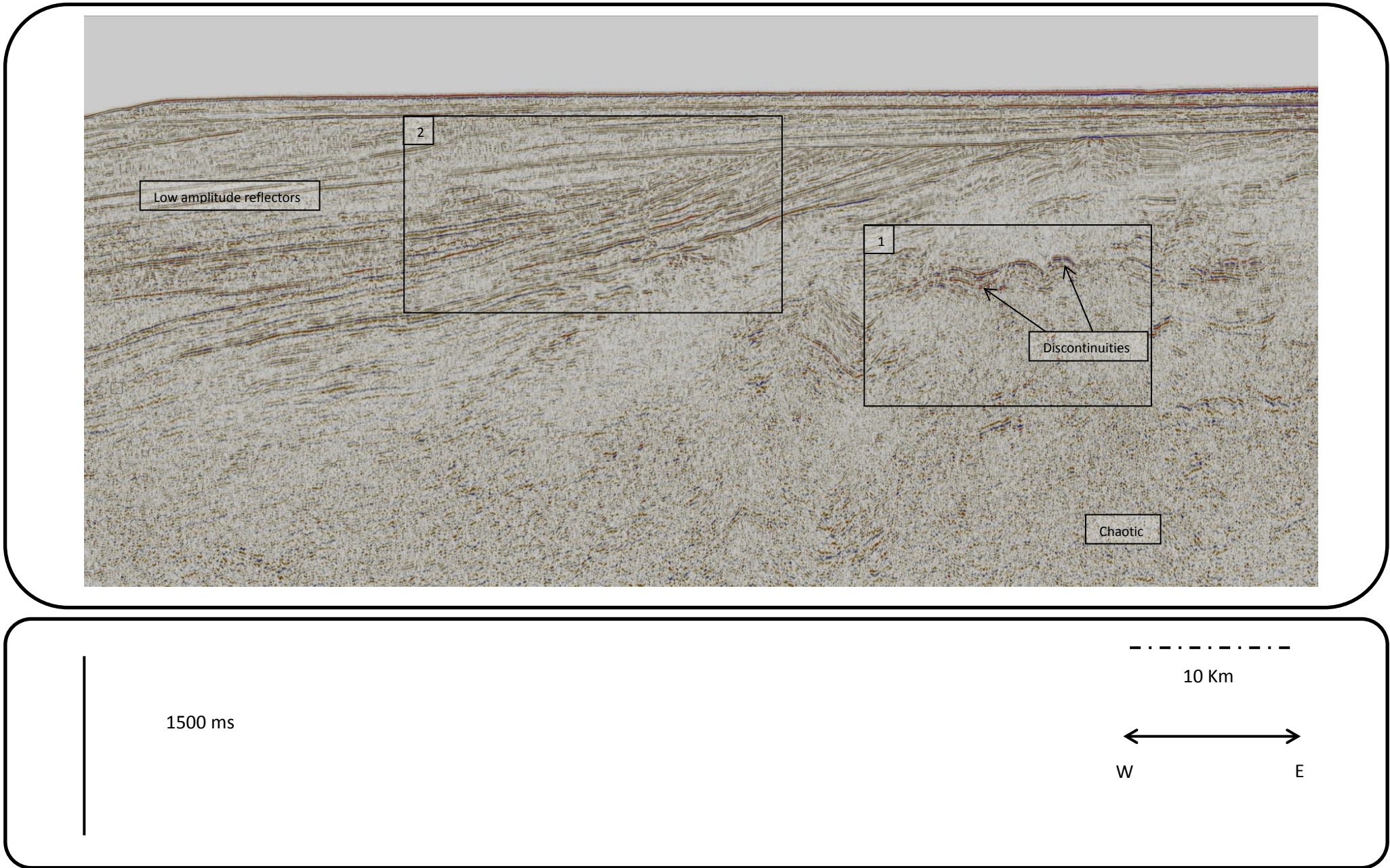
Figure 57. Seismic Line NPD-BJV2-7255 with initial observation and displayed subsections.

4.6.2.　　INTERPRETATION AND GEOLOGICAL HISTORY

Upper Paleocene – Lower Eocene

Only the top of the Upper Paleocene-Lower Eocene strata was interpreted, mainly based in the seismic patterns. The HAR are absent, suggesting that the volcanic activity was not present in this area.

Only the faulted section in the eastern part was suggested as Upper Paleocene-Lower Eocene strata (see section 1). The origin of these faults is probably related to the continental breakup of the Norwegian-Greenland Sea and the shear margin that dominated the entire area (trantensional effects could explain this faulting).

Middle Eocene- Late Miocene

In these strata only were possible interpreted one intra middle Eocene horizons. The interpretation was mainly based following seismic patterns, because the base line does not cross this line and the North-South line (NPD-BJV2-86-1645) cross it far away on the eastern section.

According to some authors, thick Miocene strata were deposited, but it was mainly eroded by a Late Miocene-Pliocene Uplift (Faleide et al., 2008). Other theories suggest a condensed Miocene section that was also eroded by the tectonic uplift (Eidvin et al., 1998).

Miocene to Pliocene

The Base Pliocene marks the evidence of the major tectonic uplift during these times. After this initial tectonic uplift, a several episodes of uplift and erosion affected this area through all the Pliocene and Pleistocene times. Initial tectonic uplift is followed by intensive glacial erosion, compensated by isostatic uplift, which induce an elevated glacial terrain (Dimakis et al., 1998). Easterly tilting was facilitated by subsidence of the hanging walls along the eastern boundary fault and the central eastern fault. Some Oligocene fault reactivation is proposed as consequence of this major tectonic event (Eidvin et a.l, 1998).

Pleistocene-Pliocene

A major erosional surface marks the boundary between the Pliocene-Pleistocene wedge (Glacial) and older strata (Pre-glacial). The Base Pliocene surface was created by the

proposed tectonic uplift and successive erosion during late Miocene times (BP, figures 58 and 59). It can be distinguished at least two intra-Pliocene surfaces that indicated a clear erosional truncation of the reflectors (IP 2, IP 5, Figures 58 and 59). These intra-Pliocene erosional surfaces should be related to uplift events and glacial cycles. It is possible distinguish at least three recent and distinct Quaternary erosional cycles in the seismic (Base Quaternary, IQ 1 and IQ 2).

— Sea bottom	— EE-LP= Early Eocene/ Late Paleocene
— Intra Pleistocene I	
— Intra Pleistocene II	
— Base Pleistocene/ Base Quaternary	
— Intra Pliocene V	
— Intra Pliocene II	
— Base Pliocene	
— Intra Middle Eocene III	

1500 ms

10 Km

W ←——————→ E
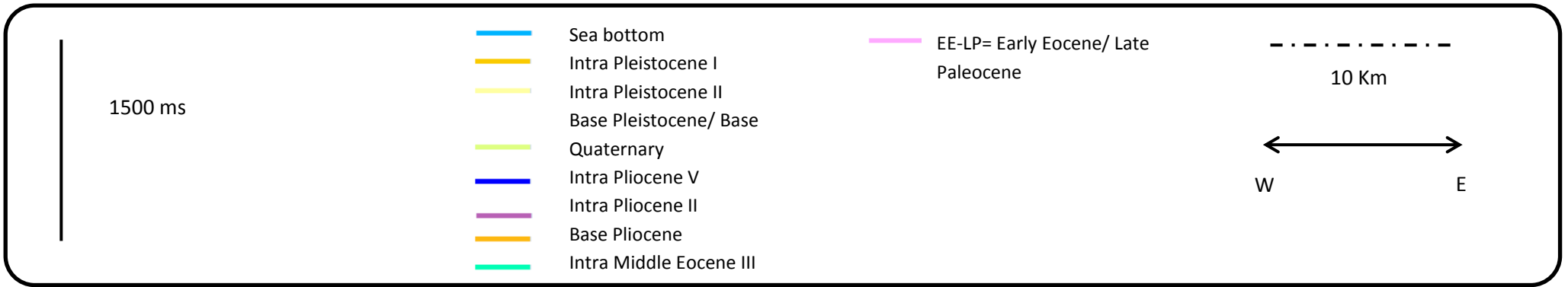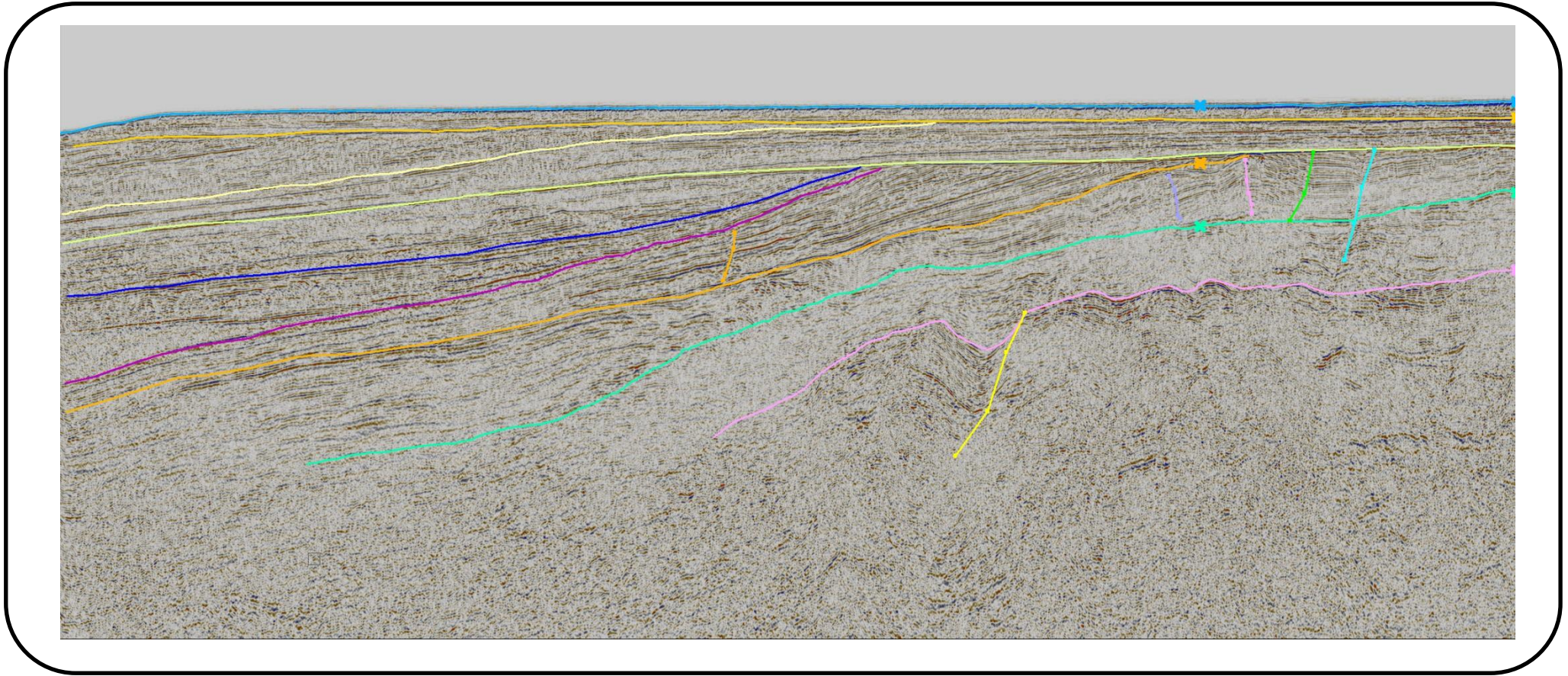
Figure 58. Interpreted horizons in the seismic line NPD-BJV2-7255.
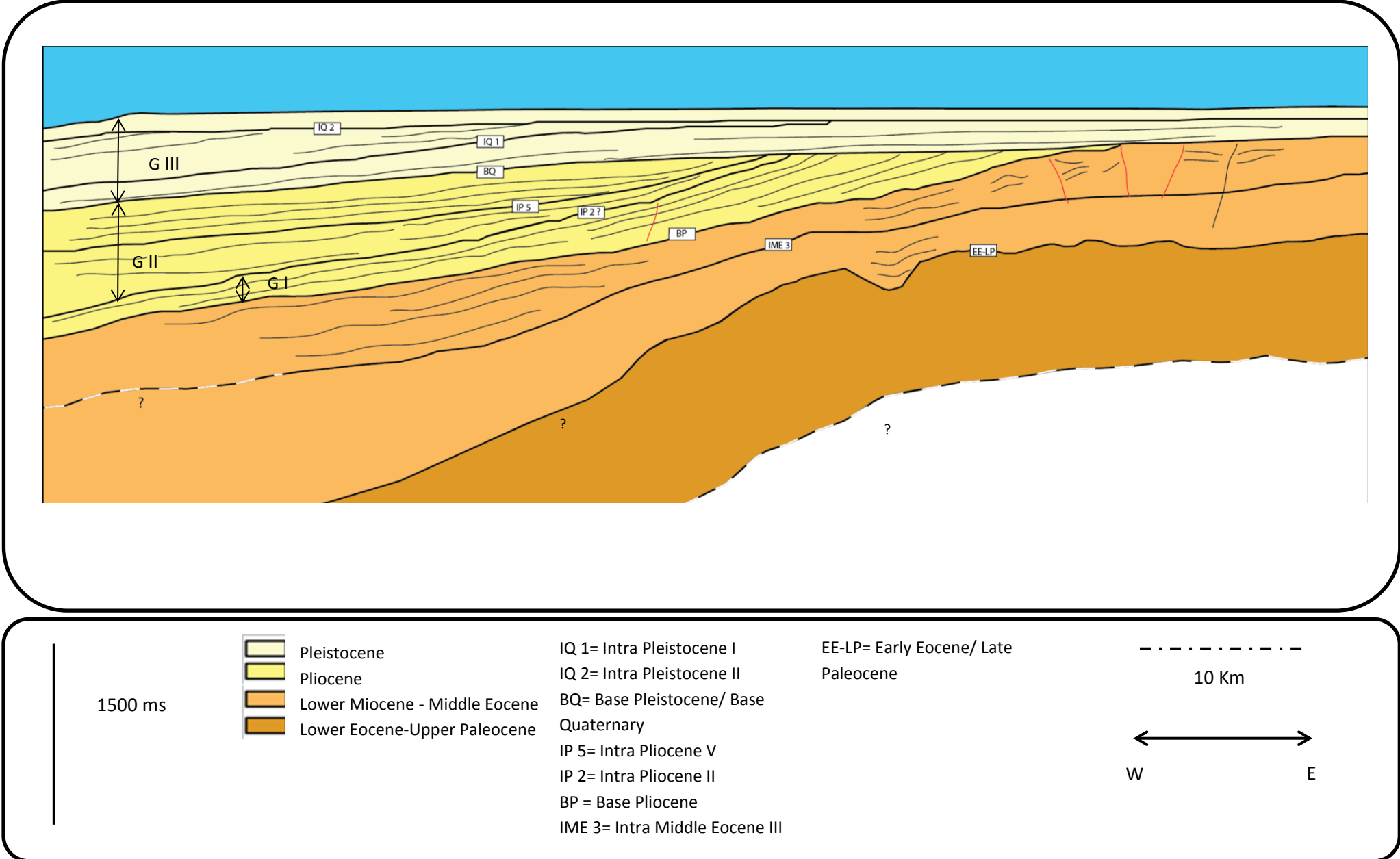
Figure 59. Geological model from the seismic line NPD-BJV2-7255.

4.7. NPD-BJV2-86-1645

The Line NPD-BJV2-86-1645 is the only seismic line with north-south direction. It is also de only seismic line that crosses all the seismic lines in this study.

This is the longest seismic line in this study with 290 km but were mainly were mainly interpreted 75 km (focused in the section crossed by the other seismic lines, see figure 23 with the colored section). According to the structural maps of the area, the study section of the seismic line is mainly over the Sørvestsnaget basin and just in one extreme is possible interpreted the Vestbakken Volcanic Province (see figure 23).

The main features also appear in this seismic line, but with a different point of view: The Eastern boundary fault, the western sub-basin, and a short section of the Vestbakken Volcanic Province. Only the upper thin part of the Pliocene-Pleistocene wedge (Bjørnøya fan) performs in this seismic image.

4.7.1.   OBSERVATIONS

Parallel and divergent reflections with medium to high amplitude predominate in the upper-north part of the seismic section (later interpreted as the western sub-basin). In the upper-south part predominates medium to low amplitude reflectors. The lower part has low resolution, showing a chaotic pattern. Three subsections were selected to improve the description of this seismic line:

1. Subsection 1 shows a short segment of the High amplitude reflections (HAR). Above HAR, it is possible observe low amplitude reflectors with a more coherent pattern. Beneath the HAR predominates a chaotic pattern (see figure 60).the HAR appears but shifted in two sections. This feature could be interpreted as fault activity after the volcanic extrusion.
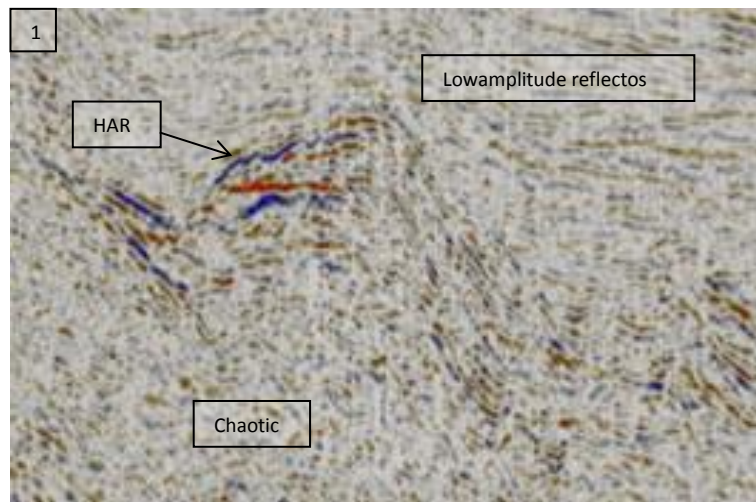
Figure 60. Subsection 1 from the seismic line NPD-BJV2-86-1645 (see figure 63). It is possible observe the high amplitude reflectors originated by the volcanic activity in the Vestbakken Volcanic Province. This segment of the HAR only represents a short section of all the extension of this volcanic activity.

2. Subsection 2 is characterized by the presence of a divergent pattern in the north part (see figure 61). Some truncations are visible and a main discontinuity in the extreme north part. Strong to middle amplitude reflectors are above middle to low amplitude reflectors (see figure 61). Several discontinuities in the reflectors are visible along this section, showing a tectonically complex history.
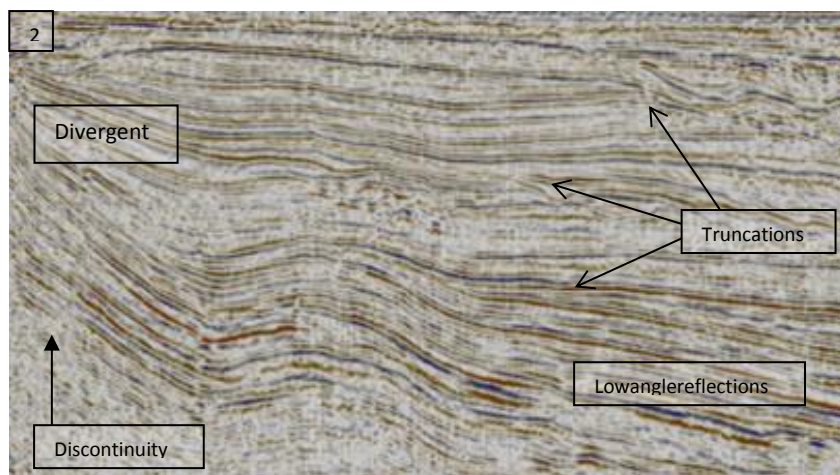
Figure 61. Subsection 2 from the seismic line NPD-BJV2-86-1645 (see figure 63). The main discontinuity in the North part (left hand of the image) is interpreted later like the eastern boundary fault.

The divergent pattern is possible consequence of the fault activity. The truncations mark historical erosional events, studied with more details in the interpretation section.

3. Subsection 3 shows the discontinuities in the middle upper part of the image. Also there are divergence and truncation of the strata. The low amplitude and chaotic reflectors in the lower part tends to go up in the south area, probably as consequence of the eastern boundary fault (appears like a mean discontinuity, see figure 62).
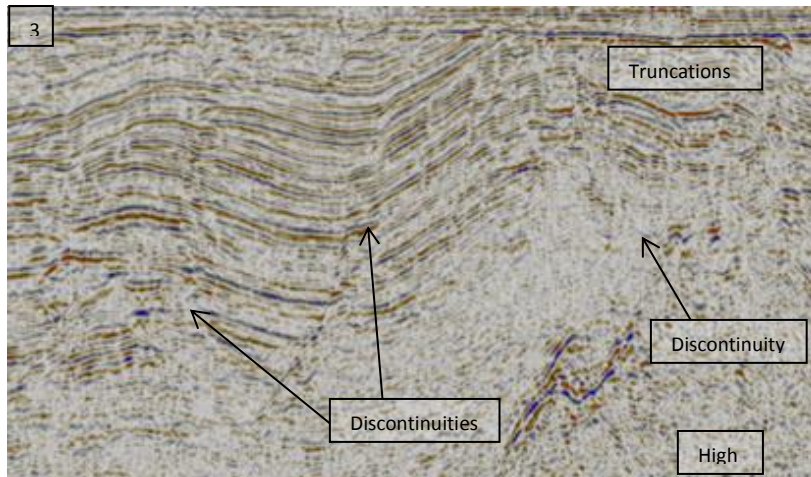
Figure 62. Subsection 3 from the seismic line NPD-BJV2-86-1645 (see figure 63). The subsection 3 was selected with the purpose of remark the presence of discontinuities in the middle upper part of the image. These set of discontinuities was later interpreted as part of the eastern boundary fault setting. Also some divergent pattern appears close to the main fault, probably as consequence of the faulting activity.
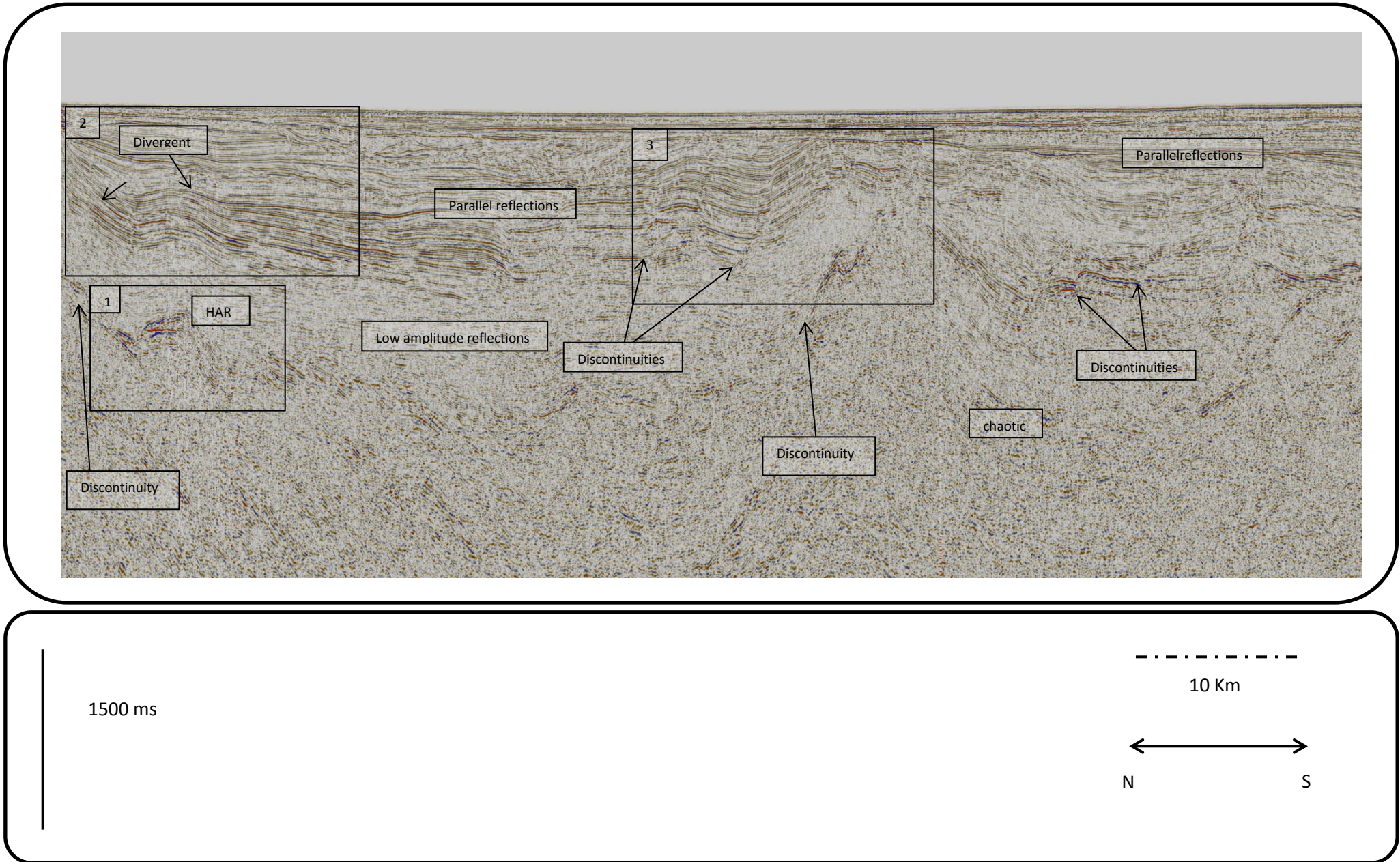
Figure 63. Seismic Line NPD-BJV2-1645 with initial observation and displayed subsections.

4.7.2.   INTERPRETATION AND GEOLOGICAL HISTORY

Upper Paleocene – Lower Eocene

Like the HAR only represent a short section in this seismic image, were used other seismic features to follow the top of this package (follow strong amplitude reflections, distinguishing between the seismic patterns, etc.). In general, The Top of the Upper Paleocene-Lower Eocene strata shows 2 highs and one bending shape in the western sub-basin, probably caused by the subsidence and fault activity of the eastern boundary fault. This main fault crosses 2 times the seismic line (see figure 64).

The High amplitude reflector (HAR) was interpreted like the top of the Upper Paleocene-Lower Eocene. The HAR are interpreted specifically like volcanic rocks originated during the rifting and continental breakup of the Norwegian-Greenland Sea during Late Paleocene to Early Eocene times. Under this interpreted volcanic intrusion was no possible due to the masking effect.

In the southern part is possible observe some faulting (see figure 64). The origin of these faults is probably related to the continental breakup of the Norwegian-Greenland Sea and the shear margin that dominated the entire area (trantensional effects could explain this faulting).

Middle Eocene

In these strata were possible interpreted three intra middle Eocene horizons. The interpretation was mainly based crossing and following the horizons interpreted in the base line and comparing the seismic patterns and features. The observed divergent pattern appears close to the main fault, probably as consequence of the faulting activity. This pattern could be consequence of the subsidence and the syn-deposition during the periods of extensional faulting activity during middle Eocene times (Eidvin et al., 1998).

Early Oligocene – Late Miocene

In these strata, it was no possible interpreted an intra-horizon (Intra Oligocene or Intra/Base Miocene) only the base Oligocene and the top of the Miocene strata (base Pliocene wedge). After a period of transpression during Eocene-Oligocene transition, it is proposed a gentle subsidence during the early Oligocene. Extension (Middle Oligocene- Upper Oligocene) after

the compressional event could explain faulting in the Middle Eocene and some of the Oligocene strata. These faults could be also explained by the Early Oligocene fault reactivation (Faleide et al., 2008).

Similar to the history of the previous lines, some suggested syn-deposition of lower Miocene strata is observed in the seismic line; it was probably originated during reactivation of the Eastern boundary fault, and eventual subsidence of the western flanks. According to some authors, thick Miocene strata were deposited, but it was mainly eroded by a Late Miocene-Pliocene Uplift (Faleide et al., 2008). Other theories propose a condensed Miocene section that was also eroded by the tectonic uplift. This condensed section was originated during the transpression and activation of some Oligocene faults (Eidvin et al., 1998).

Miocene to Pliocene

After this initial tectonic uplift, a several episodes of uplift and erosion affected this area through all the Pliocene and Pleistocene times. A clear evidence of this event is the clear base Pliocene truncation, which appears in all the seismic line. Initial tectonic uplift was followed by intensive glacial erosion, compensated by isostatic uplift, which induce the maintenance of an elevated and glaciated terrain (Dimakis et al., 1998). Easterly tilting was facilitated by subsidence of the hanging walls along the eastern boundary fault. Some Oligocene fault reactivation is proposed as consequence of this major tectonic event (Eidvin et al., 1998).

Pleistocene-Pliocene

Only the upper thin part of the Pliocene-Pleistocene wedge appears in this seismic image, something expected by the location of the line (in the other seismic lines, it cross the upper and thin part of the large depositional wedge). The Base Pliocene mark the erosive surface created by the proposed tectonic uplift and successive erosion during late Miocene times (BP, figures 64 and 65).

It could be interpreted only one intra-Pliocene surface that indicated an erosional truncation of the reflectors (IP 4, Figures 64 and 65). This intra-Pliocene erosional surface should be related to uplift events and glacial cycles. It is possible distinguish at least two recent and distinct Quaternary erosional cycles are presents in the seismic (Base Quaternary and Intra Quaternary II, IQ 2). Glacio-Isostatic tectonic cycles could also explain the origin of these Pliocene-Pleistocene erosional surfaces.
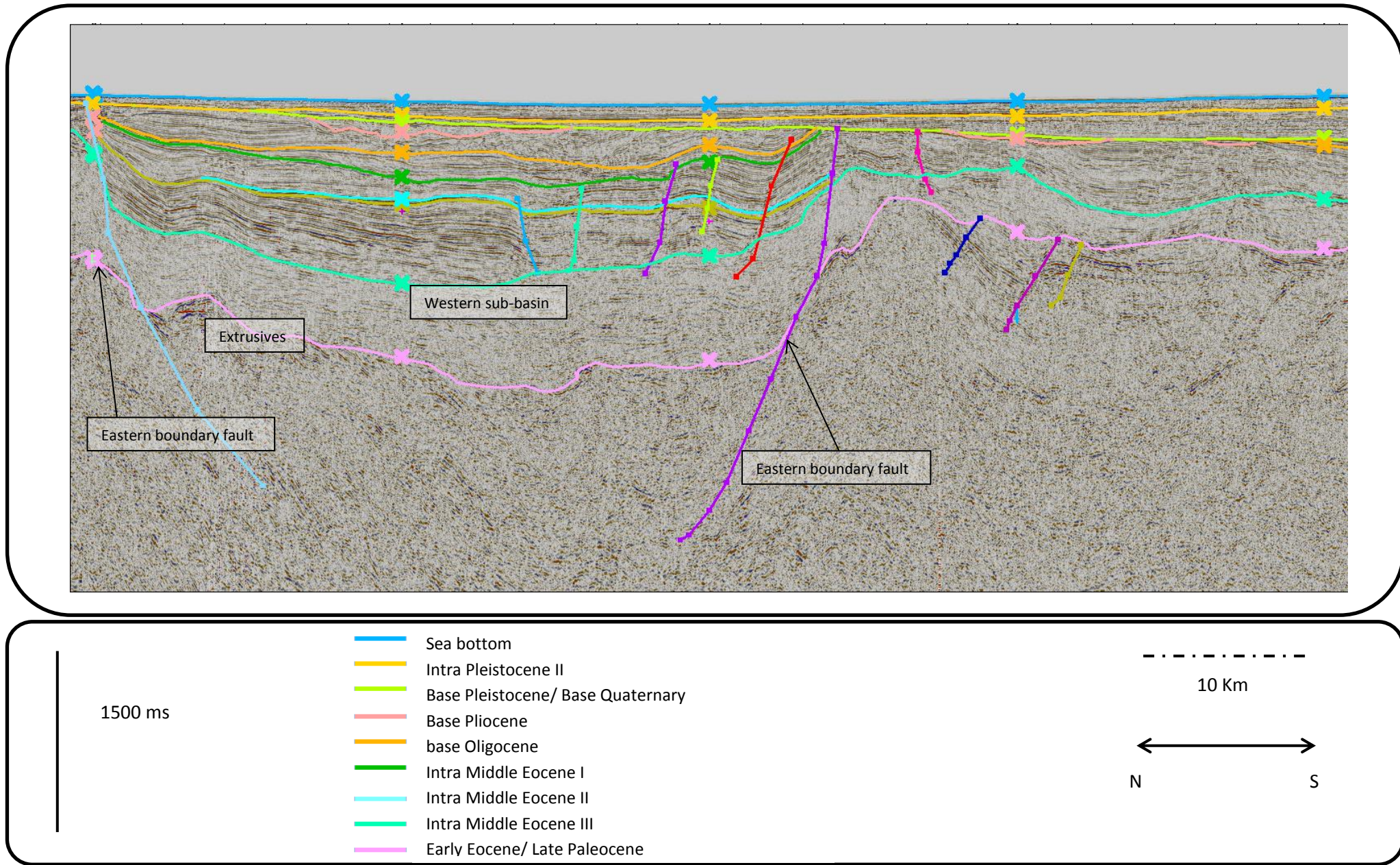
Figure 64. Interpreted horizons and other main features in the seismic line NPD-BJV2-7335.
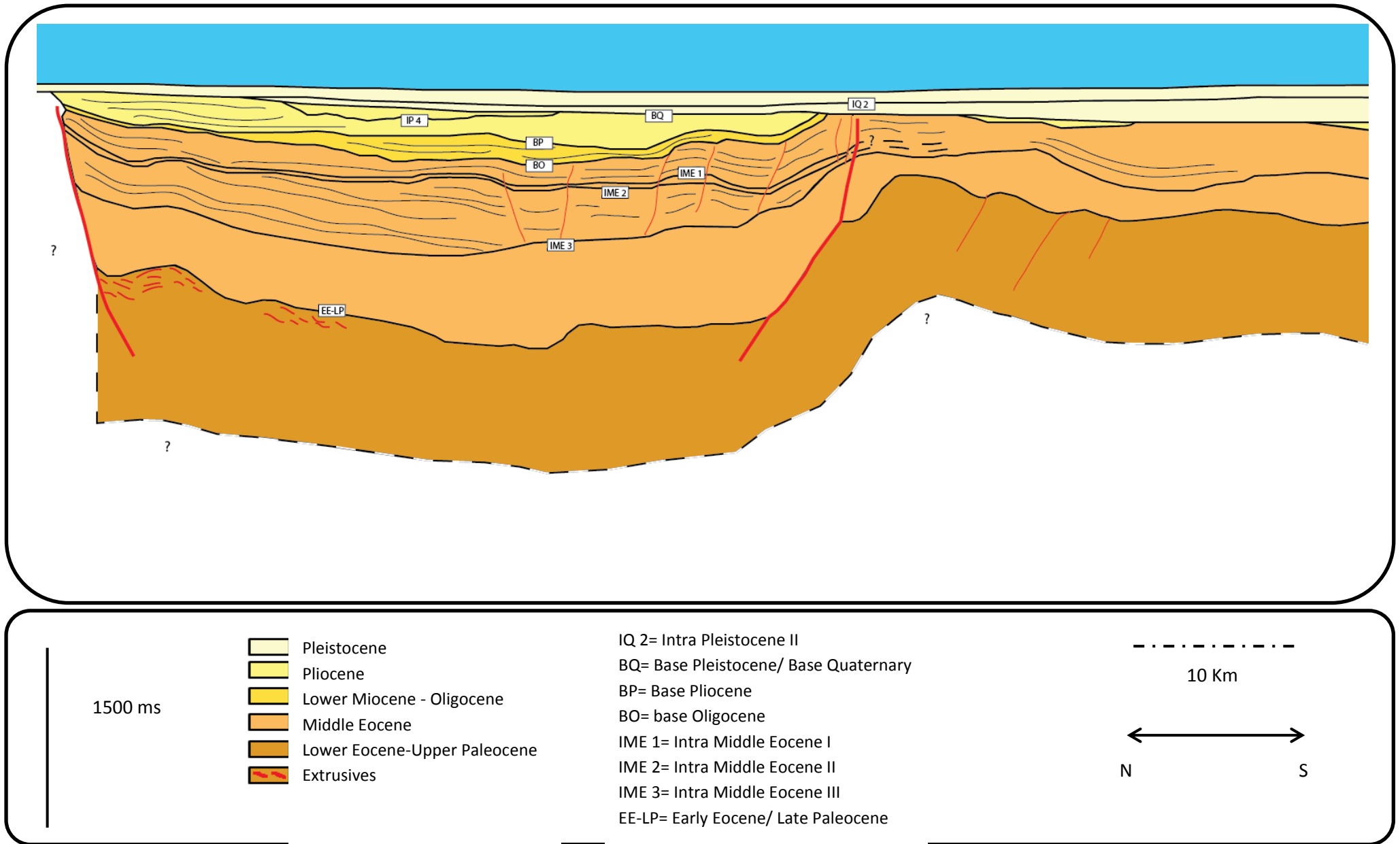
Figure 65. Geological model from the seismic line NPD-BJV2-1645.

4.8. TWO WAY TRAVEL TIME MAPS BASED IN THE SEISMIC INTERPRETATION

After interpreted the main horizons in the seven lines of this study, the next procedure was built the TWT of the tops horizons and other relevant intra-horizons. These maps will give us an idea of depth (in time) and topography of these surfaces. These results should be seen as a general view of the area, because the sampling is really rough (seven seismic lines in an area of almost 7500 km^2) and the interpolation usually creates features due to the mathematical interpolation, not based in the reality. The interpolation method used was the minimum curvature method, and it showed the best correlation with the expected geological model.

4.8.1.   TOP UPPER PALEOCENE-LOWER EOCENE

The Top-Upper Paleocene – Lower Eocene TWT (see figure 66) show some expected main features in the topography:

1. The eastern boundary fault marking the area between higher depths in the west and lower depths in the east.

2. The deeper areas in the west are consequence of the downward movement of the west flank and general subsidence due to the Pleistocene-Pliocene deposition.

3. The interpreted sub-basin in the line NPD-BJV1-86-7305 (section 4.5 of this chapter) appears clearly the western part of the map.

Figure 66. Two way travel time (TWT) map from the Top Upper Paleocene-Lower Eocene horizon

4.8.2.   BASE OLIGOCENE
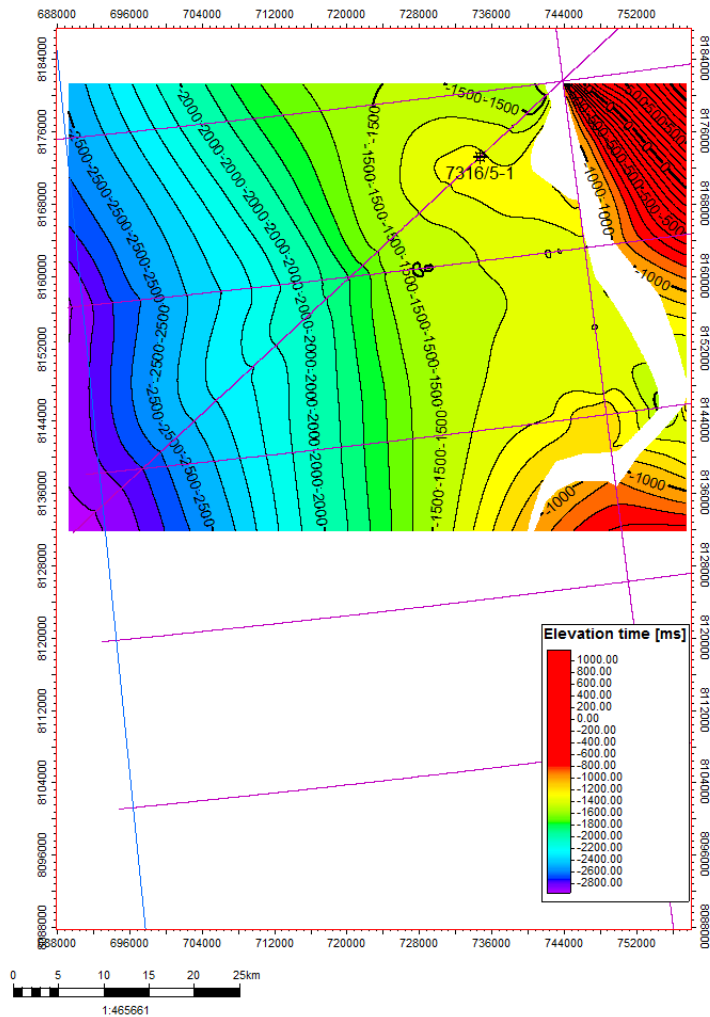
Figure 67. Two way travel time (TWT) map from the Top Upper Paleocene-Lower Eocene horizon

Only the base Oligocene horizon is showed in these TWT (see figure 67). The main features are distinguished:

1. The eastern boundary fault marking the area between higher depths in the west and lower depths in the east.

2. The deeper areas in the west are consequence of the downward movement of the west flank and general subsidence due to the Pliocene-Pleistocene wedge deposition.

3. The interpolated data in the east part of the eastern boundary fault is not completely dependable, because probably corresponds more to the mathematical extrapolation.

4.8.3.   PLESITOCENE - PLIOCENE HORIZONS

The Base Pliocene and four Intra Pliocene horizons were used to build the two way travel time maps from these strata (figure 68 and 69). The main characteristic of these five horizons, according to the TWT maps, is the tendency of get higher depths in the western part. This is probably helped by the subsidence caused by the deposition of thick Pliocene-Pleistocene sedimentary wedge. Also, the topographical setting after Oligocene times (starting of the passive margin) is an important factor to take account, because the lower areas (depocenter) were mainly located in the west. For the Pleistocene strata, two horizons were showed in these two way travel time maps (see figure 69). These Pleistocene maps have the same feature that the Pliocene horizons: general tilting to the west areas.
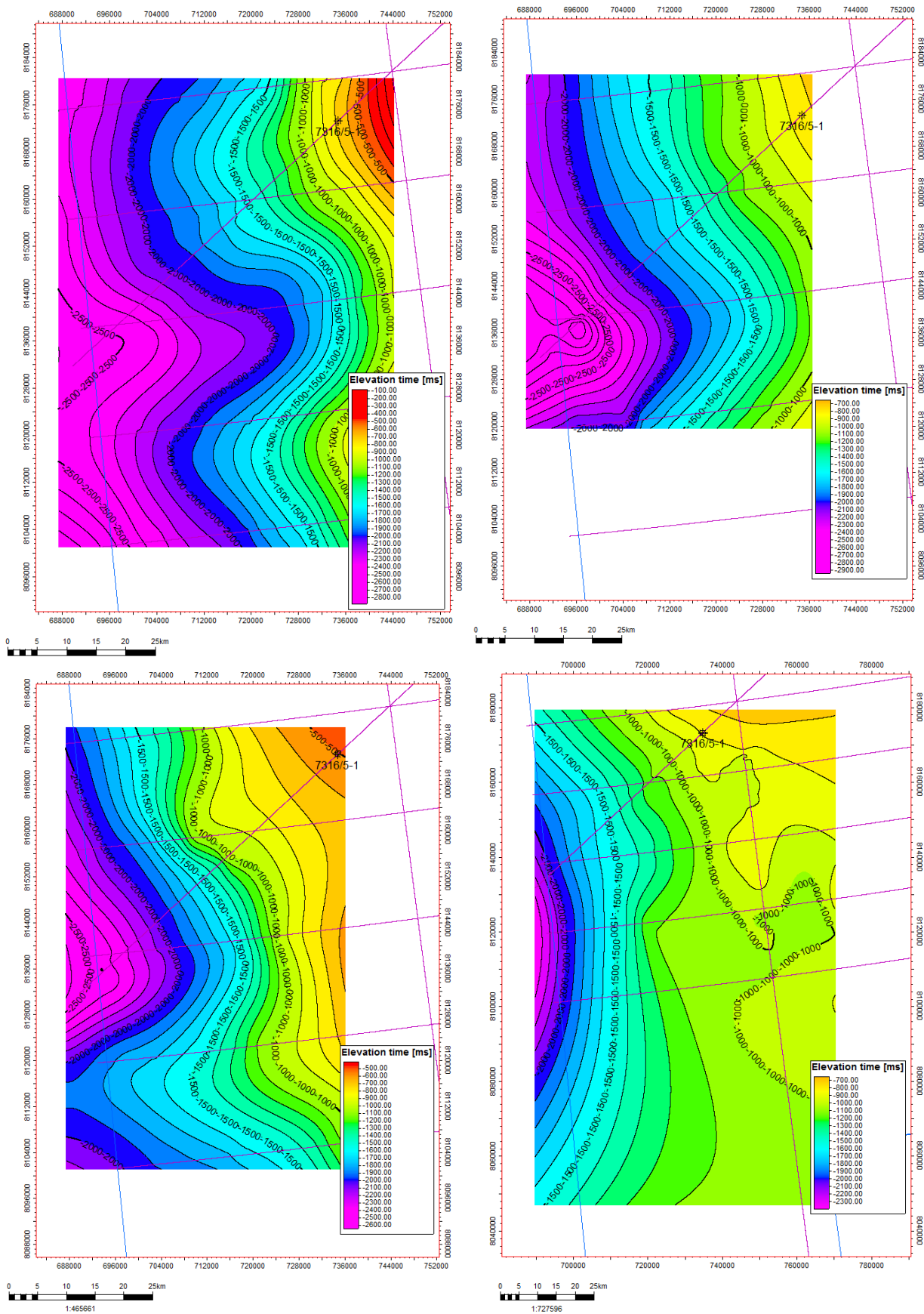
Figure 68. From top left to bottom right: Intra Pliocene II, Intra Pliocene III, Intra Pliocene IV and Intra Pliocene V horizons (for more details, check the previous sections of this chapter).
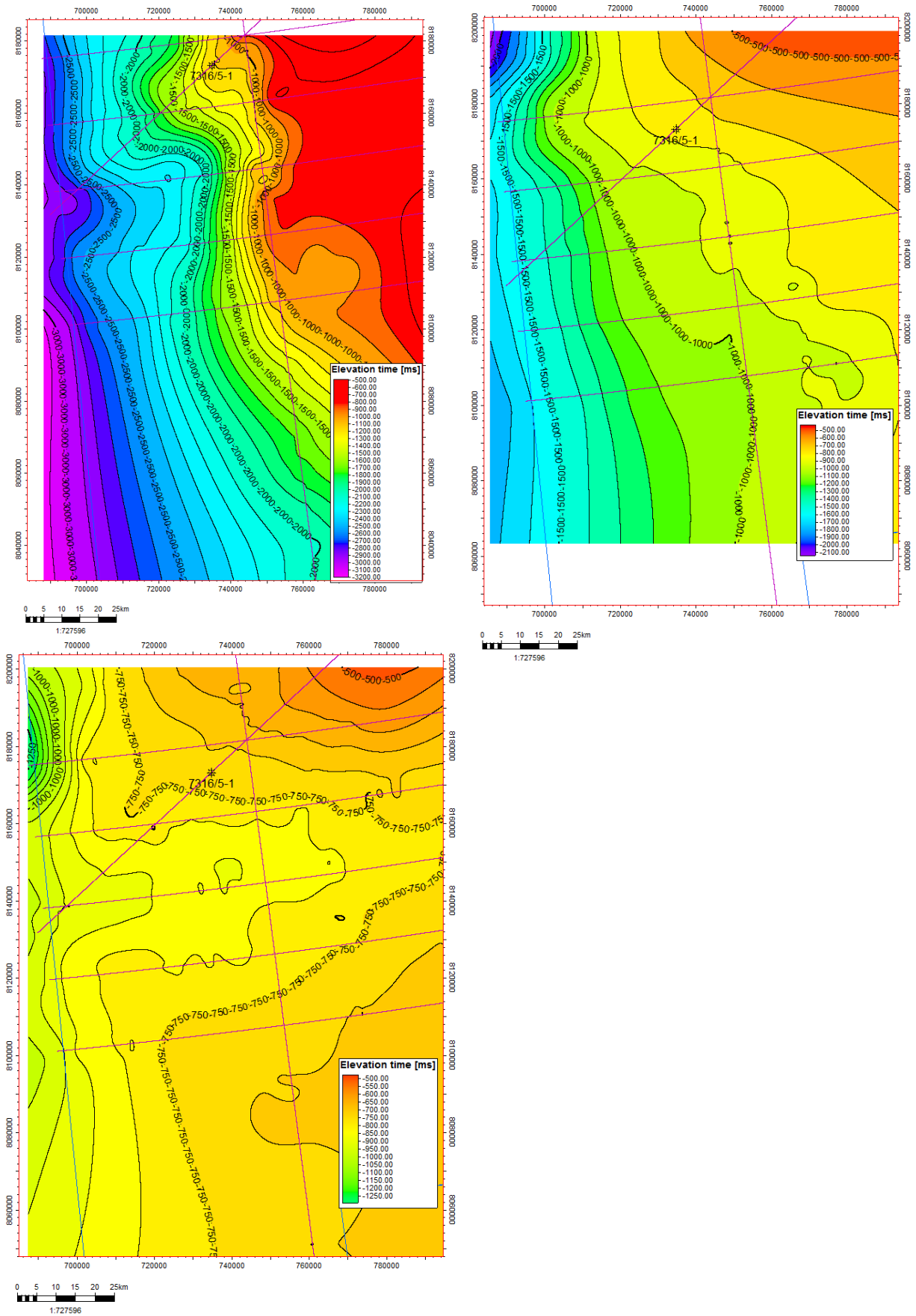
Figure 69. Top left: Two way travel time map from the Base Pliocene horizon. This map shows the base topography of the large sedimentary Pliocene-Pleistocene wedge. Top right: Base Quaternary. Bottom left: Intra Quaternary II.

4.9. ESTIMATION OF UPLIFT USING EMPIRICAL POROSITY-DEPTH TRENDS AND WELL DATA

Using empirical porosity-depth from the North Sea (Avseth et al., 2005), it was possible create an empirical gradient of the porosity according to depth. In the other hand, using logs from the well data and estimating the rock matrix density and fluid density, it was possible create a porosity curve from the density log. It was decided use the standard values for density: 2.65 g/cc for matrix (Standard Quartz density) and 1.00 g/cc for fluid (Standard water density).

These empirical formulas from Avseth et al. (2005) are based in the models of Ramm and Bjørlykke (1994). According to Avseth et al. (2005) the general trend of porosity for shales and sandstones should follow the next formula:

$$\varphi = 45e^{-(0.10+(0.27x0.1))Z} \quad \text{(formula for sandstones porosity)}$$

$$\varphi = 60e^{-(0.01+(0.22x2.0))Z} \quad \text{(formula for shale porosity)}$$

The Sands were calibrated with clean Heimdal formation sands at 2150-2160 m, and it was supposed a critical porosity of A=45. Shales were calibrated using Lisa formation shales at 2140-2154m, and the critical porosity was supposed A=60 (Avseth et al., 2005).

The main procedure to estimate the uplift, is first obtain the porosity from the density log and calculate the empirical depth-porosity trend suggested for Avseth et al. (2005). The second step consisted in adjust visually the empirical depth-porosity trend with the density porosity trend values, changing the depth values in the empirical trend and using a calibration point in the density-porosity curve. The difference between the depth value in the empirical trend and the depth value in the adjust trend is probably the value of the uplift.

The main assumption is that the shales or sandstones show porosities from bigger depths because these rocks were moved from depth areas to shallower during the uplift event. It is for that reason that was necessary change the value of Z to adjust the empirical curve to the density-porosity curve. The second assumption is that the Barents Sea formations have more or less the same burial depth time, and other burial variables like in the North Sea.

In the well 7316/5-1 were applied two trends, Sandstone trend and shale trend. But, according to the well data, the section where the formula should be more accurate (mechanical compaction stage) is mainly in the shale formation interval. For that reason, the shale trend was considered the most adequate to our purpose. The values to adjust the sand and shale depth-porosity curve were the next: Z for shale trend= Z±900 m; Tie point for shale =2250 m. The selection of the Tie point was based in the lithology suggested by the well (Sands should be dominant between the 500 until 900 m and the shales from 900 m until 2900 m).

A Middle Miocene Shale between 1100-2900 m was used to calibrate the empirical trend. Then the trend was visually moved from their original location, changing the value of Z.

In the figure 70 appears three logs: The first log contains the Gamma ray values of the well, and help us to differentiate roughly the sandstones from shales; The second log contains the shale and sand depth-porosity trends and the density-porosity log; The second log contains the shale and sand depth-porosity adjust trends and the density-porosity log.

According to this result and taking account some assumptions, the uplift in this area during Tertiary and Quaternary times was around 900±100 m (including the uncertainty in the adjustment of the trend).

This same procedure was applied to the well 7216/11-1S but was not necessary any adjustment (see figure 71). This well is also located in the western Barents Sea margin and it was expected a value of uplift (probably around 700 m). But, the adjustment due to uplift was not necessary because the lithology that penetrated this well are mainly Pliocene-Pleistocene rocks, deposited after the uplift and during the late Cenozoic glaciations.

The well 7216/11-1S shows almost 2000 m of thick Pliocene-Pleistocene sediments from the sedimentary wedge. The strata (sandstones and mainly shales) from this well correspond to recent material consequence of the uplift and glacial erosion. For that reason it was not necessary any uplift adjustment like in the well 7316/5-1 that shows shales affected by the tectonic uplift and subsequent rebound. In some way, this well can be taken as a control sample to valid the method and results obtained in the well 7316/5-1.

In the lower part of the well there are presences of sands and carbonates, corresponding to pre-glacial strata. Uplift adjustment was not applied because it could be correspond more to the chemical compaction stage and the adjustment is not clear to implement for the lithological composition (shales with interbreed carbonates and sands, Ryseth et al., 2003).
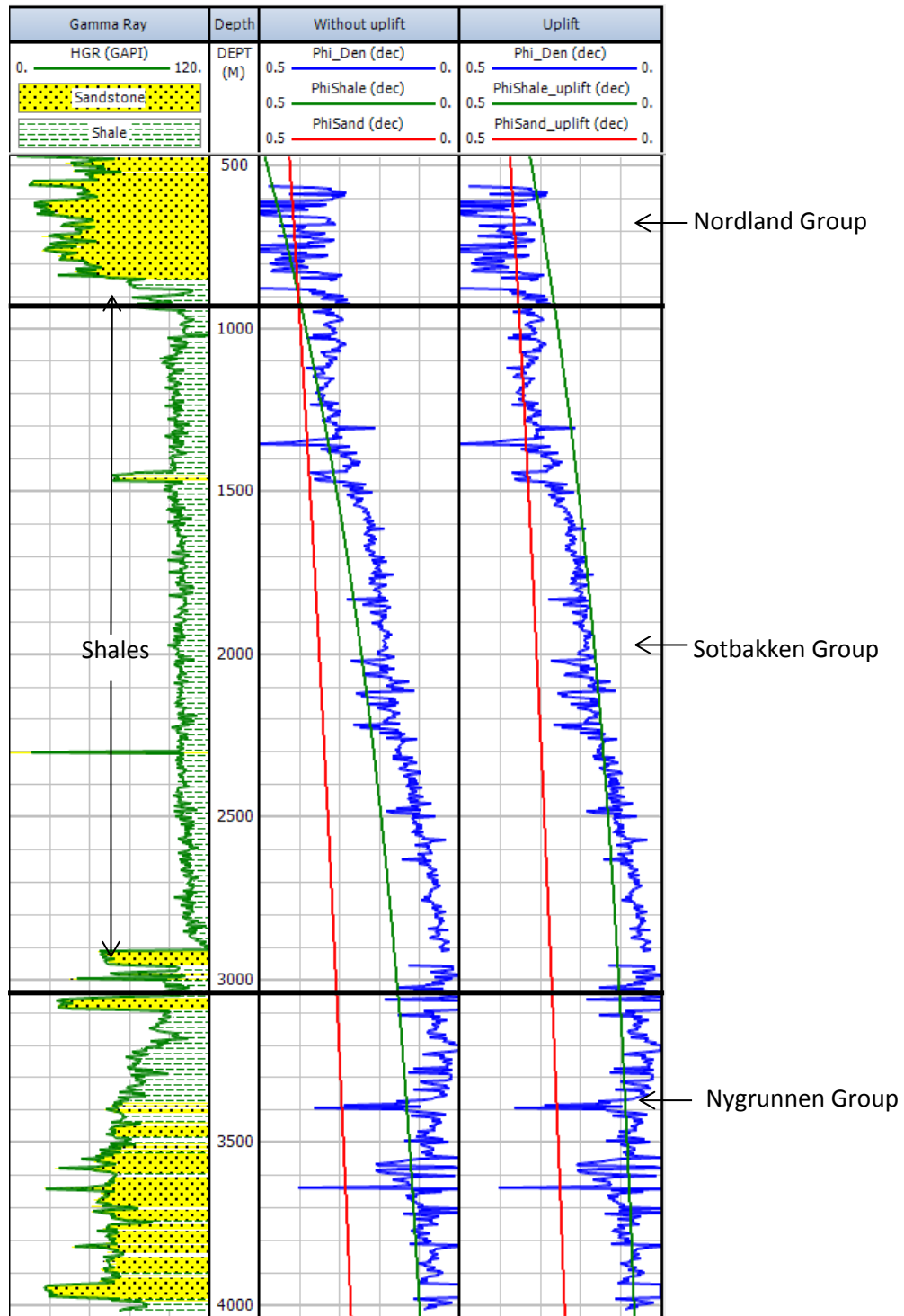
Figure 70. Adjustment of the empirical formulas for depth-porosity trends in shales and sands using the well 7316/5-1. The shale trends are mark in green and the sand trends are mark in red. In the picture, it is possible see the application of the adjustment in the shale curve, given an estimated uplift of 900-1000 m. This estimation is based in several assumptions and including more variables could improve the results.
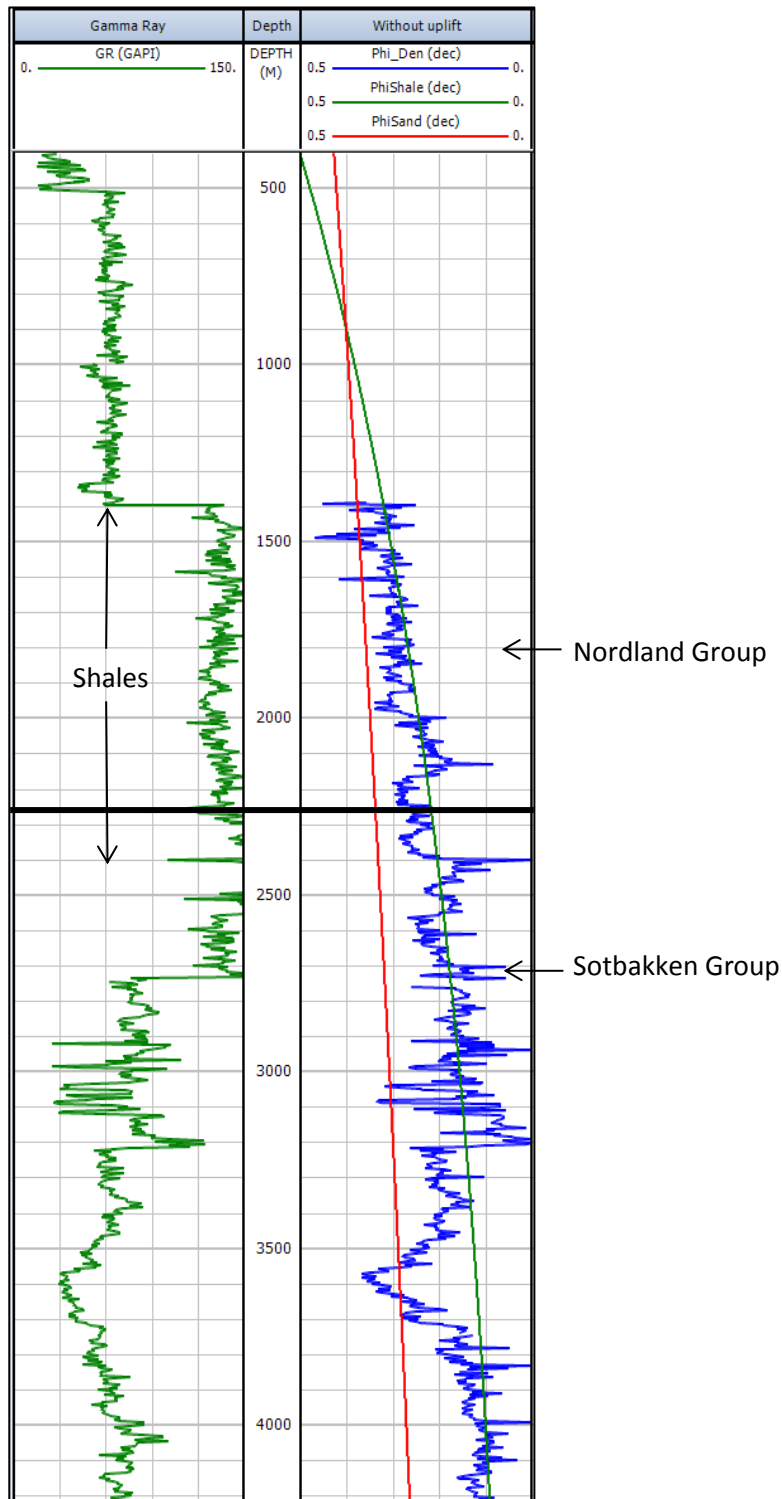
Figure 71. Depth-porosity trends in shales and sands using the well 7216/11-1S. Observe that the shales from the Nordland group (From 361 m up to 2246 m, Ryseth et al., 2003) does not require any adjustment because these shales correspond to glacial sequences from the Pliocene-Pleistocene strata and not from the pre-glacial strata affected by the uplift. Adjustment for the Sotbakken group (below 2246 m and Miocene to Late Paleocene strata) was not apply because of the lithological composition and the possible beginning of the chemical compaction stage.

5. DISCUSSIONS

5.1. MAIN STRUCTURES IN THE SEISMIC LINES

5.1.1. VESTBAKKEN VOLCANIC PROVINCE

The Vestbakken Volcanic Province was easily recognized by the seismic patterns created by the volcanic flows. These volcanic flows appear in the seismic as High Amplitude Reflectors (HAR) and are visible in almost all the seismic lines (with exception of the most southern seismic line, NPD-BJV2-86-7255).

Following the extension generated by these extrusive rocks, it was possible to map the Vestbakken Volcanic Province (see figure 72). Comparing this map with the fact map from the Norwegian Petroleum Directorate (NPD, see figure 23) there are plenty of similarities between both maps. There are just some differences in the boundary according to our results.

The well 7316/5-1 confirmed the presence of volcanic rocks in the area. The seismic tie well confirmed the direct relation between the HAR and the volcanic rocks.

The Vestbakken Volcanic Province was originated during the rifting and breakup of the Norwegian-Greenland Sea during Paleocene-Eocene times. A more detailed historical description has been made in the interpretation and historical section for each line (the base line NPD-BJV1-86-BV-04-86 includes the most complete description because it was tied with the seismic well 7316/5-1). The HAR were interpreted only as landward flows, mainly based in their signature and distribution according to the seismic image. All the stages of breakup volcanism were not interpreted in the seismic images. Probably the reason is that the study area was not a simple rifted margin setting, but it also involved a shear margin setting. The HAR created a masking effect under the strata below and for that reason, it was not possible to interpret deeper reflectors (also because the loss of resolution with depth).

5.1.2.   MAIN FAULTS AND FAULT SETTINGS

The eastern boundary fault appears in the three more northern seismic lines with E-W direction, the base line with SW-NE direction and the north-south line. This extension was showed in the final interpretation map (Figure 7). The eastern boundary fault started to be active since middle Eocene times, and the syn-deposition of the Lower Miocene strata suggests activity until Miocene-Pliocene times (Eidvin et al., 1998). The history of this fault and deposited strata associated therewith, is found in the interpretation of the base line (section 4.1) and briefly in the other lines where it appears (sections 4.2, 4.3, 4.4, and 4.7).

The west area from the eastern boundary fault is characterized by the presence of a faulted sub-basin, and the central east fault. According to the seismic images there is a fault setting along the west part of the eastern boundary fault, expressed as a main fault (named central east fault, sections 4.2 and 4.4) or as a setting of more smaller faults (sections 4.1 and 4.4). The continuity of the central east fault through all the western part was not possible, for that reason the continuity of this feature does not appear clearly in the final interpretation map (Figure 72).

The central east fault has a similar history to the eastern boundary fault (more details, section 4.2.2). The fault setting in the west part was probably originated during Late Eocene to Oligocene times (more details in section 4.1.2) by reactivation of faults (Faleide et al., 2008) or by extensional efforts during Oligocene times (Eidvin et al., 1998).

The major normal faults and fault setting of this area (Knølegga fault, eastern boundary fault, central east fault and western fault setting) are historically connected, and are consequence from the historical shear margin setting which involves periods of transtesion, transpression and inversion, until the passive margin dominated the area.

5.1.3.   FINAL INTERPRETATION MAP
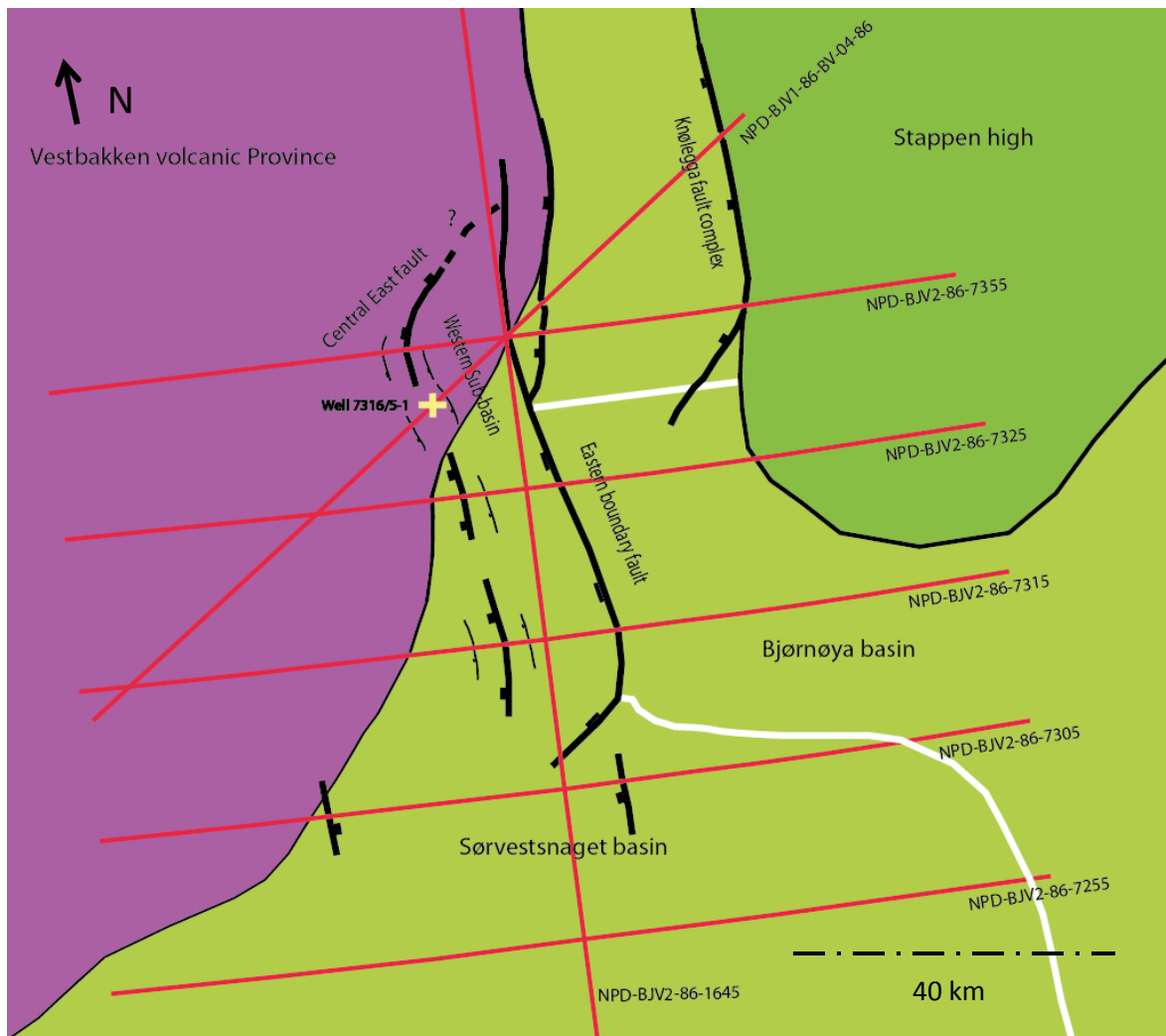
Figure 72. The main structural features are showed in this map. The Vestbakken Volcanic Province was delimited according to the extension of the HAR, interpreted as extrusive rocks. The main faults and fault settings are showed according to the seismic images and based on previous structural maps. The continuation of the central east fault along the western area of the eastern boundary fault was not interpreted in the seismic images and for that reason the continuity does not appears in the map.

5.2. CENOZOIC UPLIFT AND EROSION

After the continental breakup of the Norwegian–Greenland Sea, several authors have proposed a relevant Cenozoic uplift as consequence of this tectonic event. This Cenozoic uplift caused a sub-aerial land that was massively eroded, creating prograding wedges along the western Barents Sea Margin (Faleide et al., 2008; Dahlgreen et al., 2005; Dimakis et al., 1998).

Recent studies have suggested that the southwestern Barents Sea and Svalbard have experienced considerable uplift and erosion during Cenozoic times (Fiedler and Faleide, 1996; Dimakis et al., 1998; Vågnes E., 1997, Riis and Fjeldskaar, 1992; Rasmussen and Fjeldskaar, 1996).

A wide variety of methods have been proposed to estimate the Cenozoic uplift and erosion: vitrinite reflectance, shale compaction, interval velocities, clay mineral diagenesis, etc. (Fiedler and Faleide, 1996).

5.2.1. MAJOR CONSEQUENCES OF THE CENOZOIC UPLIFT AND EROSION – EVIDENCE FROM SEISMIC IMAGES

Base Pliocene truncation

The Base Pliocene is visible in all the seismic lines of this study and is evident along the entire western Barents Sea margin. The Base Pliocene unconformity marks the boundary between the Pliocene-Pleistocene glacial sediments and the pre-glacial sediments. According to several authors, this erosional surface is consequence of uplift and erosion which took place event during Miocene-Pliocene times (Faleide et al., 2008; Eidvin et al., 1998) and subsequent isostatic uplift and erosion (Dimakis et al., 1998). In the figure 73 there is an example showing the location of this main erosive surface.

Other erosional surfaces (example, Base Quaternary/Base Pleistocene) are clear evidence of the complex erosional history in this area, highly influenced by the glaciation during Pleistocene-Pliocene times.

Prograding Pleistocene-Pliocene wedge

The glacial units (GI, GII and GIII) form a large fan along the western Barents Sea margin (also known as trough mouth fans, Dahlgreen et al., 2005). These classification glacial units have been proposed by Fiedler and Faleide (1996) and Faleide et al. (1996) and describe the main glaciations phases during Cenozoic times. The internal sequences of the fan show prograding clinoforms at the slop and parallel layering at the basin floor (Fiedler and Faleide, 1996).

In this seismic data over the Bjørnøya trough (mainly in the upper part of the fan, see figure 74) was possible identified the glacial sequences using the imagess and descriptions proposed by Fiedler and Faleide (1996) and Faleide et al. (1996). In Figure 74 appears the Mega-sequences described by Faleide et al. (1996) over the Vestbakken Volcanic Province. Also this image give a more complete perspective of the entire depositional wedge over the western Barents Sea margin, because in this study is only possible see the upper/continental section of the wedge.

The Upper Regional Unconformity (URU, appears in the interpretation with the abbreviation BQ, Base Quaternary) have been described by Solheim and Kristoffersen (1984) and it is visible in the entire Barents Sea shelf (Fiedler and Faleide, 1996). The URU appears with the name of R1in the Fiedler and Faleide model (see figure 73).
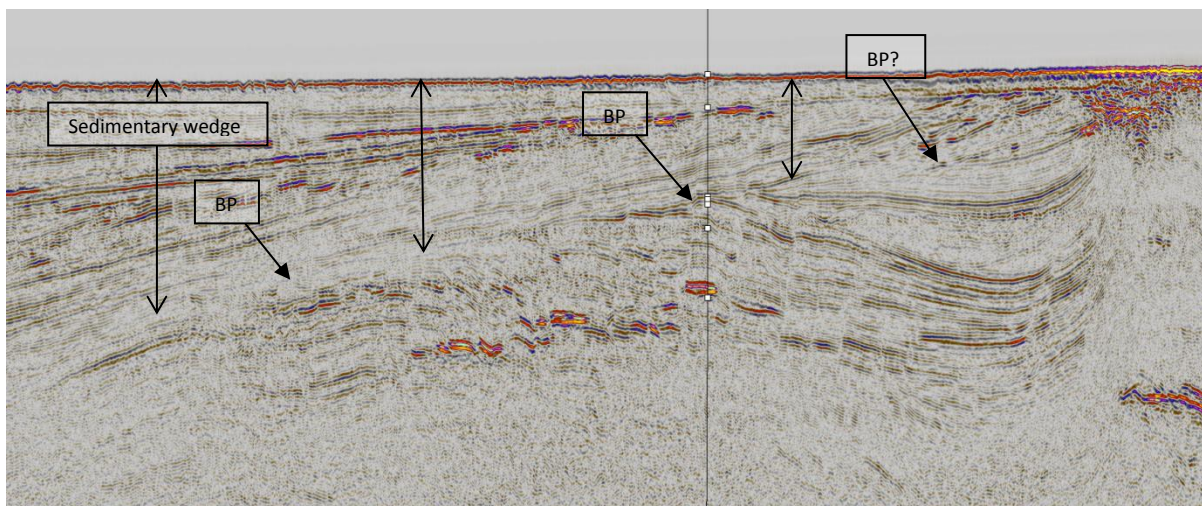
Figure 73.The Base Pliocene reflector is pointed along the image. This reflector represents a main erosive truncation visible in all the seismic lines. Section selected from the seismic line NPD-BJV1-86-BV-04-86. The arrows marks the thickness (thinning to the east) of the Pliocene-Pleistocene sedimentary wedge. BP= Base Pliocene.

The reflector set (R1-R7) proposed by Fiedler et al. (1996) were tentatively identified in this study with different names: R1 is equivalent to BQ (Base Quaternary/Base Pleistocene/ URU); R2 appears as IP 6 (Intra Pliocene VI); R3 appears possible as IP 5 (Intra Pliocene V); R4 was interpreted as IP 3 (Intra Pliocene III); R5 as IP 2 (Intra Pliocene III, base of the Glacial sequence GII); R6 as IP 1 (Intra Pliocene I); and R7 appears as the base of the Pliocene-Pleistocene wedge (BP).
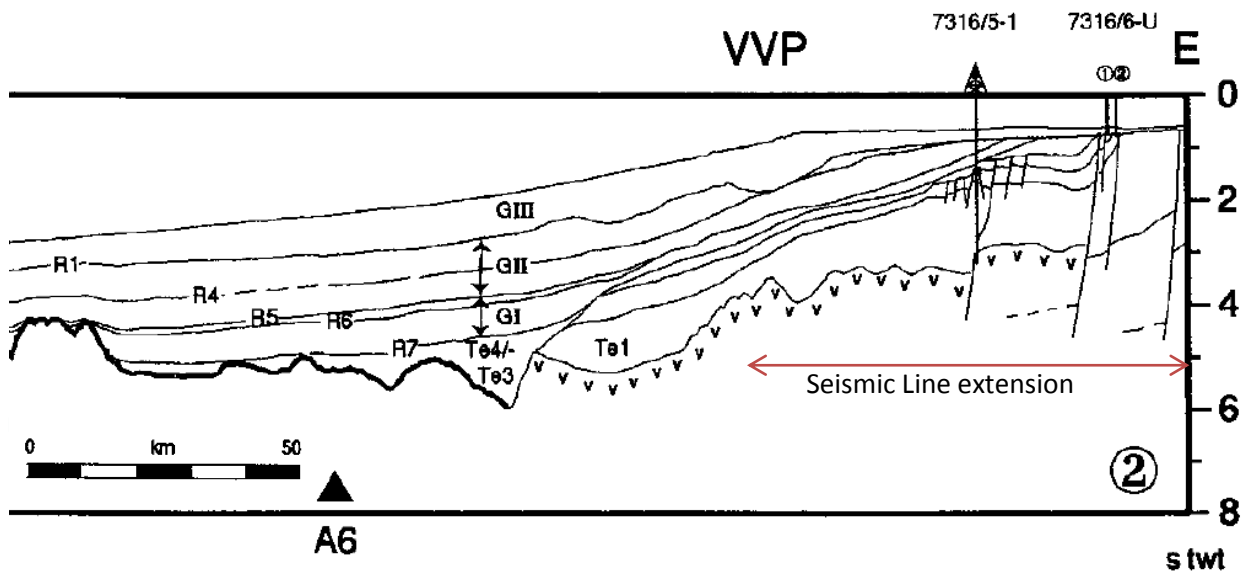
Figure 74.The reflector set R1-R7 has an equivalent in this seismic study over the Vestbakken Volcanic Province. R1 is equivalent to BQ (Base Quaternary/ Base Pliocene); R2 appears as IP 6; R3 appears possibly as IP 5; R4 equivalent would be IP 3; R5 equivalent would be IP 2; R6 was interpreted as IP 1; and R7 appears as the base of the Pliocene-Pleistocene wedge (BP).In this picture is possible observed a bigger view from the sedimentary wedge, which extends kilometers over the oceanic crust. In the seismic lines from this study (marked in the picture), it is possible see only the upper part of the Bjørnøya fan (modified From Faleide et al., 1996).

5.2.2.   CAUSES OF THE CENOZOIC UPLIFT – SOME PROPOSAL MODELS

There are different models that explain the uplift in previous transform margins. The next following thermal models (conductive, viscous coupling and combined models) are based in the three- stage evolution of a transform margin after the continental breakup, but previous to the final passive margin stage. The three-stage model explains these phases between the continental breakup and the passive margin stage that finally experiment a transform margin.

The first stage consist in a continent-continent transform margin, the second stage in an ocean-continent transform margin and the third stage consist in a passive transform margin (Reid I., 1989).

Conductive model

The conductive model is based in the thermal heat conduction from the newer oceanic crust to the older continental crust during the transform margin stage (Todd and Kenn, 1989). This model estimates uplift along a transform continental margin in response to heat conduction during the ocean-continent transform stage, creating distinguish structures possible to see in several areas with previous transform margin features.

Lorenzo and Vera, 1992, proposed this model to explain the uplift in the southern Exmouth Plateau, Australia. Using a geodynamical model, they compared the uplift predicted by the simulation with the uplift suggested estimating the thick of the eroded strata (Lorenzo and Vera, 1992). Gadd and Scrutton (1997) calculated 1300-1400 m of uplift due to thermal effects for a 900 km long transform segment using a 2D numerical model. These values are reduced considerably when considering regional isostatic effects (Gadd and Scrutton, 1997).

Viscous coupling model

Viscous coupling model proposed by Reid (1989) considers the lithospheric behavior below the brittle-ductile transition as a Newtonian viscous medium. Also considering a model of the lithosphere intersected by a transform fault, the sharp transition between the lithospheric plates in the upper and brittle part of the lithosphere will be increasingly smeared out with depth due to mechanical coupling of the ductile parts of the plates (Vågnes , 1997).

Coupling would be higher during continent-continent stage, where cold continental lithosphere is present on both sides. Nevertheless, when the ocean-continent transform stage starting, viscous coupling cease as the spreading axis approaches. During this stage, material is dragged from the ocean-continent part of the transform, where viscous coupling is weaker, to continent-continent part of the transform. These results in a mass deficiency that is supplied by material of the Asthenosphere, but led a crustal thinning during the ocean-continent transform stage (Vågnes, 1997). This crustal thinning induces uplift by isostasy due to the reduction of material.

Combined model

E. Vagnes (1997) simulated these two models, conductive and viscous coupling model, to estimate the uplift in the Senja fracture zone and also propose a combined model resulting from these two. Thermal conduction and thinning of the lithosphere are the main elements that combine this proposal models from Vågnes. To make possible the computational modeling, two simplify combined models have been proposed:

Model C1: This model is based in the supposition that the viscous coupling ends instantaneously at the beginning of ocean-continent transform stage. All the crustal thinning predicted by the viscous coupling model occurs at this time (Vågnes ,1997).

Model C2: in this model, viscous coupling does not decrease until the time of ridge pass; then it ends instantaneously, causing crustal and lithospheric thinning (Vågnes , 1997).
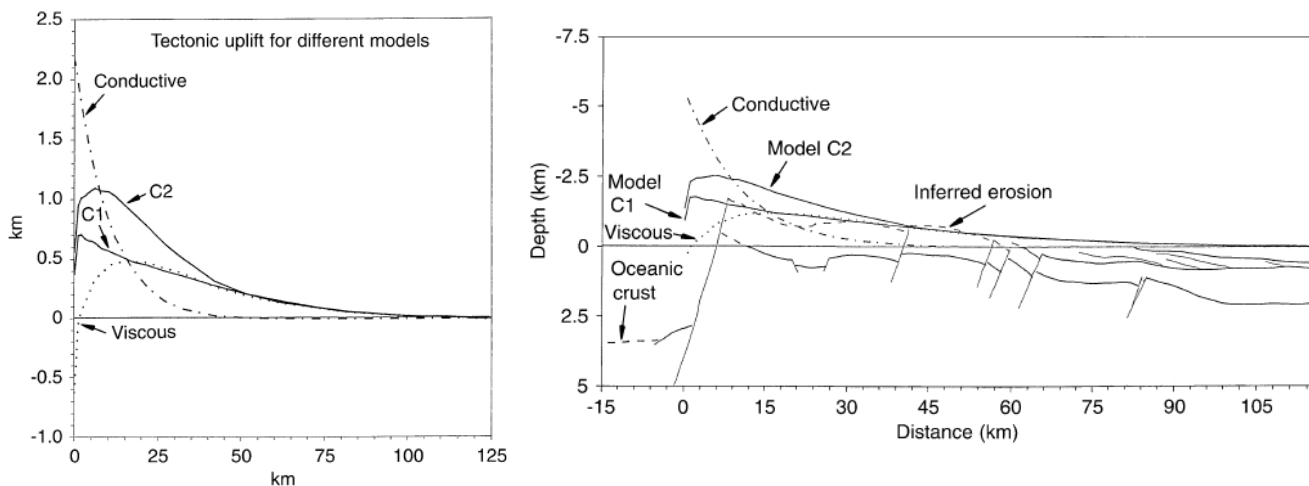
Figure 75. Left: predicted tectonic uplift for different models at the time of ridge pass (maximum uplift prediction). Right: predicted tectonic uplift converted to erosion estimates for different models and the inferred erosion in the Senja Fracture zone. Modified from Vågnes, 1997.

It was inferred the eroded mass using seismic interpreted lines of the area. According to this supposition, all the sub-aerial and subsequent eroded mass marks the maximum uplift. These inferred eroded sediments that show the possible maximum uplift, was compared with the results from different model and simulations. The combined models suggested by E. Vågnes presents the most accurate results in comparison with the erosion estimates (see Figure 75.). The combined C1 model shows just a half of the uplift estimated by the conductive model, and it shows a more accurate shape in comparison with the viscous coupling model that not include the heat transfer from the oceanic crust.

According to Vågnes simulations, using the model C1 was estimated 700 m of uplift, and almost 1000 m of uplift for the model C2. The model C1 shows a better correlation with the inferred erosion, making this model the most accurate. These results contrast with the 2000 m predicted by the conductive model and the 400 until 500 m predicted by the viscous coupling model (Vågnes , 1997).

The Senja fracture zone is adjacent to our area of study, for that reason it represents a proper example for comparison. These modeling and results could be considered a good extrapolation to understand the Cenozoic uplift in the entire western Barents Sea margin, specifically over the Vestbakken Volcanic Province.

Mechanical models

Pure shear or mechanical flexure during the shear margin setting could result in lithospheric necking and uplifting of the area. A theoretical study of these processes (Beek, 1995) has shown that mechanical uplift can result in high amplitude uplift but minor longitude of influence along the margin. This model contrast with the thermal uplift models that show smaller uplift amplitude but larger longitude of influence. For that reason, only the thermal models adjust properly to the inferred uplift and longitude of influence: 1000 of uplift and 500 km of longitude in the southwestern Barents Sea (Dimakis et al., 1998).

5.2.3.   COMPARISON BETWEEN DIFFERENT UPLIFT ESTIMATED RESULTS

There is not a unique value or model that explains the uplift along the western Barents Sea margin. Also there is not a precise consensus in the causes and timing that involved this major uplift and erosional events.

According to Dimakis et al. (1998) initial uplift was followed by intensive glacial erosion, compensated by isostatic uplift which induced the maintenance of an elevated and glaciated terrain. They estimated a pre-glacial elevation around 500 m; this was interpreted as consequence of the initial tectonic uplift. The values of the subsequent isostatic uplift are variable, because in some areas of the margin there was bigger uplift and erosion rates than in others. For highly eroded areas was estimated an uplift of 1300-1400 m (mainly northern

areas and Svalbard region) and 400-500 m in least eroded areas (southern areas of the Barents Sea margin). But, these estimations require more detailed studies to have a clear history of the Uplift and glacial erosion (Dimakis et al., 1998).

The result using the depth-porosity trend method to estimate the uplift in this area was around 900-1000 meters. This model estimated the total uplift in the area, and does not distinguish between the first tectonic uplift and the isostatic uplift suggested by Dimakis et al. For that reason, if we add the minimum results for both events proposed by Dimakis et al. (900 m, in the SW Barents Sea margin) and compare with the depth-porosity trend results (900-1000 m), there is a good correlation between both ranges of values.

According to Rassmussen and Fjeldskaar (1996) they estimated the first tectonic uplift around 500-2000 m (2000 m in the Svalbard region and 500 m in the Southwestern Barents Sea margin) with subsequent sub-aerial erosion. Then, they propose a second step characterize by massive glacial erosion and isostatic net uplift in order of 400 m in the Bjørnøyrenna, and 200-300 m in the central Barents Sea (Rassmussen and Fjeldskaar, 1996). Adding both uplift values (around 700 until 900 m) and comparing with the depth-porosity trend estimation (900±100 m) there is a good correlation between both results.

There are other studies that proposed different scenarios and estimations for this major Cenozoic event. According to Vågnes (1997), using different models was estimated at least 4 tentative maximum uplift values: 2000 m (conductive model), 500 m (viscous coupling model), 700 m (combined model C1) and 1000 m (combined model C2). Vågnes (1997) does not make difference between the initial tectonic uplift and the subsequent isostatic rebound in this study.

Ohm et al. (2008) estimated the total amount of uplift in the southwestern Barents Sea around 500-1500 m with an uncertainty of 500 m. Using the vitrinite reflectance vs depth method (R_0 maturity trends) in several wells along the Barents Sea was possible built a tentative map of the total uplift and its impact in the maturity of the petroleum systems (Ohm et al., 2008). Haltenbanken (Mid-Norway) was used as reference maturity trend to estimate the uplift in the Barents Sea (Ohm et al., 2008).

In table 9 there is a brief summary comparing some of the different estimation for the amount of Cenozoic uplift in the Barents Sea. The Estimation of this study is also included.

Reference	Pre-glacial elevation (tectonic uplift)	Isostatic Uplift
Dimakis et al. (1998)	500- 1000 m	1300-1400 m (Svalbard area). 400-500 m (SW Barents Sea).
Rassmussen and Fjelskaar (1996)	500-2000 m (400-600 m in the SW Barents Sea)	400 m (Bjørnøyrenna) 200-300 m (central Barents Sea)
E. Vågnes (1997)	Total uplift*: 2000 m (conductive model, Senja Fracture zone) 500 m (viscous coupling model, Senja Fracture zone) 1000 m (combined C2 model, Senja Fracture zone) 700 m (combined C1 model, Senja Fracture zone)	
S. Ohm et al. (2008)	Total Uplift: 500-1500 ± 500 m (Vestbakken Volcanic Province) 1500 ± 500 m (location well 7316/5-1)	
Depth-porosity trend estimation	Total Uplift: 900 ± 100 m (Vestbakken Volcanic Province, location well 7316/5-1)	

Table 9. Comparison between the different estimation of the Cenozoic Uplift according to different authors. * Vågnes E. (1997) does not take account the isostatic rebound in its study.

5.2.4.   ESTIMATED EROSION DURING CENOZOIC TIMES

The erosion that affected the western Barents Sea margin has been studied by several authors: Fiedler and Faleide, 1996; Riis and Fjeldskaar, 1992; Richardsen et al., 1993a; Vorren et al., 1991. Typical estimations of erosion for the western Barents Sea indicates 1000-1500 m in the central parts, 1500-2000 m in the southern parts and less than 1000 m in western part (Fiedler and Faleide 1996).

According to Fiedler and Faleide (1996), their estimations of erosion using mass balance was around 1000 m in the southwestern Barents Sea margin. Riis and Fjeldskaar (1992) estimate erosion around 800-1000 m using present-day topography and bathymetry. Richardsen et al.

(1993a) use an interval velocity method to estimate erosion around 600-1200 m and 650-950 m.

In the Table 10, there is a brief summary of some erosion estimation according different studies. There are different methods to estimate the Cenozoic erosion and each one show different results, making uncertainty and inaccuracy in these results.

Reference	Estimated erosion in western Barents Sea margin
Vorren et al (1991)	1200 m
Riis and Fjeldskaar (1992)	800-1000 m
Richardsen et al (1993a)	650-950 m
Fiedler and Faleide (1996)	1000 m

Table 10. Comparison between the different estimation of the Cenozoic erosion according to different authors.

5.2.5 SOME REMARKS ABOUT THE ESTIMATION OF UPLIFT USING EMPIRICAL POROSITY-DEPTH TRENDS AND WELL DATA

There are some assumptions in the depth-porosity trend model that makes this estimation uncertain and subject for revision. The first weakness in this model is the use of empirical depth-porosity trends based in sands and shale formations from the North Sea and not from the Barents Sea formations without uplift, assuming more or less the same burial depth time, and other burial variables. However, this is part of the assumption and the North Sea sands and shales could be seen as the reference formations to make possible the adjustment.

The second weakness is the omission of the deposition and subsidence after the uplift episodes and glacial events. It means that this estimation is probably over-estimated due to subsequent deposition that could increase compaction, reducing even more the porosity of shales and sandstones. The impact of later subsidence in the porosity of these shales and sands was not included in this model. A final assumption is that these shales never reach the chemical compaction stage, in other words, it was only taken account mechanical compaction to explain the loss of porosity in this interval.
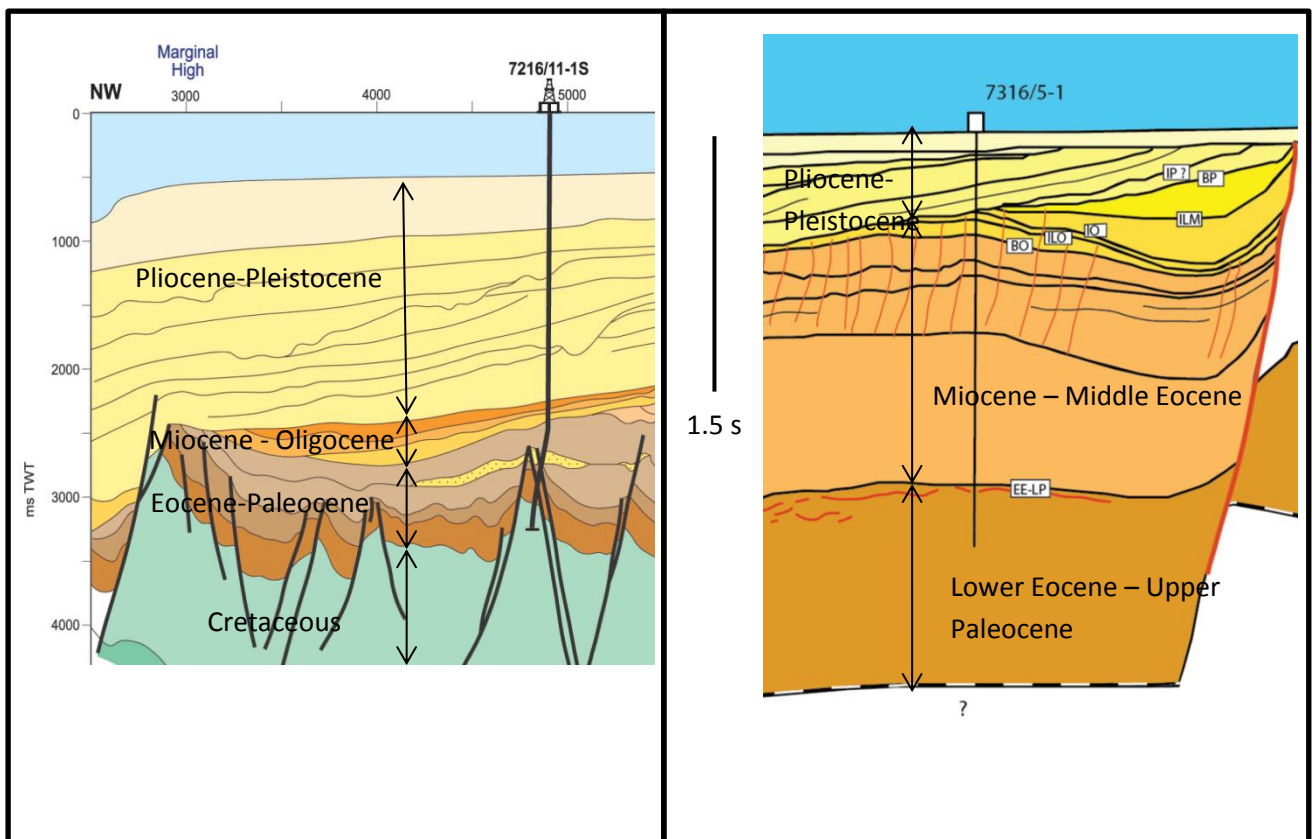
Figure 76. Seismic sections and stratigraphy from wells 7216/11-1S (Left) and 7316/5-1 (right). Noticed that the well 7216/11-1S (Seismic interpretation from Ryseth et al., 2003) was drilled in a thicker section of the prograding wedge (Bjørnøya fan) in comparison with the well 7316/5-1 (interpretation from this study). (modified from Ryseth et al., 2003).

The depth-porosity trend adjustment was applied in the Middle Eocene shales from the well 7316/5-1, and these strata showed a tentative uplift of 900 ± 100 m. The well 7216/11-1S shows almost 2000 m of thick Pliocene-Pleistocene sediments from the sedimentary wedge (see figure 76). The strata (sandstones and mostly shales) from this well correspond mainly to recent material consequence of the previous uplift and glacial erosion. For that reason, it was not necessary any uplift adjustment because the well shows newer strata, not like the well 7316/5-1 that shows shales affected by the tectonic uplift and subsequent rebound. In some way, this well could be considered as the control sample to valid the method and results obtained in the well 7316/5-1.

However, the absence of manual adjustment of the depth-porosity trends for the Pliocene-Pleistocene strata (well 7216/11-1S) could result from other burial factors and not necessarily consequence of the lack of uplift. This is part of the main assumption of this thesis, the

differences in the depth-porosity trends are consequence of the uplift and not by other burial factors. The depth-porosity trend method was not applied in older strata of the well 7216/11-1S (lower than 2300 m) because were too depth rocks, probably bounding with the chemical compaction stage. Also, the logs do not show a clear sand or shale configuration, and carbonates are present in the well (see figure 71).

5.3. SHEAR MARGINS: SOME EXAMPLES AROUND THE WORLD

5.3.1.   GULF OF GUINEA – IVORY COAST AND GHANA TRANSFORM MARGIN

The Ivory Coast and Ghana transform margin is related to the formation of the central Atlantic ocean (118 million years ago) and the continental breakup of the South American and African plates (Bird, 2001).As consequence of this breakup, transform margins were created along the boundary of these two plates. A very steep and narrow transition zone is described between the continental crust and the Oceanic crust, lined up with an oceanic fracture zone (Basile et al., 1998).

The main stages of a transform margin have been described in this area: (1) Intra-continental transform faulting stage; (2) Continent/ocean transform stage and finally (3) Transform margin stage. An elevated and elongated marginal ridge extends the transform domain along the border of the adjacent passive basin (Basile et al., 1998). This Marginal ridge marks the southern boundary of the Deep Ivorian basin over the continental shelf (See figure 77).

There was not an absolute (relative to sea level) uplift associated with the contact between continental crust and passing hot oceanic rifting center. The only visible consequence of this passing is the increasing tilting of the marginal ridge, creating an apparent uplift respect to the subsided Ivorian basin (Basile et al., 1998). There are several theories that tentatively explain this absence of significant thermal uplift in the area. A first theory suggests that thermal uplift had been substantially reduced by coupling of continental and oceanic lithospheres. A second theory is based in the absence of thermal conduction between both lithospheres, as consequence of the nature of the adjacent oceanic lithosphere which was relative cold in comparison with the continental platform (Basile et al., 1998).

5.3.2. EXMOUTH PLATEAU – AUSTRALIA

Lorenzo et al. (1991) proposed a two stage model for continent-ocean transform in the Exmouth Plateau, northwestern Australia. The Exmouth Plateau is a continental block, deformed during Jurassic rifting previous to Early Cretaceous Indian ocean seafloor spreading (see figure 78). During the rift stage, detachment surfaces were formed and then sheared by lateral strike-slip motion and fault block rotations (Bird, 2001).
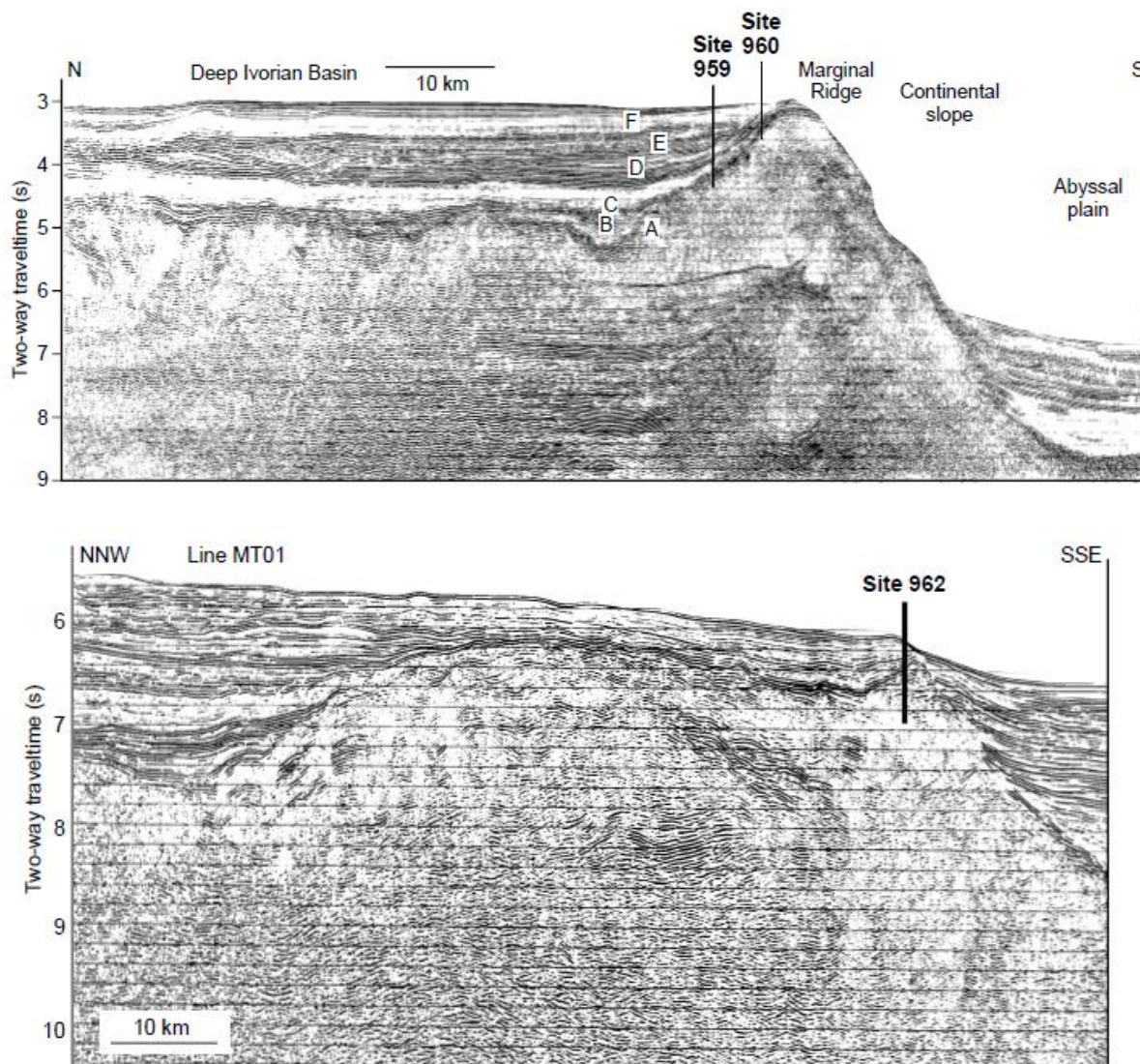
Figure 77.Top: Seismic line across the deep Ivory Coast – Ghana basin, the marginal ridge and the abyssal pain .Bottom: Seismic line across the deep Ivory Coast – Ghana basin, and termination of the marginal ridge (from Basile et al., 1998).

Lorenzo and Vera (1992) also estimated the thermal uplift and erosion in the Exmouth Plateau boundary caused by the interaction between the new seafloor and the continental block. A numerical geodynamic model was created to simulate the effects of heat conduction across the transform margin. Lorenzo and Vera (1992) reports a maximum of 3.5 km of eroded material and also described a local isostatic rebound due to sub-aerial erosion, induced by the first uplift.
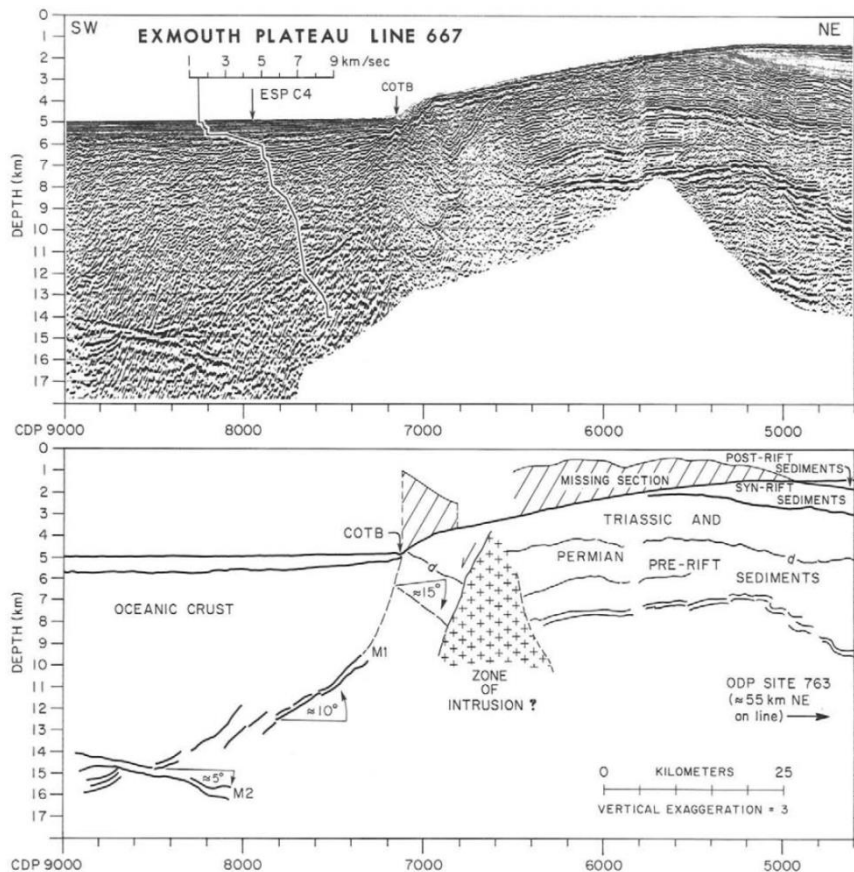
Figure 78.Top: seismic section profile across the margin of the Exmouth Plateau .Bottom: interpretation of the seismic line (From Lorenzo and Vera, 1992).

5.3.3. COMPARISON WITH THE WESTERN BARENTS SEA MARGIN

The two previous examples show a close geological history with the southwestern Barents Sea margin: continental breakup that results in a transform margin (continent/continent and then continent/ocean shearing) until concludes in a passive margin stage (see the three stage model, chapter 2, Subsection 2.1). In the Exmouth Plateau and the Ivory Coast/Ghana

transform margins is possible see a marginal ridge (or zone of intrusion in the Exmouth Plateau). In the seismic lines over the Vestbakken Volcanic Province is not possible see the marginal ridge, due to the location of the seismic lines. A more western or southern seismic image (close to The Senja fracture zone) would show the marginal ridge. This marginal ridge is consequence of igneous intrusion during the interaction between plates during the transform stage margin (Lorenzo and Vera, 1992). It is possible distinguish between a deep oceanic basin and a high continental shelf in both margins (in the seismic images over the Vestbakken Volcanic Province and the Sørvestsnaget basin are only over continental shelf areas).

The main difference between the recent geological history of the western Barents Sea margin and the Ivory Coast and Ghana transform margin is the absence of thermal uplift and subsequent massive erosion. According to Basile et al. (1998) in the Ivory Coast and Ghana transform margin is not possible distinguish induced thermal event, marking a distinctive difference with the western Barents Sea margin. A main consequence of the thermal uplift in the western Barents Sea margin is the sub-aerial erosion. Including the effect of glaciation that increases the erosion, it created a large sedimentary wedge along the margin and adjacent oceanic basins (Dahlgreen et al., 2005). Massive erosion and erosive surfaces are not significant in the Ivory Coast/Ghana transform margin in comparison with the western Barents Sea (see figure 77). It is possible see a depositional wedge over the abyssal plain in the Ivory Coast and Ghana transform margin, but it probably was caused by other type of erosion and sedimentation (submarine fans, alluvial sources from the continent, etc.).

Comparing the western Barents Sea with the Exmouth Plateau, there are evidences of uplift and erosion in both cases. According to Lorenzo et al. (1991), the Exmouth Plateau was uplifted and there are some proposal thermal models to explain this event. However, the erosive processes in the Northern Australia were different that the erosive processes in the western Barents Sea. Glacial erosion was the main factor in the erosion of the western Barents Sea, leading the creation of large Pliocene-Pleistocene wedges. Comparing the images in the western Barents Sea and the image in the Exmouth Plateau (see figure 78) is clearly that the western Barents Sea suffered more intense erosion. This erosion was mainly caused by glaciations that created a massive depositional wedge along the margin. These depositional wedges are not clearly visible in the Exmouth Plateau.

In the table 11 there is a brief summary of the comparison between these three margins. The three examples have a similar tectonic origin, however they present remarkable differences in their geological evolution.

Transform Margin	Uplift and Erosion	Prograding wedge
Southwestern Barents Sea	Yes (succeeded by an isostatic rebound)	Yes (due to Pliocene-Pleistocene glacial erosion)
Exmouth Plateau, Australia	Yes (succeeded by an Isostatic rebound)	No*
Ivory Coast and Ghana transform margin	No	Yes (different origin, over the Abyssal plain)

Table 11. Comparison between some examples of transform margins, focused in uplift and depositional wedge presence. Difference in the tectonism and erosional factors change considerably the main features in each wedge. *Over the oceanic crust of the Exmouth Plateau margin is possible interpreted some sedimentation but is fairly different in magnitude, thick and shape from the massive sedimentary wedge in the western Barents Sea margin.

6. CONCLUSIONS

The first objective in this study consisted in the interpretation of seismic profiles and the use of the provided well 7316/5-1, to build the geological models and understand the history of this area based in all the previous regional studies and resources. Some of the most important features described were the Vestbakken Volcanic Province, the pre-glacial sediments, the glacial sediments (composed by the prograding wedge) and the fault setting.

The Vestbakken Volcanic Province (VVP) was marked and delimited during the seismic interpretation. These volcanic flows were easy to distinguish in the seismic lines and the presence of these volcanic rocks was confirmed by the only deep well in the area (7316/5-1). The pre-glacial sediments (Paleocene-Lower Miocene) were deposited and affected during the shear margin setting that dominated the southwestern Barents Sea during those times. Transpression and transtension during this stage, explain the configuration of these strata. The glacial sediments (Pliocene-Pleistocene) were deposited after the Cenozoic uplift and massive glacial erosion. These glacial sediments formed a massive prograding wedge, visible along the entire margin.

The fault setting affected mainly the pre-glacial strata (under the transtensional effects caused by the shear margin stage) and it was closely involved in the development of this pre-glacial sediments. All the faults were interpreted mainly as normal faults.

The second objective consisted in determining the consequences of the major Cenozoic uplift and giving an estimation using well data and empirical depth-porosity trends. Some of the main consequences of the Cenozoic uplift and erosion are clearly visible in the seismic lines: (1) The Base Pliocene erosive surfaces and other erosive events related to glacial activity (2) The prograding wedge as consequence of the glacial erosion that affected the sub-aerial terrains in response to the uplift.

According to the depth-porosity trend adjustment applied in this study, the uplift was estimated to be around 900±100m. These results include the first tectonic event and the subsequent isostatic rebound. Comparing these results with previous studies, there is a good correlation with the variable range estimated for the total uplift (from 700 m until 1500 m in the southwestern Barents Sea margin).

When comparing the southwestern Barents Sea margin with other old transform margins, it was possible to distinguish the unique features of the southwestern Barents Sea; the tectonic uplift plus isostatic rebound (not proposed in the Ivory coast/Ghana margin) and the massive glacial erosion which led to the deposition of the massive Pliocene-Pleistocene wedge (not visible in the Exmouth Plateau margin).

7. REFERENCES

Attoh, K., Brown, L., Guo,J., Heanlein, J. "Seismic stratigraphic record of transpression and uplift on the Romanche transform margin, offshore Ghana." *Tectonophysics 378*, 2004: 1-16.

Avseth, P.,Mukerji,T. and Mavko, G. *Quantetative Seismic Interpretation: Applying Rock Physics Tools to reduce interpretation risk.* Cambridge University Press , 2010 .

Basile, C., Mascle,J., Benkhelil,J.,Bouillin,J.P. "Geodynamic evolution of the Cote d´Ivore-Ghana transform margin: an overview of Leg 159 results." *Proceedings of the Ocean drilling program, scientific results, Vol 159*, 1998.

Beek, P.A. "Tectonic Evolution of continental rifts: Inferences from numerical Modeling and Fission Tracks Thermochronology." *Proefschrift, Vrije Universiteit Amsterdam* , 1995.

Berndt, C., Planke, S., Alvestad, E., Tsikalas,F. and Rasmussen T. "Seismic volcanostratigraphy of the Norwegian Margin: constraints on tectonomagmatic break-up processes." *Journal of the Geological Society, 158*, 2001: 413-426.

Bird, D. "Shear Margins: Continent-ocean transform and fracture zone boundaries." *The Leading Edge, 20*, 2001: 150-159.

Bradley, D.C. "Passive margin through earth history." *Earth-Science Reviews, 91*, 2008: 1 - 26.

Breivik, A.J., Faleide, J.I., Gudlaugsson, S.T. "Southwestern Barents Sea margin: Late Mesozoic sedimentary basins and crustal extension." *Tectonophysics 293*, 1998: 21-44.

Brown, A. *Interpretation of three dimensional seismic data.* AAPG memory 42, 1996.

Czuba, W., Grad,M.,Mjelde,R.,Guterch,A.,Libak,A.,Kruger,F.,Murai,Y.,Schweitzer,J. & Group. "Continent-ocean transition across a trans-tensional margin segment off Bear island, Barents Sea." *Geophysical journal international, 184* , 2010: 541-554.

Dahlgren, T.K.I, Vorren, T.O.,Stoker, M.S., Nielsen, T., Nygård, A and Sejrup,H.P. "late Cenozoic prograding wedges on the NW European Continental margin: their formation and relationship to tectonics and climate." *Marine and Petroleum Geology, 22*, 2005: 1089-1110.

Dick, H.J.B.,Lin,J. and Schouten,H. "An ultraslow-spreading class of ocean ridge." *Nature, 426* , 2003: 405-412.

Dimakis, P., Braathen, B. I., Faleide, J.I., Everhøi, A. and Gudlaugsson, S. "Cenozoic erosion and the preglacial uplift of the Svalbard-Barents Sea region." *Tectonophysics, 300*, 1998: 311-327.

Eidvin, T., Goll, R., Grogan, P., Smelor, M. and Ulleberg K. "The Pleistocene to Middle Eocene stratigraphy and geological evolution of the western Barents sea continental margin at well site 7316/5-1 (Bjornoya West Area)." *Norwegian Geological Journal*, 1998: 99-123.

Ewing, T. *AAPG Datapages/ seach and Discovery - Synthetic Seismograms: preparation, calibration and associated issues.* 2001. http://www.searchanddiscovery.com/documents/geophysical/Ewing/ (accessed June 05, 2014).

Faleide, J.I., Gudlaugsson, T., Jacquart, G. "Evolution of the western Barents Sea." *Marine and Petroleum Geology Vol 1*, 1984: 123-150.

Faleide, J.I., Myhre,A. and Eldholm,O. "Early Tertiary volcanism at the western Barents Sea margin." *Geological society, London, Sepecial publications, 39*, 1988.

Faleide, J.I., Solheim, A., Fiedler,A., Hjelstuen,B.,Andersen,S.,Vanneste,K. "Late Cenozoic evolution of the western Barents Sea-Svalbard continental margin." *Global and Planetary Change 12*, 1996: 53-74.

Faleide, J.I., Tsikalas,F.,Breivik,A.J.,Mjelde,R.,Ritzmann,O.,Engen,O., Wilson,J. and Eldholm,O. "Structure and evolution of the continental margin off Norway and the Barents Sea." *Episodes, 31*, 2008: 82-91.

Faleide, J.I., Vagnes,E.,Gudlaugsson,S.T. "Late Mesozoic-Cenozoic evolution of the south-western Barents Sea in a regional rift-shear tectonic setting." *Marine and Petroleum Geology, vol 10*, 1993a: 186-214.

Fiedler, A., Faleide, J.I. "Cenozoic sedimentation along the southwestern Barents Sea margin in relation to uplift and erosion of the shelf." *Global and Planetary change 12*, 1996: 75-93.

Fossen, Haakon. *Structural Geology*. New York: Cambridge University Press, 2010.

Gabrielsen, R.H., Faerseth, R.B., Jensen,L.N., Kalheim, J.E. and Riss,F. "Structural elements of the Norwegian continental shelf." *NPD-Bulletin,6*, 1990.

Heshthammer, J., Landro, M. and Fossen, H. 2001. "Use and abuse of the seismic data in reservoir characterization." *Marine Petroleum Geology, 18*, 2001: 635-655.

Hintz, K., Eldholm, O., Block, M. and Skogseid, J. "Evolution of North Atlantic volcanic continental margins." *London, the geological society*, 1993 .

Knies, J., Matthiesse, J., Vogt, C., Laberg, J.S., Hjelstuen, B.O., Smelror, M., Larsen, E., Eidvin, T. and Vorren, T.O. "The Plio-Pleistocene glaciation of the Barents Sea-Svalbard region: a new model based on revised chronostratigraphy." *Quaternary Science Reviews 28*, 2009: 812-829.

Knutsen, S.M. and Larsen, K.I. "The Late Mesozoic and Cenozoic evolution of the Sorvestnaget Basin: A Tectonostratigraphic mirror for regional events along the southwestern Barents Sea Margin ?" *Marine and Petroleum Geology 14*, 1997: 27-54.

Libak, A. Mjelde, R., Keers, H., Faleide, J.I. and Murai, Y. "An Integrated geophysical study of Vestbakken Volcanic Province, western Barents Sea continental margin, and adjacent oceanic crust." *Marine Geophysical research, 33*, 2012: 185-207.

Lister, G.S., Etheridge, M.A., Symonds, P.A. "Detachment faulting and the evolution of passive continental margins." *Geology*, 1986: 246-250.

Lorenzo, J.M., Mutter, J.C., Larson, R.L. "Development of the continent-ocean transform boundary of the southern Exmouth Plateau." *Geology V. 19*, 1991: 843-846.

Lorenzo, J.M., Vera, E.E. "Thermal Uplift and erosion across the continent-ocean transform boundary of the southern Exmouth Plateau." *Earth and Planetary Science letters, 108*, 1992: 79-92.

Lundin, E. and Doré, A.G. "Mid-Cenozoic post-breakup deformation in the ´passive´ margins bordering the Norwegian-Greenland Sea." *Marine and Petroleum Geology, 19*, 2002: 79-93.

Macdonald, K.C. *Encyclopedia of Ocean Sciences. Mid-Ocean Ridge Tectonics, Volcanism and Geomorphology.* Academic Press., 2001.

Macdonald, K.C. "Mid-Ocean Ridges: Fine Scale Tectonic, VOlcanic and Hydrothermal Processes within the Plate Boundary Zone." *Annual Reviews in Earth and Planetary Sciences*, 1982: 155-190.

Magara, K. "Comparison of porosity-depth relationships of shale and sandstone." *Journal of Petroleum Geology* (Journal of Petroleum geology, 3), 1980: 175-185.

Magara, K. "Comparison of porosity-depth relationships of shale and sandstone." *Journal of Petroleum Geology, 3*, 1980: 175-178.

Mascle, J., Lohmann,P.,Clift,P. "Development of a passive transform margin: Cote d´Ivore-Ghana transform margin . OPD leg 159 preliminary results." *Geo-Marine Letters, 17*, 1997: 4-11.

McKenzie, D. and Blickle, M.J. "The olume and composition of Melt generated by extension of the Lithosphere ." *Journal of Petrology, 29*, 1988: 625-679.

Mckenzie, D. "Some remarks on the development of sedimentary basins. ." *Earth and Planetary Sciences Letters, 40* , 1978: 25-32.

Morgan, J. "Hotspots tracks and the early rifting of the atlantic." *Tectonophysics, 94*, 1983: 123-139.

Natural history Museum - Oslo. *Norwegian Stratigraphic Lexicon .* n.d. http://nhm2.uio.no/norges/litho/Barents_Chart.html (accessed June 03, 2014).

NOAA. *Bathymetry Data viewer [Online].* 2014. http://maps.ngdc.noaa.gov/viewers/bathymetry/ (accessed June 06, 2014).

NPD. *NPD: Norwegian Petroleum directorade. Fact Map [online].* March 20, 2014. Available: http://npdmap1.npd.no/website/npdgis/viewer.htm.

NPD. *NPD: Norwegian petroleum Directorate. factpage [Online].* n.d. http://factpages.npd.no/ReportServer?/FactPages/PageView/strat_Litho_level1_group _formation&rs:Command=Render&rc:Toolbar=false&rc:Parameters=f&NpdId=154& IpAddress=129.241.65.229&CultureCode=en (accessed June 3, 2014).

NPD: Norwegian petroleum. *NPD, factpages.* n.d. http://factpages.npd.no/ReportServer?/FactPages/PageView/strat_Litho_level1_group _formation&rs:Command=Render&rc:Toolbar=false&rc:Parameters=f&NpdId=154& IpAddress=129.241.65.229&CultureCode=en (accessed June 3, 2014).

Ohm, S.E., Karlsen,D.A., and Austin,T.J.F. "geochemically driven exploration models in uplifted areas: Examples from the Norwegian Barents Sea." *AAPG Bulletin, V. 92, No. 9*, 2008: 1191-1223.

Planke, S. and Alvestad, E. "Seismic Volcanostratigraphy of the extrusive breakup complexes in the Northeast Atlantic: Implications from ODP/DSDP drilling." *Proceedings of the Ocean Drilling Program, Scientific results, 163*, 1999: 3-16.

Planke, S., Symonds, P.A, Alvestad, E. and Skogseid, J. "Seismic volcanostratigraphy of large-volume basaltic extrusive complexes on rifted margins." *Journal of Geophysical research, 105*, 2000: 335-351.

Rammm, M. and Bjørlykke, K. "porosity/Depth trends in reservoir sandstones: assessing the quantitative effects of varying pore-pressure, temperature history and mineralogy." *Norwegian Shelf data, clary minerals 29*, 1994: 475-490.

Rasmussen, E. Fjeldskaar, W. "Quantification of the Pliocene-Pleistocene erosion of the Barents Sea from present-day bathymetry." *Global and Planetary change 12*, 1996: 119-133.

Reid, I. "Effects of Lithospheric flow on the formation and evolution of a transform margin ." *Earth planetary Science letters, 95*, 1989: 38-52.

Richardsen, G., Knutsen, S., Vail, P.R. and Vorren T.O. "Late Miocene sedimentation on the southwestern Barents Shelf margin." *Artic Gology and Petroleoum potential. Nor.Pet.Soc, Elsevier* , 1993a : 539-571.

Riis, F. and Fjeldskaar, W. "On the magnitude of the Late Tertiary and Quaternary erosion and its significance for the uplift of Scandinavia and the Barents Sea." *NPF Special publication 1* , 1992: 163-185.

Ryseth, A. Augustson, J.H., Charnock, M., Haugerud,O., Knutsen,S., Mildboe,P.S., Opsal,J.G. and Sundsbo,G. "Cenozoic stratigraphy and evolution of the Sorvestnaget Basin, southwewestern Barents Sea." *Norwegian Journal of Geology, 83*, 2003: 107-130.

Scrutton, R.A., and Gadd,S.A. "An integrated thermomechanical model for transform continental margin evolution." *Geo-Marine letters, 17*, 1997: 21-30.

Semple, R.T. Bulman, R. *Final Well Report, Well 7316/5-1.* . Norsk Hydro AS, 1993.

Solheim, A. and Kristoffersen, Y. "Sediments above the upper regional unconformity: thickness, seismic stratigraphy and outline of the glacial history." *Norsk Polarinst Skrift, 179B*, 1984.

Todd, B.J. and Keen, C.J. "Temperature effects and their geological consequences at tranform margins." *Canadian Journal of Earth Science*, 1989: 2591-2603.

Vågnes, E. "Uplift and Thermo-mechanically coupled ocean-continent transforms: Modeled at the Senja Fracture Zone, southwestern Barents Sea ." *Geo-Marine letters*, 1997: 100-109.

Vorren, T., Henriksen, E. "Cenozoic erosion and sedimentation in the western Barents Sea." *Marine and Petroleum Geology, Vol 8*, 1991: 317-340.

White, R. and McKenzie,D. "Magmatism at rift zones: the generation of volcanic continental margins and flood basalts." *Journal of geophysical science, 94*, 1989: 7685-7729.